REPUBLIC OF TURKEY

YILDIZ TECHNICAL UNIVERSITY

GRADUATE SCHOOL OF SCIENCE AND ENGINEERING

SYNTHESIS OF POLY(OXANORBORNENE) DERIVATIVES CONTAINING PHTHALOCYANINE AND INVESTIGATION OF THEIR ANTIMICROBIAL PHOTODYNAMIC PROPERTIES

Erem AHMETALİ

DOCTOR OF PHILOSOPHY THESIS

Department of Chemistry

Inorganic Chemistry Program

Supervisor

Prof. Dr. M. Kasım ŞENER

October, 2022

REPUBLIC OF TURKEY

YILDIZ TECHNICAL UNIVERSITY

GRADUATE SCHOOL OF SCIENCE AND ENGINEERING

SYNTHESIS OF POLY(OXANORBORNENE) DERIVATIVES CONTAINING PHTHALOCYANINE AND INVESTIGATION OF THEIR ANTIMICROBIAL PHOTODYNAMIC PROPERTIES

A thesis submitted by Erem AHMETALİ in partial fulfillment of the requirements for the degree of DOCTOR OF PHILOSOPHY is approved by the committee on 26.10.2022 in Department of Chemistry, Inorganic Chemistry Program.

Prof. Dr. M. Kasım ŞENER
Yıldız Technical University
Supervisor

Approved By the Examining Committee

Prof. Dr. M. Kasım ŞENER, Supervisor
Yildiz Technical University _____

Prof. Dr. Tarık EREN, Member
Yildiz Technical University _____

Assoc. Prof. Dr. Abdullah AYDOĞAN, Member
Istanbul Technical University _____

Prof. Dr. Metin TÜLÜ, Member
Yildiz Technical University _____

Prof. Dr. Amitav SANYAL, Member
Boğaziçi University _____

I hereby declare that I have obtained the required legal permissions during data collection and exploitation procedures, that I have made the in-text citations and cited the references properly, that I haven't falsified and/or fabricated research data and results of the study and that I have abided by the principles of the scientific research and ethics during my Thesis Study under the title of Synthesis of Poly(oxanorbornene) Derivatives Containing Phthalocyanine and Investigation of Their Antimicrobial Photodynamic Properties supervised by my supervisor, Prof. Dr. M. Kasım ŞENER. In the case of a discovery of false statement, I am to acknowledge any legal consequence.

Erem AHMETALİ

Signature

This study was supported by the Scientific and Technological Research Council of Turkey (TUBITAK) Grant No: 219Z271

Dedicated to everyone with

the courage to try better

ACKNOWLEDGEMENTS

I would like to start by thanking my supervisor Prof. Dr. M. Kasım ŞENER who expanded my horizon with his ideas about the design and synthesis of original molecules and always was a very important idol for me with his knowledge and ability to follow the literature. He guided me on how to write scientific projects and articles during my Ph.D. and supported me to work in different laboratories to improve myself.

I would like to thank Prof. Dr. Tarık EREN who opened his laboratory's facilities to us in order to carry out collaboration. Moreover, he enabled me the possibility to enter the research area of polymer chemistry by supporting our collaborative work to be my thesis.

I would like to thank Prof. Dr. Metin TÜLÜ, Assoc. Prof. Dr. Abdullah AYDOĞAN and Prof. Dr. Amitav SANYAL who are the esteemed jury members honored us by spending their time and efforts.

I would like to thank Dr. Pınar ŞEN and Prof. Dr. Tebello NYOKONG who contributed to my thesis with their studies.

I would like to thank Prof. Dr. Anzhela GALSTYAN who has share in my thesis, encouraged me to write a DAAD project and hosted me to gain knowledge and experience about photochemistry in her laboratories.

I want to thank my friend and colleague Dr. Burak YILDIZ. We have worked together for five years in the laboratory and he is one of the rare people who impressed me with his diligence and logic in the academic community.

I'm also grateful for my professors and friends Dr. Armağan ATSAY and Dr. Ömer Tahir GÜNKARA whose minds and experiences I have always consulted throughout my academic life.

I want to thank my students Münevver YAVUZ, Lina ZENGİL, Durmuş Yiğit EMİR and Tahsin Can TEZEL, who helped me during my thesis and gave me strength with their energies.

I want to thank my family Erol AHMETALİ and Emine AHMETALİ, who have always supported me.

I would like to express my deepest gratitude to my professor and mentors Dr. Mahmut PARLAK and Levent SALGANCAK who have the biggest share in the development of both my personal and academic point of view.

And the most special thank goes to my partner Dr. Azra KOCAARSLAN who I am always so proud of with her ideas, perspective and diligence. She has always inspired me with her courage and effort to achieve better and has been my only constant in my life where I believe that every variation is possible.

I would like to thank The Scientific and Technological Research Council of Turkey (TUBITAK) and DAAD (Deutscher Akademischer Austauschdienst) for supporting our projects and me personally.

Erem AHMETALİ

TABLE OF CONTENTS

LIST OF SYMBOLS **ix**
LIST OF ABBREVIATIONS **x**
LIST OF FIGURES **xi**
LIST OF TABLES **xiii**
ABSTRACT **xiv**
ÖZET **xvii**
1 INTRODUCTION **20**
1.1 Literature Review 20
1.2 Objective of the Thesis 28
1.3 Hypothesis 28
2 GENERAL INFORMATION **30**
2.1 Bacteria and Antibacterial Treatment 30
2.2 Ring Opening Metathesis Polymerization and Poly(Norbornene)s 32
2.3 Antimicrobial Photodynamic Therapy 35
2.4 Phthalocyanines 37
2.5 Polymeric Phthalocyanines 39
3 EXPERIMENTAL PART **45**
3.1 Materials 45
3.2 Instruments 45
3.3 Synthesis of Compounds 46
3.4 Antimicrobial Photodynamic Activities 53
4 RESULTS AND DISCUSSION **55**
4.1 Synthesis of Monomers and Polymers 55
4.2 Characterization of Monomers and Polymers 59
4.3 Photophysical Studies 63
4.4 Singlet Oxygen Quantum Yields (Φ_{Δ}) 67
4.5 Triplet Quantum Yield (Φ_{T}) and Lifetimes (τ_{T}) 69
4.7 Antimicrobial Photodynamic Activities in Biofilms 74
4.8 Bacteria Imaging Studies 76
4.9 Conclusion 79
REFERENCES **80**

A SPECTRA **90**
PUBLICATIONS FROM THE THESIS **117**

LIST OF SYMBOLS

gr	Gram
L	Liter
mg	Milligram
mL	Milliliter
mmol	Millimol
mol	Mol

LIST OF ABBREVIATIONS

aPDT	Antibacterial Photodynamic Therapy
AsymPc	Asymmetrical Phthalocyanine
ATRP	Atom Transfer Radical Polymerization
$CHCl_3$	Chloroform
DCM	Dichloromethane
DMAC	Dimethyl Acetamide
DMAE	Dimethyl Amino Ethanol
DMF	Dimethyl Formamide
DMSO	Dimethyl Sulfoxide
DBU	1,8-Diazabicyclo(5.4.0)undec-7-ene
FT-IR	Fouirer Transform Infrared
MALDİ	Matrix-Assisted Laser Desorption/İonization
MPc	Metallophthalocyanine
NMR	Nuclear Magnetic Resonance
PDT	Photodynamic Therapy
PEG	Polyethylene Glycol
PN	Poly(Norbornene)
PON	Poly(Oxanorbornene)
PPc	Polymeric Phthalocyanine
PZnPc	Polymeric Zinc Phthalocyanine
PS	Photosensitizer
Pc	Phthalocyanine
RAFT	Reversible Addition Fragmentation Chain Transfer
ROS	Reactive Oxygen Species
ROMP	Ring Opening Metathesis Polymerization
SEM	Scanning Electron Microscope
SiPc	Silicon Phthalocyanine
SymPc	Symmetrical Phthalocyanine
THF	Tetrahydrofuran
UV-vis	Ultraviolet Visible
ZnPc	Zinc Phthalocyanine

LIST OF FIGURES

Figure 1.1 PNs with different hydrophobic groups [6] 21

Figure 1.2 Synthesis of PONs derivatives containing different phosphonium groups [7] 21

Figure 1.3 Synthesis of PNs derivative containing biocompatible PEG moiety [8] 22

Figure 1.4 Asymmetric ZnPcs used in aPDT [14] 23

Figure 1.5 Symmetric ZnPc containing alkylpyridyloxy groups of different hydrocarbon chain lengths used in aPDT [15] 23

Figure 1.6 A PPc have been synthesized with the help of polymer-bound precursor technique [19] 24

Figure 1.7 Structure of PN which are containing Pc and fullerene units as pendant [23] 26

Figure 1.8 Chemical structure of star-shaped PZnPc containing DMAE groups in the arms [28] 26

Figure 1.9 SiPc hydrogel containing chitosan [29] 27

Figure 1.10 PZnPc example from literature prepared with side chain method [30] 28

Figure 2.1 Strategies used by bacteria for inactivation of drugs [38] 31

Figure 2.2 Some action mechanisms of antimicrobial peptides (A) Barrel-Stave model (B) Carpet model (C) Toroidal pore model [43] ..32

Figure 2.3 ROMP mechanism proposed by Chauvin in 1970 [20] 33

Figure 2.4 Grubbs catalyst derivatives [50] 34

Figure 2.5 Jablonski diagram showing the aPDT mechanism [54] 36

Figure 2.6 Substitution points of Pcs 37

Figure 2.7 An example to typical UV-vis spectrum of MPcs 39

Figure 2.8 Synthesis of network PPc [67] 40

Figure 2.9 Preparation of ZnPc hydrogel containing chitosan and difloxacin [77] 41

Figure 2.10 Chemical Structure of main chain PPc [84] 42

Figure 2.11 Synthesis strategies of the side chain PPcs 43

Figure 2.12 Structure of star-shaped PZnPc containing poly(ε-caprolactone)s in the arms [92] 44

Figure 4.1 The synthetic route A....56
Figure 4.2 The synthetic route B for monomer synthesis....56
Figure 4.3 The structures of first series polymers....57
Figure 4.4 Synthesis of monomer M5....58
Figure 4.5 The structures of second series polymers....58
Figure 4.6 ^{1}H NMR spectra of M2 and P1-P3....60
Figure 4.7 ^{1}H NMR spectra of P4-P7 in DMSO-d_6....61
Figure 4.8 ^{1}H-NMR spectra of M5, M3 and P8-P11 in DMSO-d_6....63
Figure 4.9 Absorption, excitation and emission spectra of P5 (excitation wavelength: 617 nm)....64
Figure 4.10 Fluorescence decay (blue), χ2 fitting (black) and IRF (green) curves for P3 in DMSO....65
Figure 4.11 (a),(b) UV-vis spectra (c),(d) fluorescence spectra of copolymers (P9-P11) in DMF and H_2O (concentration: 10 μg/mL)....66
Figure 4.12 Determination of singlet oxygen quantum yield of P5 (a) in DMSO using DPBF (b) in 5% DMSO-water using ADMA....68
Figure 4.13 (a) Decay curves of DPBF (b) Decay curves of ADMA in presence of corresponding PSs....69
Figure 4.14 Triplet absorption decay (black) and fitting (red) curve for P3 in DMSO....71
Figure 4.15 Antimicrobial activities of copolymers (P4-P7) (a) against *S. aureus* (b) against *E. coli*....72
Figure 4.16 (a) Viability of *B. subtilis* (b) Viability of *E. coli* in dark and after irradiation in the presence of P8-P11. Overall light dose 18 J/cm^2....74
Figure 4.17 (a) Viability of *B. subtilis* (b) Viability of *E. coli* in biofilms....76
Figure 4.18 SEM micrographs of (a) *S. aureus* untreated (b) *S. aureus* treated by P5 at MIC value (c) *S. aureus* treated by P5 at supra-MIC value....77
Figure 4.19 Fluorescence microscopy images of Live/Dead stained *B. subtilis* after incubation with 10 μg/mL of corresponding polymers and irradiation with red light of 18 J/cm^2 doses....78
Figure 4.20 Fluorescence microscopy images of Live/Dead stained *E. coli* after incubation with 10 μg/mL of corresponding polymers and irradiation with red light of 18 J/cm^2 doses....78

LIST OF TABLES

Table 2.1 Strain energies of some cyclic olefins [40].....35

Table 4.1 Photodynamic parameters of P3-P7 in DMSO and 5% DMSO-water.....70

Table 4.2 Photodynamic parameters of P8-P11 in DMF and Water.....70

Table 4.3 Log reduction and percentage cell survival (% survival) values of *S. aureus* and *E. coli* after 80 min irradiation in the presence of first series polymers (P3-P7).....73

ABSTRACT

Synthesis of Poly(oxanorbornene) derivatives Containing Phthalocyanine and Investigation of Their Antimicrobial Photodynamic Properties

Erem AHMETALİ

Department of Chemistry

Doctor of Philosophy Thesis

Supervisor: Prof. Dr. M. Kasım ŞENER

Bacterial infection is a serious problem in today's world. Excessive use of traditional drugs such as antibiotics has given rise to the development of resistance mechanisms of bacteria to these drugs. Thus, the search for potential agents that can inactivate bacteria is increasing day by day. Antibacterial polymers have taken attention because they successfully mimic antibacterial peptides and can be synthesized quickly and on purpose in the laboratory environment. Their mechanism of action originates from the electrostatic interaction between the negatively charged cell membrane of the bacteria and the cationic side of polymer, and the hydrophobic interaction between the tail groups of the phospholipids in the cell wall and the hydrophobic groups on the polymer. PONs are polymeric structures that are synthesized by the ROMP method with the help of various metal complexes. They have a significant place among the stars of antibacterial polymers thanks to being easily changed their substituents and controlled of their parameters such as molecular weight and charge density. On the other hand, aPDT

is an important method based on ROS formation on the inactivation of bacteria. When the molecules called PS interacts with the light of the appropriate wavelength, they can achieve intersystem crossing and produce ROS. Thus, they lead to protein dysfunction, DNA damage, cell membrane disruption and provide photoinactivation of bacteria. Pcs are among the most used PSs with the convenient absorption wavelength, long triplet lifetime, and high ROS generation. In addition, Pcs can carry hydrophobic, hydrophilic or cationic groups in their many positions that can contribute to the struggle against bacteria.

Within the scope of this thesis, two antimicrobial agents (cationic PON and PS ZnPc), each with a different antimicrobial mechanism, have combined in a single molecule and the antibacterial properties of synthesized structures containing these components in different ratios were examined comparatively.

In the first part of the thesis, the synthesis of PONs containing *tert*-butyl substituted ZnPc in their side chains was aimed. For this purpose, firstly, the “Polymer Bound Precursor” method was used. Oxanorbornene substituted phthalonitrile compound was synthesized (M1), this compound was polymerized by ROMP method (P1) and P1 was reacted with excess amount of *tert*-butyl substituted phthalonitrile compound for the synthesis of Pc-containing polymer (P2). However, although the monomer and the starting polymer were successfully synthesized and characterized (M1 and P1), the characteristic polymer peak could not be seen in the ^{1}H NMR of the final product and it was understood that the polymer backbone could not be protected during Pc formation reaction (P2). Therefore, it was decided to change the synthesis strategy and use the "Pc-Containing Monomer" method. For this purpose, oxanorbornene monomer (M2) containing *tert*-butyl substituted ZnPc was synthesized for the first time, and other oxanorbornene monomers (M3, M4) containing phosphonium groups were synthesized according to the literature. Then, the synthesis and characterization of homopolymer (P3) containing only M2 monomer and copolymers (P4-P7) containing M2, M3 and M4 monomers in different ratios were carried out. Photophysical and photochemical parameters of all polymers (P3-P7) (first series) were measured, and aPDT activities against gram-negative *E. coli* and gram-

positive *S. aureus* were investigated. In addition, the bacterial-polymer interaction has been demonstrated by scanning electron microscopy.

In the second part of the thesis, in order to increase biocompatibility, oxanorbornene monomer (M5) containing PEG substituted ZnPc in its side chains instead of *tert*-butyl groups was synthesized, and then the synthesis and characterization of its homopolymer (P8) and copolymers (P9-P11) containing M3 and M5 monomers in different ratios were carried out. Photophysical and photochemical parameters of all polymers (P8-P11) (second series) were measured and aPDT activities were investigated against *B. subtilis* as gram-positive bacteria and *E. coli* as gram-negative bacteria. The bacterial-polymer interaction was proved with the help of fluorescence microscopy.

Keywords: poly(oxanorbornene), ring-opening metathesis polymerization, phthalocyanine, antimicrobial photodynamic therapy, macromolecular photosensitizer, singlet oxygen generation

ÖZET

Ftalosiyanin İçeren Poli(oksanorbornen) Türevlerinin Sentezi ve Antimikrobiyal Fotodinamik Özelliklerinin İncelenmesi

Erem AHMETALİ

Kimya Anabilim Dalı

Doktora Tezi

Danışman: Prof. Dr. M. Kasım ŞENER

Günümüzün dünyasında bakteriyel enfeksiyon ciddi bir problemdir. Antibiyotik gibi geleneksel ilaçların aşırı kullanımı ve bakterilerin bu ilaçlara direnç mekanizmaları geliştirmesinden dolayı bakterileri etkisiz hale getirebilecek potansiyel ajanların arayışı gün geçtikçe artmaktadır. Antibakteriyel polimerler, antibakteriyel peptitleri başarıyla taklit etmeleri ve laboratuvar ortamında amaca uygun ve hızlı bir şekilde sentezlenebilmelerinden dolayı dikkat çekmektedirler. Polimerlerin etki mekanizması bakterinin negatif yüklü hücre zarı ile polimerin katyonik tarafı arasındaki elektrostatik etkileşimden ve hücre duvarındaki fosfolipidlerin kuyruk grupları ile polimerin hidrofobik grupları arasındaki hidrofobik etkileşimden ileri gelmektedir. PON'ler çeşitli metal kompleksleri yardımıyla ROMP metodu ile sentezlenen bileşiklerdir. Kolaylıkla modifiye edilebilmeleri ve molekül ağırlığı, yük yoğunluğu gibi parametrelerinin kolaylıkla kontrol edilebilmesi sayesinde antibakteriyel polimerler sınıfının yıldızları arasında kendilerine yer bulmuşlardır. Diğer yandan, aPDT bakterilerin etkisiz hale getirilmesinde reaktif oksijen türlerinin üretimini esas alan önemli bir

yaklaşımdır. Uygun dalga boyunda ışık ile etkileştiğinde sistemler arası geçiş yapabilen PS adındaki moleküllerin ürettiği reaktif oksijen türleri protein, DNA ve hücre membranının tahribine neden olmakta ve bakteri etkisiz hale gelmektedir. Pc'ler absorpsiyon yaptıkları dalga boyu, sistemler arası geçişte uzun süre kalabilmeleri ve yüksek miktarda reaktif oksijen türleri üretebilme kapasiteleri ile en çok kullanılan PS'ler arasındadır. Ayrıca Pc'ler uygun sentez stratejileri yardımıyla bakteri ile mücadelede katkı sağlayabilecek hidrofobik, hidrofilik yada katyonik grupları pek çok pozisyonlarında taşıyabilirler.

Bu tez kapsamında her biri farklı antimikrobiyal mekanizmaya sahip iki antimikrobiyal ajan (katyonik poli(oksanorbornen) ve ışığa duyarlı çinko ftalosiyanin) tek molekülde bir araya getirilmiş ve bu bileşenleri farklı miktarlarda içeren yapıların antibakteriyel özellikleri karşılaştırmalı olarak incelenmiştir.

Tezin birinci kısmında yan zincirlerlerinde *tert*-butil sübstitüe ZnPc içeren PON'lerin sentezi amaçlanmıştır. Bu amaç doğrultusunda ilk olarak "Polimer Bağlı Başlangıç Maddesi" yöntemi denenmiştir. Bunun için öncelikle oksanorbornen sübstitüe ftalonitril bileşiği sentezlenmiş (M1), bu bileşiğin ROMP metodu ile polimerizasyonu gerçekleştirilmiş (P1) ve ftalosiyanin içeren polimer (P2) molekülünün sentezi için P1 aşırı miktarda *tert*-butil sübstitüe ftalonitril bileşiği ile reaksiyona sokulmuştur. Fakat monomer ve başlangıç polimeri başarılı bir şekilde sentezlenip karakterize edilmesine rağmen (M1 ve P1), son ürünün ^{1}H NMR'ında karakteristik polimer piki görülememiş ve ftalosiyanin oluşum reaksiyonu sırasında polimer omurgasının korunamadığı anlaşılmıştır (P2). Bundan dolayı sentez stratejisinin değiştirilmesine ve "Ftalosiyanin İçeren Monomer" yönteminin kullanılmasına karar verilmiştir. Bu amaçla *tert*-butil sübstitüe ZnPc içeren oksanorbornen monomeri (M2) ilk defa, fosfonyum grupları içeren diğer oksanorbornen monomerleri (M3, M4) literatüre uygun olarak sentezlenmiştir. Daha sonra sadece M2 monomerini içeren homopolimer (P3) ve M2, M3 ve M4 monomerlerini farklı oranlarda içeren kopolimerlerin (P4-P7) sentezi ve karakterizasyonu gerçekleştirilmiştir. Tüm polimerlerin (P3-P7) (birinci seri) fotofizik ve fotokimyasal parametreleri ölçülmüş olup, gram-negatif *E. coli*, ve gram-pozitif *S. aureus* bakterilerine karşı aPDT aktiviteleri incelenmiştir.

Bunlara ek olarak, bakteri-polimer etkileşmesi taramalı elektron mikroskobu ile kanıtlanmıştır.

Tezin ikinci kısmında biyouyumluluğu arttırmak amacıyla *tert*-butil grupları yerine yan zincirlerlerinde PEG sübstitüe ZnPc içeren oksanorbornen monomeri (M5) sentezlenmiş ardından bu monomerin homopolimerinin (P8) ve M3 ve M5 monomerlerini farklı oranlarda içeren kopolimerlerinin (P9-P11) sentezi ve karakterizasyonu gerçekleştirilmiştir. Tüm polimerlerin (P8-P11) (ikinci seri) fotofizik ve fotokimyasal parametreleri ölçülmüş ve gram-pozitif bakteri olarak *B. subtilis*, gram negatif olarak yine *E. coli* kullanılarak aPDT aktiviteleri incelenmiştir. Ayrıca bakteri-polimer etkileşmesi floresans mikroskobu yardımıyla kanıtlanmıştır.

Anahtar Kelimeler: poli(oksanorbornen), halka açılma metatez polimerizasyonu, ftalosiyanin, antimikrobiyal fotodinamik terapi, makromoleküler fotosensitizer, singlet oksijen üretimi

1
INTRODUCTION

1.1 Literature Review

Bacterial infection and resistance of bacteria to antibiotics are major problems worldwide [1]. The rapid increase in bacterial resistance to antibiotics has made the development of new generation antibiotics a necessity [2]. Moreover, another area of research to prevent the spread of infectious diseases is the development of materials that can be used on antimicrobial surfaces that limit bacterial colonization [3]. Synthetic antimicrobial polymers have come out as an important class of macromolecules that can serve both of these research areas [4]. Although different antimicrobial action mechanisms have been proposed for amphiphilic polymers, it is thought that the electrostatic interaction between the negatively charged cell membrane of the bacteria and the cationic polymer, and the hydrophobic interaction between the tail groups of phospholipids in the cell wall and hydrophobic groups at polymer backbone provide a lethal effect. Therefore, it is important that antimicrobial polymers have positively charged and hydrophobic structures in terms of interaction with bacteria [5]. Even though there are numerous polymeric structures containing effective groups against bacteria in the literature, PONs have been studied intensively because of the achievements of imitating antimicrobial peptides.

Firat Ilker et al. investigated the effect of hydrophobic groups and molecular mass differences on antimicrobial activity by synthesizing amphiphilic water-soluble homopolymers with ROMP method. This study shows that hydrophobic-hydrophilic equilibrium and molecular mass play an important role in high selectivity and antimicrobial activity. In addition, copolymers that have high activity and nontoxic structures have been synthesized thanks to mixing monomers of active and toxic polymer (poly3) and inactive and nontoxic polymer (poly2) in a certain ratio (Figure 1.1) [6].

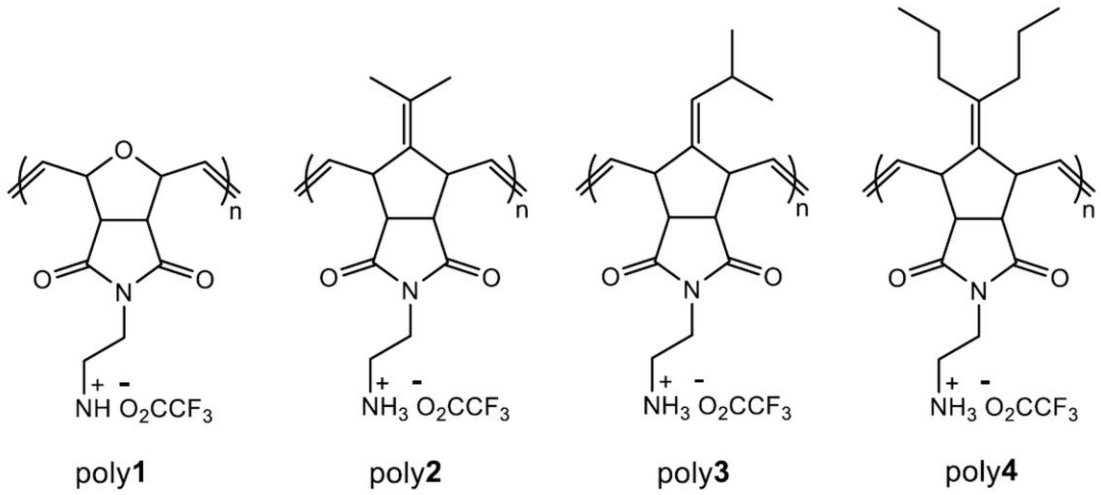

Figure 1.1 PNs with different hydrophobic groups [6]

In another study by Ceren Süer et al., amphiphilic PONs derivatives with different alkyl and aromatic phosphonium groups were synthesized. When the antimicrobial properties of the PON derivatives were examined, it was observed that the activities of the structures containing aromatic groups on the side chain were higher than those containing alkyl groups (Figure 1.2) [7].

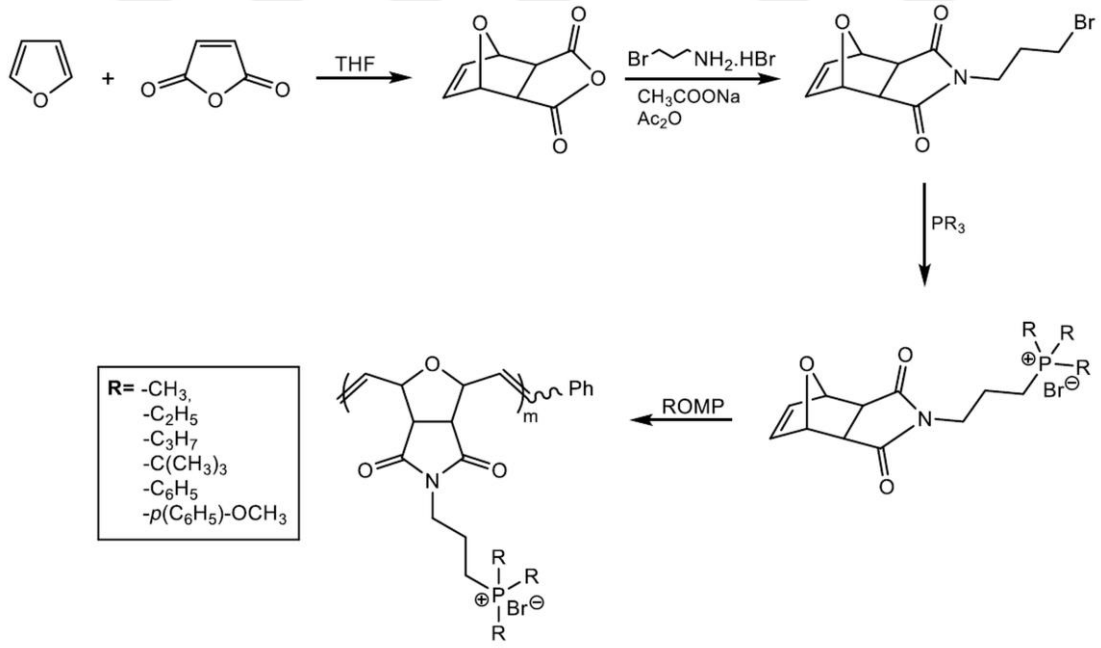

Figure 1.2 Synthesis of PONs derivatives containing different phosphonium groups [7]

Colak et al. have investigated the incorporation of hydrophilic and biocompatible groups into polymeric structures through copolymerization of suitable monomers or post-polymerization of related polymers. PEG moiety is one of them and it has been used to give the structure hydrophilic character, water solubility and biocompatibility. Antibacterial study of these polymers showed that as the hydrophilicity has increased, the activity has decreased owing to the overall charge reduction but biocompatibility increased (Figure 1.3) [8].

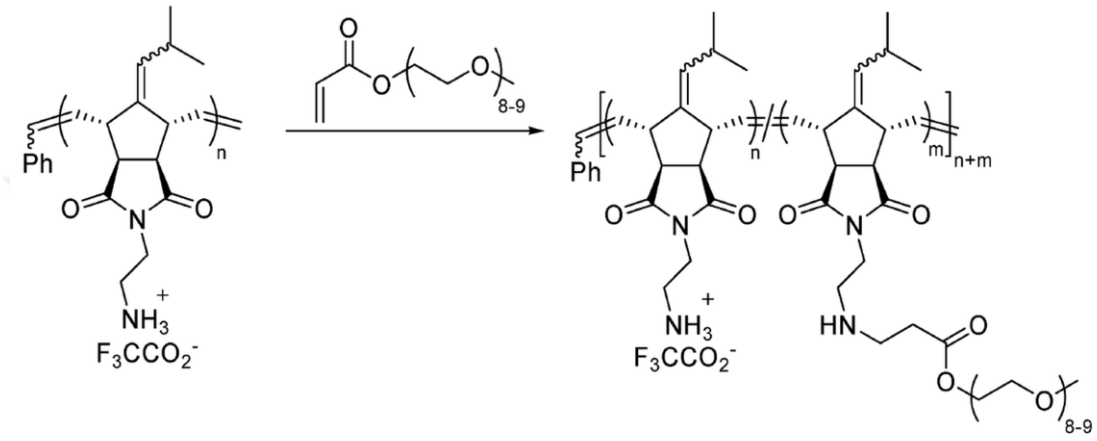

Figure 1.3 Synthesis of PNs derivative containing biocompatible PEG moiety [8]

On the other hand, aPDT has emerged as a significant alternative method to antibiotic treatment since it is hard to be developed resistance by bacteria [9]. Its action mechanism involves the interaction of light with the substances which is called PS and the resulting ROS interact with cellular components, causing damage and death of the bacteria [10, 11]. Within the scope of aPDT, Pcs are important molecules since they fulfill suitable properties (see Chapter 2.3) [12, 13].

In the study performed by Lin et al., AB_3-type asymmetric ZnPc containing triazatricyclodecane and quaternized derivative have been synthesized. The aPDT activities of these PSs against gram-positive and gram-negative bacteria have been investigated and the killing efficiency of PS which is containing the cationic group was found extremely high (99.99% killing) (Figure 1.4) [14].

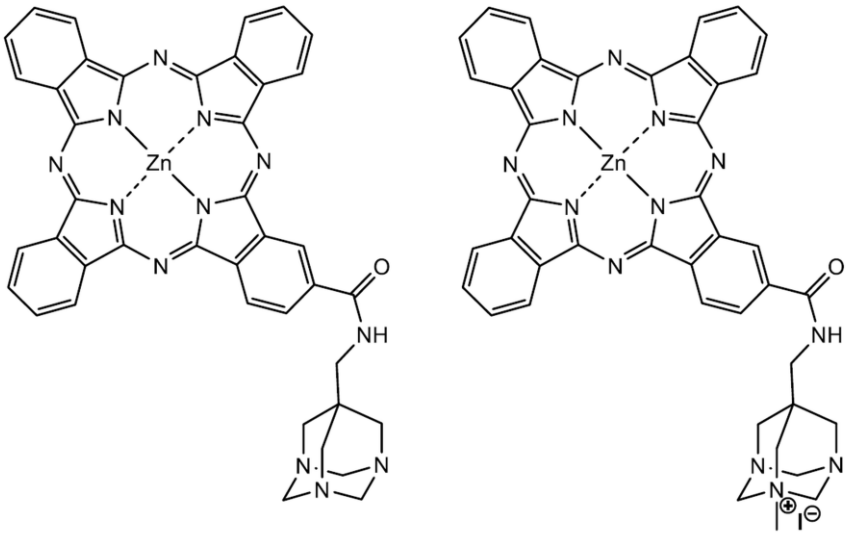

Figure 1.4 Asymmetric ZnPcs used in aPDT [14]

Veselin Kussovski et al. have examined the effect of changing the hydrophobic groups on the aPDT activity of Pcs. For this purpose, they have synthesized four different ZnPc containing alkylpyridyloxy groups of different hydrocarbon chain lengths. aPDT activities of these Pcs have been evaluated against gram-negative bacteria *A. hydrophila*. The study showed that the increase in hydrophilicity gives rise to higher accumulation capacity and aPDT activity (Figure 1.5) [15].

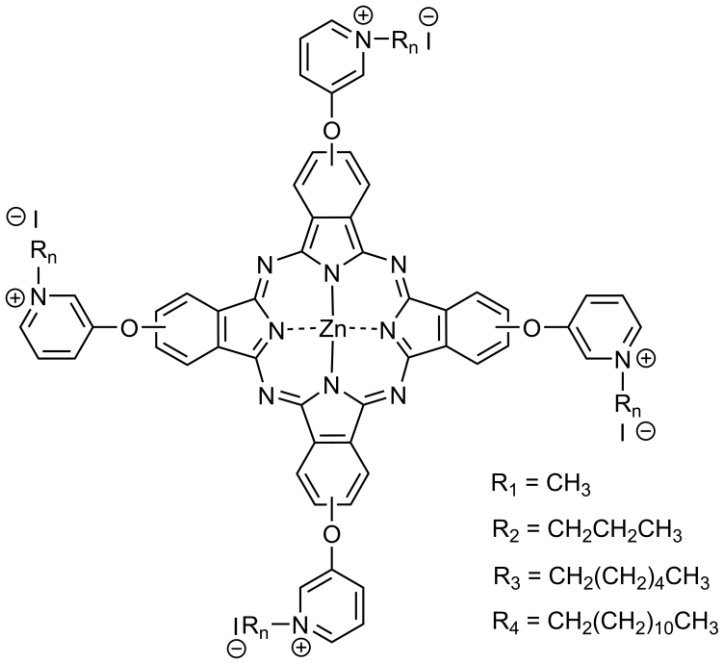

Figure 1.5 Symmetric ZnPc containing alkylpyridyloxy groups of different hydrocarbon chain lengths used in aPDT [15]

The other matter of interest is the introduction of a Pcs ring into macromolecular structures owing to the significant chemical and physical properties that both structures add to each other [16]. The importance of the combination of Pcs and polymers has shown itself in many studies thanks to the fact that Pcs can cause energy transfer as photoactive molecules and polymers can contain several functional units and have high chemical resistance [17, 18]. It is seen that although PPcs can be obtained by using different methods, sub-techniques of the side chain method are mostly preferred for synthesis of these type of structures in the literature (see Chapter 2.5).

In the study performed by Jian Zhang et al., a PPc has been synthesized with the help of a polymer-bound precursor sub-technique of side chain method (see Chapter 2.5.4). Firstly, methacryloyl chloride has been incorporated into the phthalonitrile compound and then polymerization of it has been achieved by RAFT. The desired PZnPc has been obtained by reaction between polymeric phthalonitrile and 4-(octyloxy)phthalonitrile in the presence of zinc acetate dihydrate (Figure 1.6) [19].

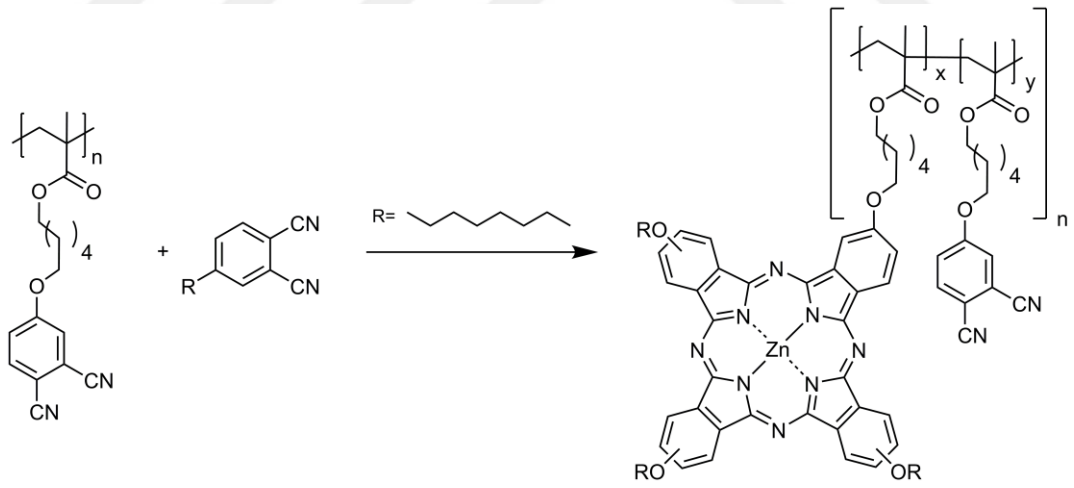

Figure 1.6 A PPc have been synthesized with the help of polymer-bound precursor technique [19]

On the other hand, ROMP has gained significance as a powerful tool for synthesizing polymers with different shapes, sizes, and functions. While the previous studies of ROMP are generally related to the polymerization of monocyclic olefins, subsequent works are carried out on bicyclic and polycyclic olefins, especially norbornene derivatives with high ring tension. High ring tension provides high polymerization amount and soft reaction conditions and offers great advantages to prepare materials that can exhibit interesting mechanical, electronic and biological properties [20, 21].

Although there are many studies using ATRP and RAFT in the synthesis of PPc with different chemical structures, ROMP has rarely been used [22-24]. While there are only a few studies in the literature in which PN and Pc are used together, there is no example except this thesis you are reading now in which PON and Pc are combined in one molecule.

One of the case studies where Pc and PN were used together belongs to Andres de la Escosura et al. They have synthesized PNs which are containing Pc and fullerene units by using Pc-containing monomer sub-technique of side chain method (see Chapter 2.5.4). For this, asymmetric Pc and fullerene-containing norbornene monomers were synthesized and polymerization was carried out through ROMP in good yields. It has been investigated whether there is electron transfer between donor Pc units and the fullerene acceptor units in copolymers and they can be used as materials for photovoltaic devices (Figure 1.7) [23].

In the literature, there are several studies on the photodynamic activities of polymeric structures which is consisting of a photoactive agent. While porphyrin or bodipy derivatives were introduced into the polymer backbone and their antibacterial properties were examined in some of them, the Pc molecule was combined with the polymer and its anticancer properties were examined in the others [25-27]. Although there are some studies which are reporting the antibacterial properties of Pc-containing polymers, they are very scarce.

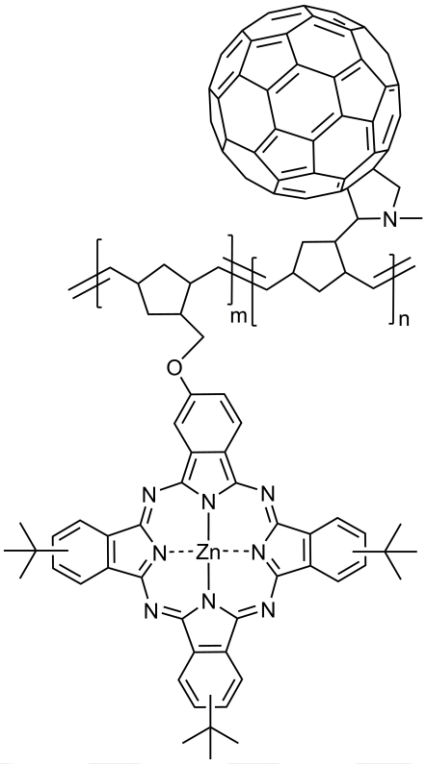

Figure 1.7 Structure of PN which are containing Pc and fullerene units as pendant [23]

In the study by Zhenlong Xu et al., star-shaped PZnPc containing DMAE groups in the arms have been successfully synthesized by RAFT polymerization. Then, the quaternization of the star polymer has been carried out and aPDT activities for the bacterial capture and bacteria-infected wound healing have been examined (Figure 1.8) [28].

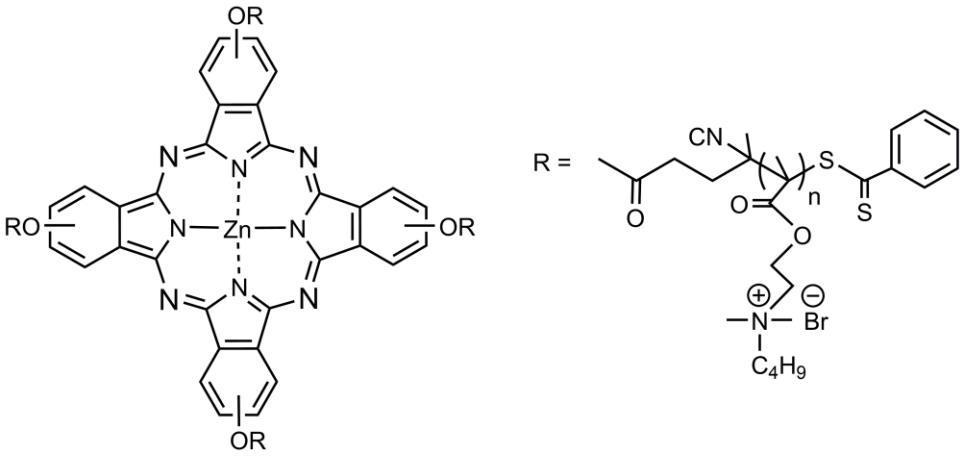

Figure 1.8 Chemical structure of star-shaped PZnPc containing DMAE groups in the arms [28]

In the study by Konstantin Strokov et al., hydrogel Pc which is composed of SiPc derivative and chitosan has been synthesized via carbodiimide-mediated amine coupling reaction. The aPDT activity of the compound has been examined against gram-negative and gram-positive bacteria (Figure 1.9) [29].

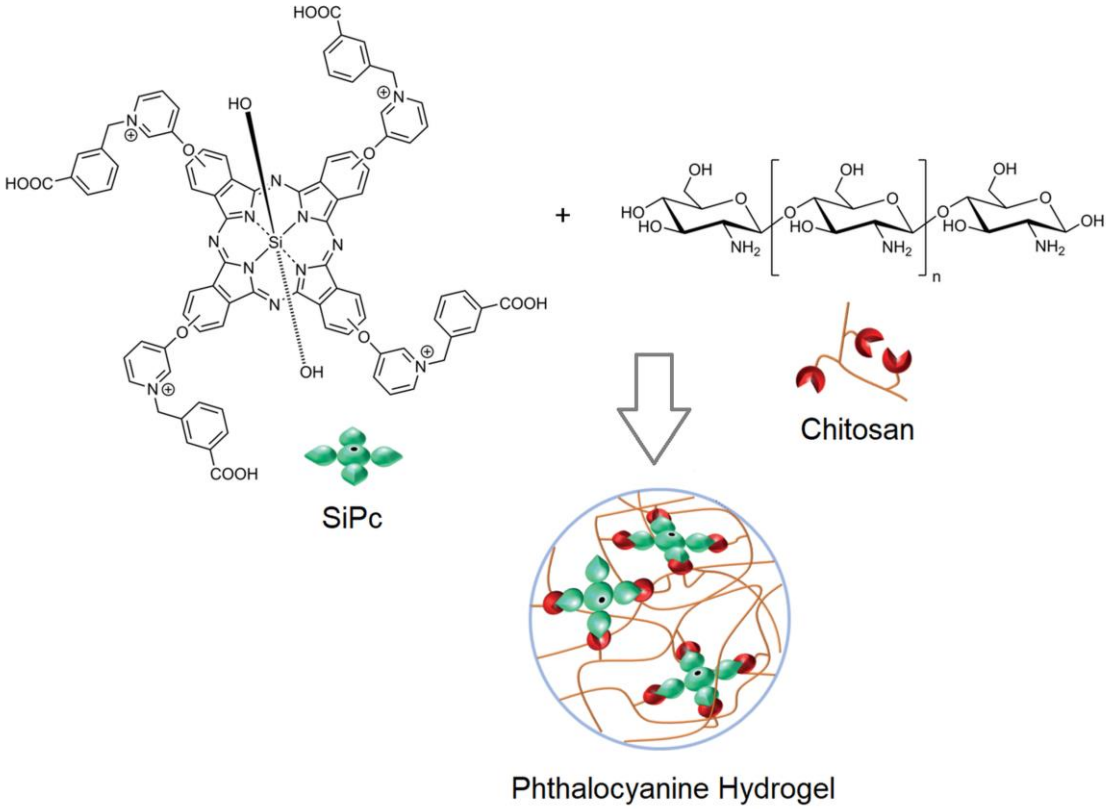

Figure 1.9 SiPc hydrogel containing chitosan [29]

In the study by Wei Tong et al., side chain PPc have been used while trying to obtain the target structure. The monoamine substituted ZnPc has been firstly synthesized and conjugation to poly(glycidyl methacrylate) is achieved via ROMP. Then, they reacted the remaining epoxy groups with excess ethylenediamine and provided dispersed the compound in aqueous solution. The aPDT activities of forming self-assembled nanoparticles have been studied extensively against *S. aureus* and *E. Coli* (Figure 1.10) [30].

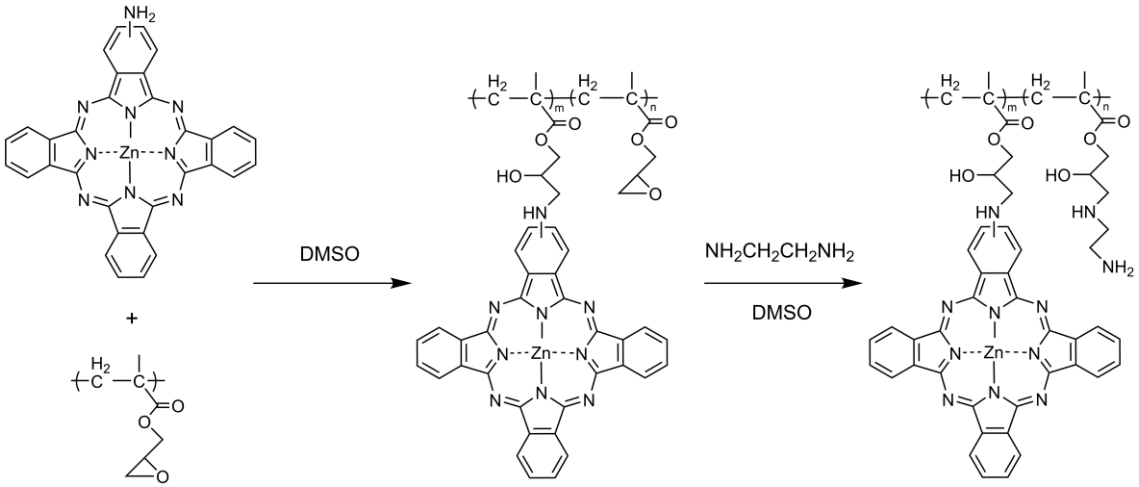

Figure 1.10 PZnPc example from literature prepared with side chain method [30]

1.2 Objective of the Thesis

In this thesis, it is aimed to bring together two molecules with different antimicrobial mechanisms. It is seen that PONs and Pcs containing suitable groups have antibacterial properties in the literature. The dual effect of these two agents when they meet in a single molecule is a matter of curiosity. Moreover, how the structure-activity relationship will change depends on the different ratios is among the questions to be answered. In line with these ideas, it was planned to synthesize Pc monomers with different substituents and oxanorbornene monomers containing cationic groups and converted them into polymers by ROMP method. By measuring the photophysical and photochemical parameters, potentials of substances were investigated and their aPDT activities against gram-positive and gram-negative bacteria were examined.

1.3 Hypothesis

Nowadays the design and synthesis of new alternative molecules to antibiotics, like antibacterial polymers, has become an important research topic due to the increasing bacterial resistance. PONs are extensively studied in this field as antibacterial agents because their monomers can be substituted with suitable groups in mild conditions and these monomers can be converted into polymers in controlled and efficient steps. On the other hand, Pcs have great interest as photoactive antibacterial agents thanks to their ability to carry a large number of

functional groups and produce ROS as a result of their interaction with light. Although there are various studies in the literature containing PS in the polymer backbone, there is no study related to PON containing Pc or any PS. In this thesis, for the first time, PON containing Pc was synthesized, and the synergistic antibacterial properties of polymers that contain two antimicrobial agents (cationic PON and PS ZnPc) were investigated.

2
GENERAL INFORMATION

2.1 Bacteria and Antibacterial Treatment

Bacteria are single-celled organisms with prokaryotic cell structures that are invisible to the naked eye but can be detected with a microscope [31]. Although bacteria are classified into many categories, the most used one is based on Gram Staining. While bacteria having a thick peptidoglycan layer and retaining the purple color of crystal violet is called “gram-positive”, bacteria having a thin peptidoglycan layer and losing crystal violet but retaining the pink/red color of counterstain safranine is called “gram-negative” [32, 33]. *B. subtilis* and *S. aureus* as gram-positive, *E. coli* and *S. typhimurium* as gram-negative are among the most well-known bacteria [34]. Even though most bacteria are harmless and even some of them are beneficial to the human body, the bacterial infection is one of the most common diseases in today’s world [1]. Especially gram-negative bacteria have become a serious threat to humankind since it is harder to deactivate them because of the additional hard and protective outer membrane, although their peptidoglycan layer is much thinner than that of gram-positive [35].

Antibiotics are the most important class of commonly used substances in the treatment and prevention of bacterial infections [36]. However, the overuse of antibiotics in recent decades has significantly led to antibiotic resistance [2, 37]. Bacteria has developed many strategies for deactivating antibiotics such as antibiotic degrading enzyme, antibiotic altering enzyme, antibiotic-efflux pump (Figure 2.1) [38]. On the other hand, antimicrobial peptides, which are another class of antibacterial agents, are natural antibiotics. These peptides are found in animals, plants and insects and they are part of the immune system. Their structures consist of short amino acid chains and carry amphiphilic character. They can show activity against gram-negative and gram-positive bacteria, fungi and some other organisms thanks to capable of killing microorganisms (biocidal) and preventing the growth and reproduction of microorganisms (biostatic) like

antibiotics [39]. In addition, they have a broad spectrum of action and do not cause bacterial resistance [40, 41]. Until now, numerous antimicrobial peptides have been isolated from natural organisms and synthetic mimics have been synthesized in vitro [42, 43].

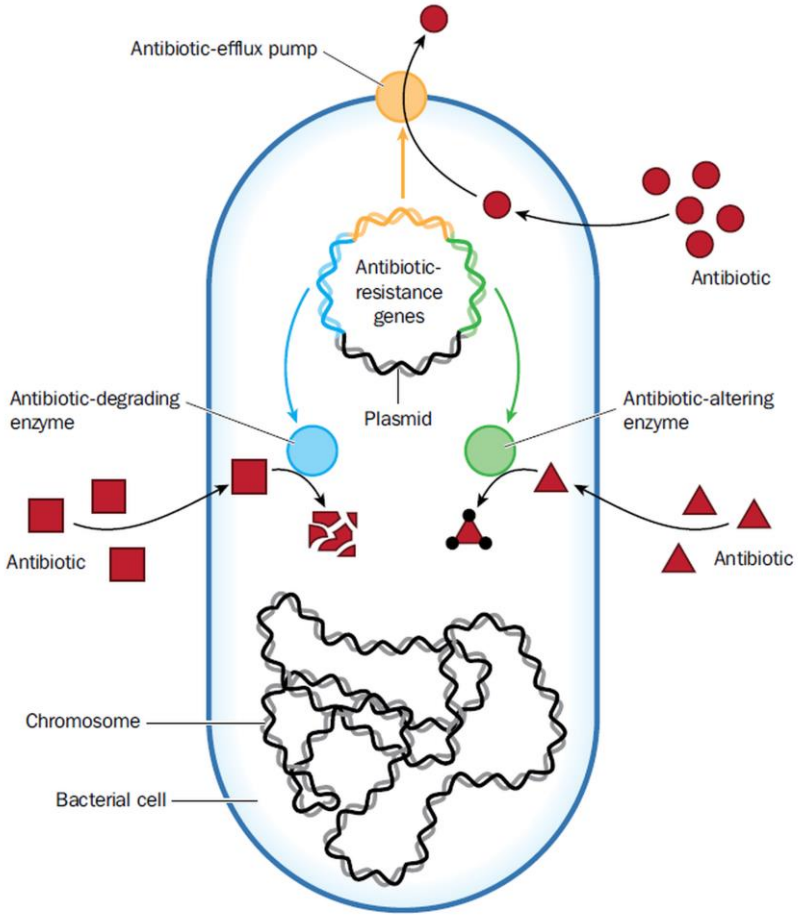

Figure 2.1 Strategies used by bacteria for inactivation of drugs [38]

Inspired by natural antimicrobial peptides, more active and less toxic antimicrobial synthetic polymers can be obtained. In addition to the therapeutic use of these substances, their use in food packaging, coating of catheter surfaces, hospital paints, textile materials and first aid equipment for protection from microbes has recently increased considerably. The facts that the synthesis of polymer structures is easy and cheaper, their structure can be functionalized according to the expected properties and their durability in ambient conditions show that they are more advantageous than peptides [40, 44, 45].

Although there are many antibacterial mechanisms for these peptides and polymers, the main interactions with bacteria are thought thanks to cationic and hydrophobic groups (Figure 2.2). While the cationic side electrostatically interacts with negatively charged cell membrane of the bacteria, the hydrophobic side interacts with tail groups of phospholipids in the cell wall. With these two phenomena, the dead is inevitable for bacteria [43, 44].

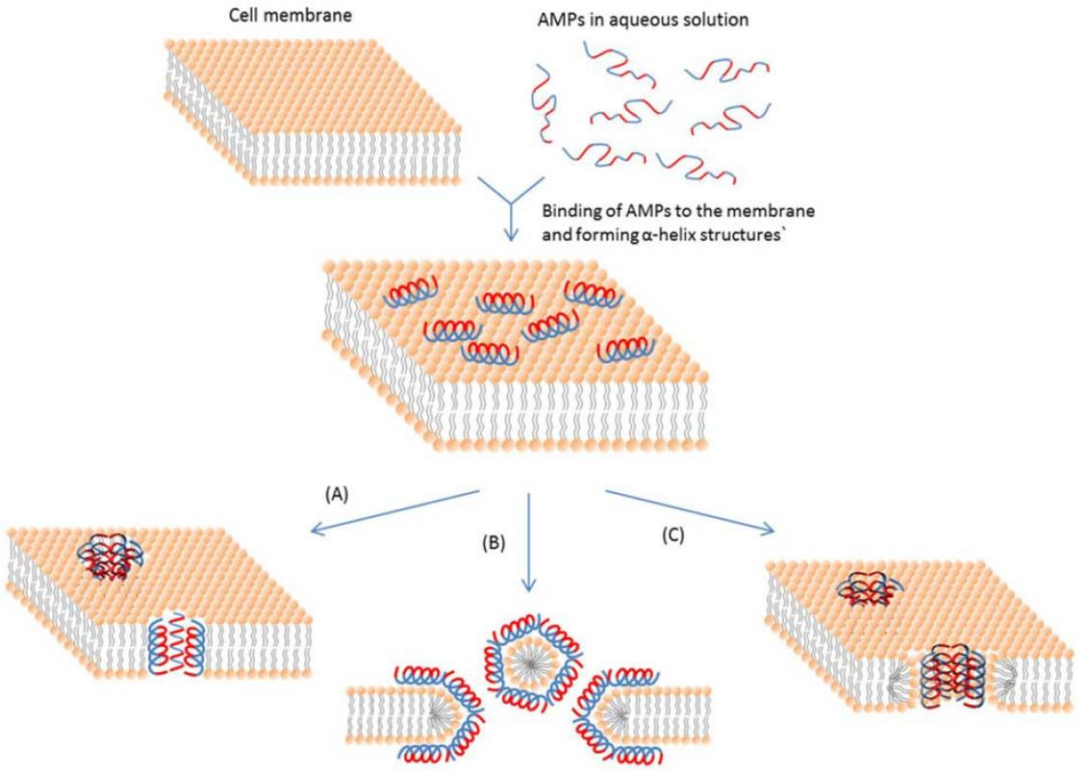

Figure 2.2 Some action mechanisms of antimicrobial peptides (A) Barrel-Stave model (B) Carpet model (C) Toroidal pore model [43]

2.2 Ring Opening Metathesis Polymerization and Poly(Norbornene)s

ROMP is one of the important controlled polymerization methods, in which chain growth polymerization takes place and cyclic olefins are converted to polymeric substances. The basis of this polymerization method consists of olefin metathesis (metal-mediated carbon-carbon double bond exchange process) [21]. Different transition metal complexes are used as catalysts in this process. The unsaturated bond of the monomer is broken by the effect of metal complexes, the ring is

opened and the polymer chain is formed which is containing new double bonds in the backbone. This is significant and distinctive characteristic property that apart ROMP from other olefinic polymerization methods [20].

The ROMP mechanism was proposed by Chauvin in 1970 [46]. Cyclic olefins coordinate to transition metal-containing alkylidene structures. This coordination is followed by [2+2] cycloaddition and cycloreversal reactions, and a new metal alkylide is formed (Initiation). Coordinating the monomer to the structure increases the size of the complex, but its activity towards cyclic olefins remains the same as that of the initiator. This allows the reaction to be repeated until all the monomer is used up and the desired polymer is obtained (Propagation). The polymerization is terminated by the external addition of the special reagent. This reagent removes the reactive metal tip at the end of the polymer and replaces it with a known functional group (Termination) (Figure 2.3) [20, 21, 46].

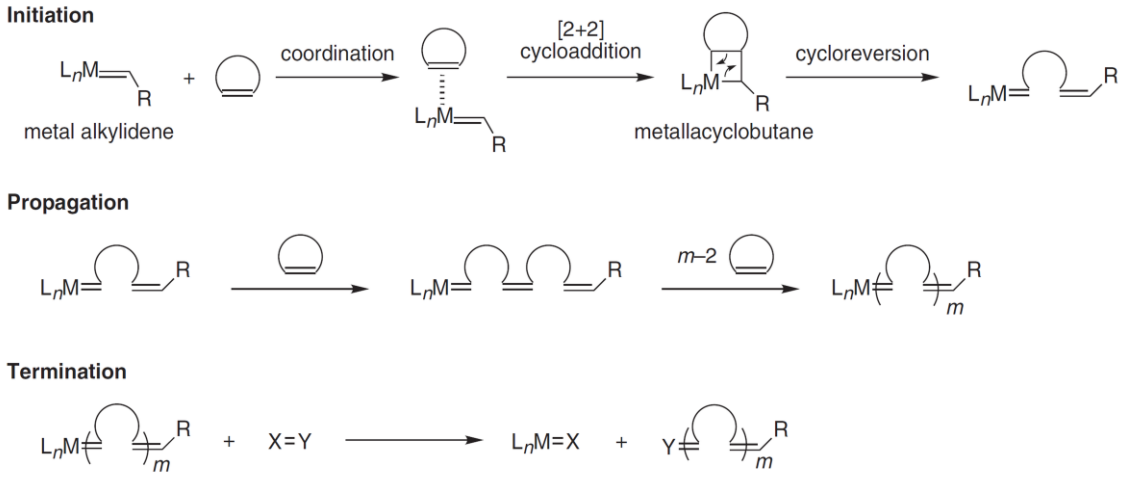

Figure 2.3 ROMP mechanism proposed by Chauvin in 1970 [20]

The basis of ROMP and the used metal catalysts goes back to the 1950s. Although there are many studies in the literature examining the effect of the catalysts on the ROMP, the most effective ones known; molybdenum complexes developed by Schrock et al. in 1993 and ruthenium-based complexes developed by Grubbs et al. in 1995 [47, 48]. Especially, Grubbs catalysts are preferred due to their selectivity to the olefinic group, being more resistant to ambient conditions like air and humidity, and being compatible with various solvents. Based on the $RuCl_2(PPh_3)_3$ structure, the first ruthenium transition metal-containing metathesis catalyst was

synthesized and this substance became a pioneer in the development of other derivatives (Figure 2.4) [49]. Robert H. Grubbs, Richard R. Schrock and Yves Chauvin were awarded the Nobel Prize in Chemistry in 2005 for “the development of the metathesis method in organic synthesis".

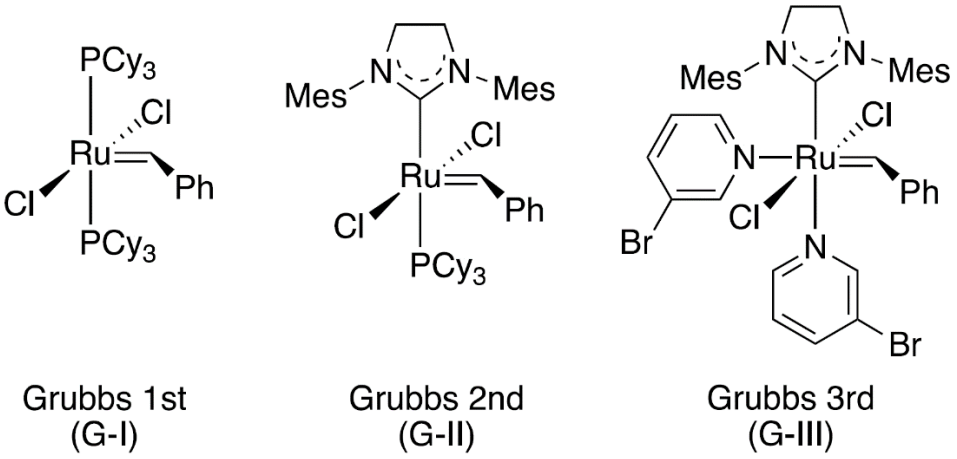

Figure 2.4 Grubbs catalyst derivatives [50]

Previous studies of ROMP are generally related to the polymerization of monocyclic olefins. However, subsequent works are carried out on bicyclic and polycyclic olefins, especially norbornene derivatives with high ring tension. High ring tension provides high polymerization amount and soft reaction conditions. For instance, while the ring tension of cyclohexene is 1.4 kcal/mol, that of norbornene is 27.2 kcal/mol and it can polymerize quickly and easily with many metal catalysts (Table 2.1). Another reason for preferring norbornene compounds as monomers is that they can be easily turned into desired derivatives by different organic reactions [40, 51].

Table 2.1 Strain energies of some cyclic olefins [40]

Olefins	Strain Energies (kcal/mol)	Olefins	Strain Energies (kcal/mol)
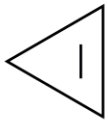	53.7	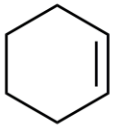	5.9
	29.8	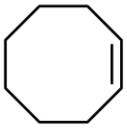	6
	5.9		27.2

2.3 Antimicrobial Photodynamic Therapy

All applications in which ultraviolet, visible or near-visible light is used therapeutically are called PDT. The fundamental of PDT is based on the fact that ROS, which is formed as a result of the activation of the substance called PS with light in the presence of molecular oxygen, interact with many biological molecules. PDT is mostly used in the treatment of acne, a common skin problem, and one of the biggest health problems of our time; cancer [11, 52].

However, nowadays, one PDT derivative which has existed since the 1990s has gained a lot of importance due to the increasing resistance of bacteria to antibiotics; aPDT. The fundamental process contains three main steps: (i) When the PSs are exposed to the light with the appropriate wavelength (usually red light), they transition from the ground state (S_0) to the first excited state (S_1) (ii) This unstable excited singlet state can cause the transition to excited triplet state (T_1) via intersystem crossing (iii) The PS in the triplet state transfers the excess energy from its structure to the surrounding molecules by two different types of mechanisms. When the PS generates radicals, such as hydrogen peroxide (H_2O_2), the superoxide anion radical ($O_2^{\cdot-}$), or hydroxyl radicals ($OH^{\cdot}$); this reaction is called a Type I reaction. The reaction in which the PS creates singlet oxygen by directly transferring its energy to molecular oxygen is called Type II reaction.

Lately, in the study Hamblin et al., the new mechanism containing oxygen-independent photoinactivation is described as a Type III mechanism. ROS leads to protein dysfunction, DNA damage, cell membrane disruption and provide photoinactivation of bacteria. This approach has many advantages over others, such as activity against resistant bacteria, short treatment times, and simple application (Figure 2.5)[53-56].

The most important and changeable factor that can contribute to activity of aPDT is the properties of the PSs. Ideal PS should have sufficient ROS generation, long triplet lifetime, negligible dark toxicity, good photostability, and biocompatibility. Moreover, absorbing light in the appropriate wavelength and having a high extinction coefficient are important requirements for a PS, which needs the ability of high tissue penetration. Chlorines, Porphyrins, BODIPYs and Pcs are among the some PS examples with suitable properties [54, 57, 58].

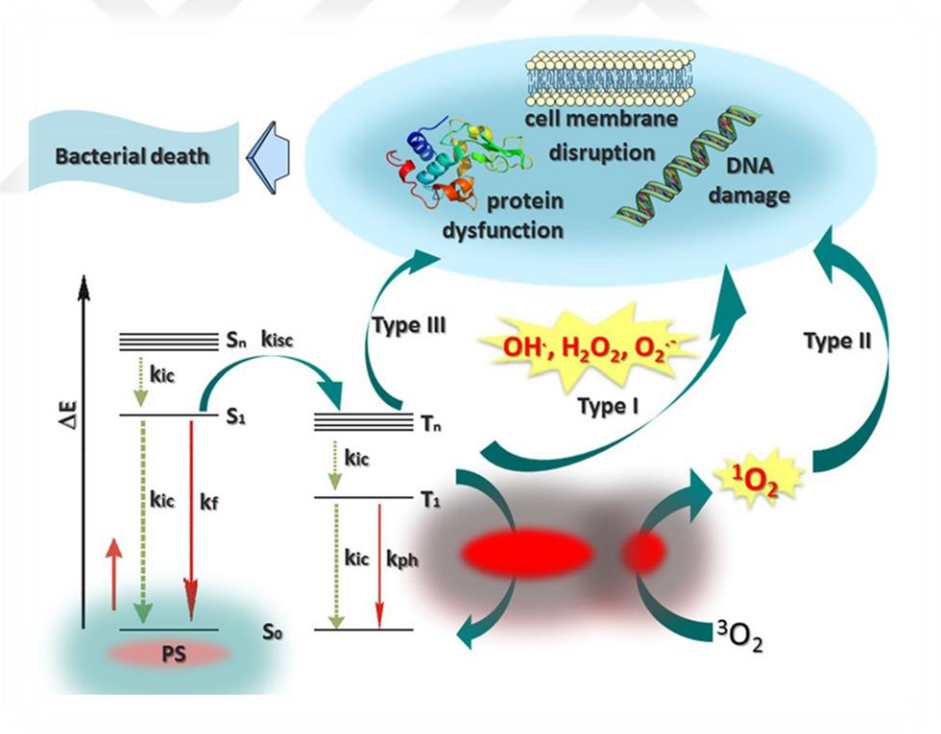

Figure 2.5 Jablonski diagram showing the aPDT mechanism [54]

2.4 Phthalocyanines

Pcs are tetrapyrrole derivative macrocyclic aromatic compounds that contain four isoindole units connected at 1,3-positions by aza bridges. They have planar structure, 18 π-electron system and the ability to bind more than 70 metal and semimetal cations in the periodic table instead of the two hydrogen atoms in their core [59-61]. Pcs were first synthesized as a blue-colored by-product by researchers named Braun and Tscherniac in 1907 by chance, and their structures were lightened thanks to the studies of Linstead and Robertson's X-ray diffraction analysis in 1933 [62, 63].

After the understanding of their structures, synthesis methods began to develop gradually and it was understood that Ps could be modified for appropriate purposes. While the positions of 2, 3, 9, 10, 16, 17, 23, 24 are called peripheral (β) and the positions of 1, 4, 8, 11, 15, 18, 22, 25 are called non-peripheral (α). They can be substituted in a total of 16 positions with eight peripheral and eight non-peripheral (Figure 2.6). Synthesis of Pcs can be carried out by the cyclotetramerization reaction of starting materials such as phthalic anhydride, diiminoisoindoline and phthalonitrile. Since it is more economical, phthalic anhydride derivatives are mostly preferred industrially in the production of Pc compounds. However, in scientific research, the most used starting compound is phthalonitrile derivatives (1,2-dicyanobenzene) because the reaction yields are much better and the possibility of forming by-products is very low [59-62].

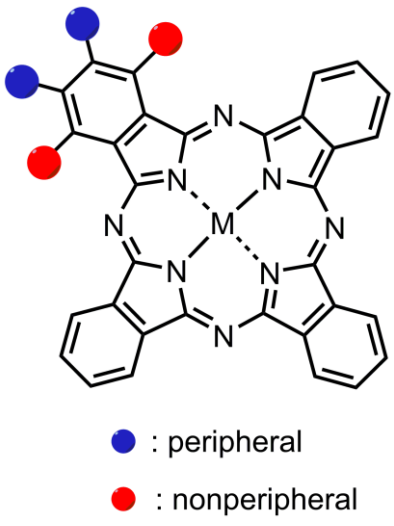

Figure 2.6 Substitution points of Pcs

The starting compounds are substituted according to the positions at which Pc is desired to be functionalized. By using a single phthalonitrile compound, the structure, in which all isoindole units contain the same substituents, can be obtained and this is called “SymPc”. On the other hand, if two different phthalonitrile compounds are used, “AsymPc” can be obtained which has isoindole units with different substituents. High temperature, a suitable solvent and a base source are needed for the synthesis of both types of Pcs (e.g., 150 °C, pentanol, DBU). However, if the solvent already has a basic character, the reaction can be carried out with only solvent (e.g., 140 °C, DMAE). Moreover, the synthesis of MPc can be achieved via the addition of metal salt to the reaction mixture. Column chromatography is an essential purification step in obtaining both SymPc and AsymPcs as pure substances [64, 65].

Pcs are very significant components that can be used in many applications such as liquid crystals, nonlinear optic, molecular magnets, solar cells, gas sensors, batteries, organic thin-film transistors and electrocatalytic reduction due to their stable structure, chemical, physical and optical properties [64-66]. In addition, they can exhibit photodynamic anticancer and antibacterial activity thanks to their long absorption wavelength maxima (650–800 nm)(Figure 2.7), high extinction coefficient ($\varepsilon \sim 2\times10^{5}$ $M^{-1}cm^{-1}$), long triplet lifetime, and high ROS generation. These properties make them one of the most used PS. However, a drawback of Pcs is the low solubility in aqueous media. This arises from its unsubstituted core which has extreme hydrophobic and planar structure, leading to the formation of aggregates and deterioration of the parameters. This disadvantage hinders the activity of the Pcs as PS. Nevertheless, this challenge can be overcome by different strategies. While Pcs can be modified up to 16 substituents with water-soluble hydrophilic groups, on the other hand, it can be taken advantage of properties as Ps by incorporating them into different structures such as micelles and polymers. It should not be forgotten that the design and synthesis of Pc with different substituents requires a meticulous and skillful effort because it is important to find the correct hydrophobic-hydrophilic balance [9-13].

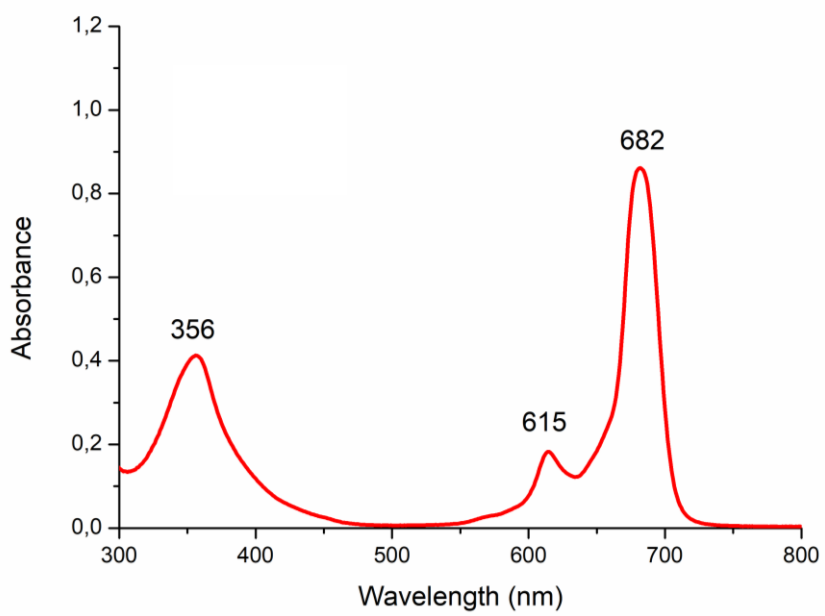

Figure 2.7 An example to typical UV-vis spectrum of MPcs

2.5 Polymeric Phthalocyanines

The incorporation of a Pc ring into macromolecular structures has been a matter of curiosity due to the important chemical and physical properties it can contribute to the polymers. Firstly, the presence of π-electrons in the ring system and d-electrons belonging to the central metal ion which can cause electron transfer are their main features. Secondly, electron or energy transfer can be provided under irradiation with visible light. With all these features, combinations of Pc and macromolecules can be used in many areas such as electrical conductivity and photoconductivity, electrocatalytic and photocatalytic reductions/oxidations, electrochemical charge/discharge, metal ion sensor and PDT. PPc can be classified based on the formation type of the macromolecule as network, hydrogel, main chain, side chain and star shaped [16, 18, 67-69].

2.5.1 Network Phthalocyanines

Network is a chemical compound in which the atoms or molecules are bonded by covalently and repeated themselves through in a 2D or 3D stucture. In a network, there are no individual molecules, and the entire crystal or amorphous solid is considered a macromolecule [70-72]. For a Pc network, a bifunctional

starting material is required such as bis(phthalanhydride) or bis(phthalonitrile) containing two pairs of ortho-nitrile groups. The desired products can be obtained by reacting these derivatives with related metal salts under Pc formation conditions (Figure 2.8) [16, 73, 74].

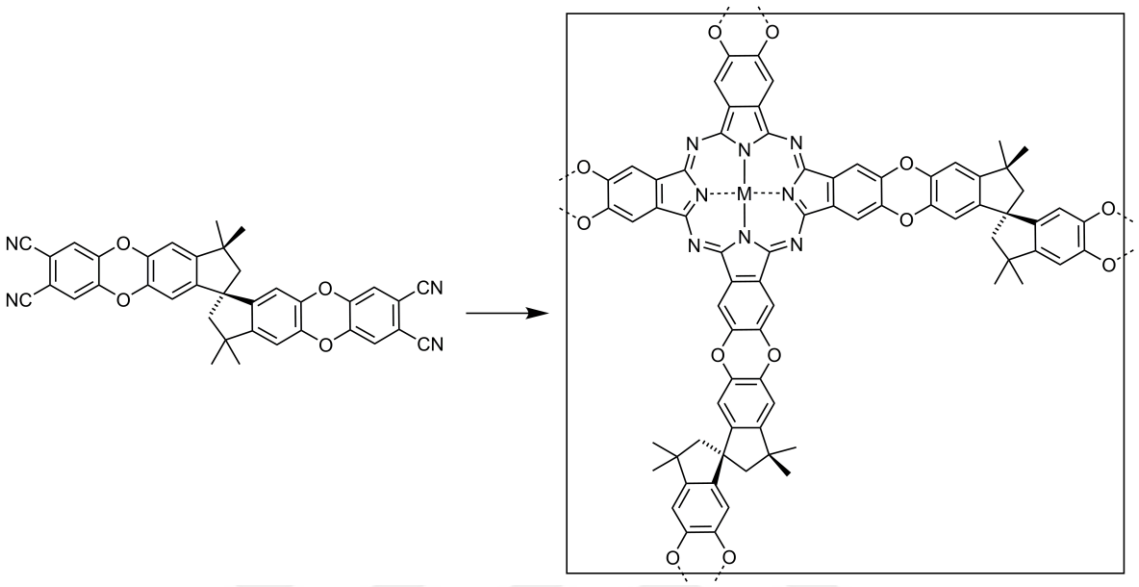

Figure 2.8 Synthesis of network PPc [67]

2.5.2 Hydrogel Phthalocyanines

Hydrogels are the type of polymeric networks which have both hydrophilic groups and cross-linked bonds in their structure. They aren't soluble in water but, they have the ability to swell with water. While their water-absorbing ability originates from hydrophilic functional groups connected to the polymeric backbone, they resist being dissolved in water because of the cross-linked bonds in the network [75, 76]. Hydrogels can be prepared via two methods; i) physical interactions (electrostatic or hydrophobic interactions ii) dynamic covalent bonds. A Pc hydrogel can be obtained by reaction between symmetrical Pc derivative and hydrophilic biopolymer which are both have functional end groups. The formation of the hydrogel can be achieved via different synthesis strategies such as Schiff-base reaction and carbodiimide-mediated amine coupling reaction (Figure 2.9) [29, 77-79].

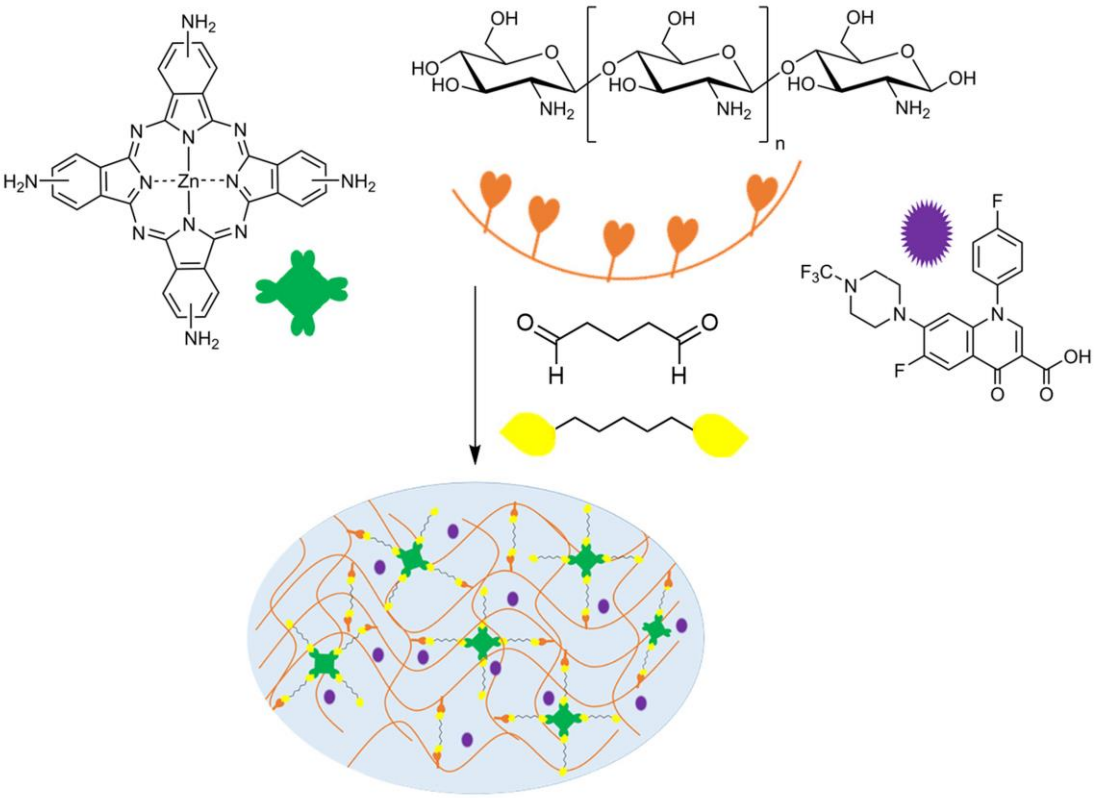

Figure 2.9 Preparation of ZnPc hydrogel containing chitosan and difloxacin [77]

2.5.3 Main Chain Polymeric Phthalocyanines

The polymer chain or simply backbone defines the main chain of a polymer that is consisting of elements that repeat themselves in a certain order. Polymers are frequently categorized concerning the elements in the main chains. While most of main chain of polymers have composed of carbon as in examples such as polyethylene and polystyrene, some of them have additional oxygen and nitrogen atoms in their backbones e.g. polyesters and polyamides [80-82]. In the main chain PPcs, the repeating element, or with the more accurate expression, “repeating unit” is the Pc itself. Obtaining a main chain PPc requires a bifunctional Pc monomer that has A_3B or A_2B_2 unsymmetrical structure (Figure 2.10) [16, 83, 84].

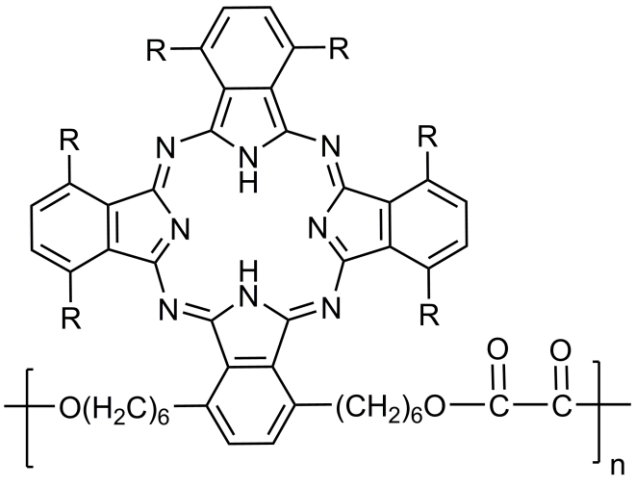

Figure 2.10 Chemical Structure of main chain PPc [84]

2.5.4 Side Chain Polymeric Phthalocyanines

Side chain is defined as chemical group that is connected to a core of a polymer backbone. It has different constitutional or configurational properties that depart from those in the main chain. A side chain molecule is also known as “pendant group” which refers the molecules’ appearance of resulting polymer [85, 86]. Three different strategies are available to synthesize the side chain Pc polymers; i) Grafting Pc onto a preformed polymer ii) The use of polymer-bound precursor iii) Polymerization of Pc containing monomer.

The first method needs two precursors; polymer backbone with functional groups that are shared along the whole chain and Pc with a functional end group. The formation of the graft polymer is achieved by the suitable reactions between these preformed compounds [16, 87, 88]. In the second method, a diiminoisoindoline or phthalonitrile compound (B) is bound to a polymer and reacted with the excess amount of different diiminoisoindoline or phthalonitrile (A) to form a Pc. It is assumed that the resulting mixture contains symmetrical Pc (A_4) and asymmetrical Pc (A_3B). Considering the solubility and chromatographic properties, symmetric Pc (A_4) is removed by washing or column chromatography method and PPc is obtained [16, 89]. The first and second methods have many difficulties like as the possibility of crosslinking and forming an insoluble polymer. Hence, it is considered that the third method, in which a Pc molecule with a polymerizable substituent is used, is the healthiest method to obtain side chain Pc polymer.

Obtaining PPc with this method requires a monofunctional Pc monomer which has A_3B unsymmetrical structure (Figure 2.11) [16, 22-24].

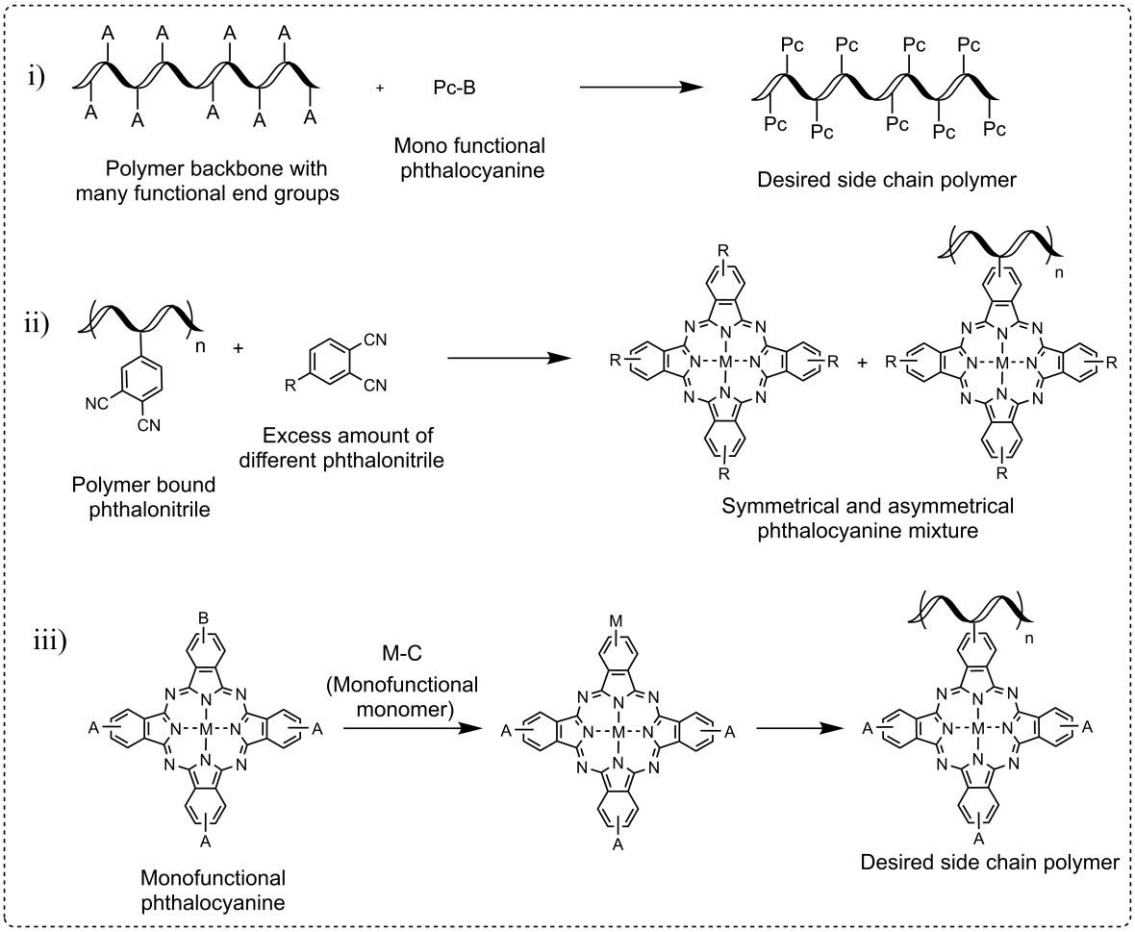

Figure 2.11 Synthesis strategies of the side chain PPcs

2.5.5 Star-Shaped Polymeric Phthalocyanines

The polymers in which secondary polymer chains are attached to a primary backbone are called “Branched Polymers” and star, H-shaped, pom-pom, and comb-shaped polymers can be given as examples for this category. The simplest class of branched polymers is star polymers. They have a number of linear chains or “arms” connected to a central core that was mentioned in the branched polymer’s definition as the primary backbone. While the core can be an atom, molecule and macromolecule, the arms can consist of many organic chains with changeable properties and lengths. Pc can be part of the star-shaped polymeric structures as a “core” [86, 90, 91].

The most widely used method to obtain a star-shaped PPc is the synthesis of a “Pc Initiator" containing a convenient group that can start the preferred polymerization reaction. Many different Pcs can be synthesized according to the number of substituents of starting compounds such as tetra, octa and hexadeca substituted. Hence, the number of substituents of Pc determines the number of arms of the star polymer (Figure 2.12) [66, 92-96].

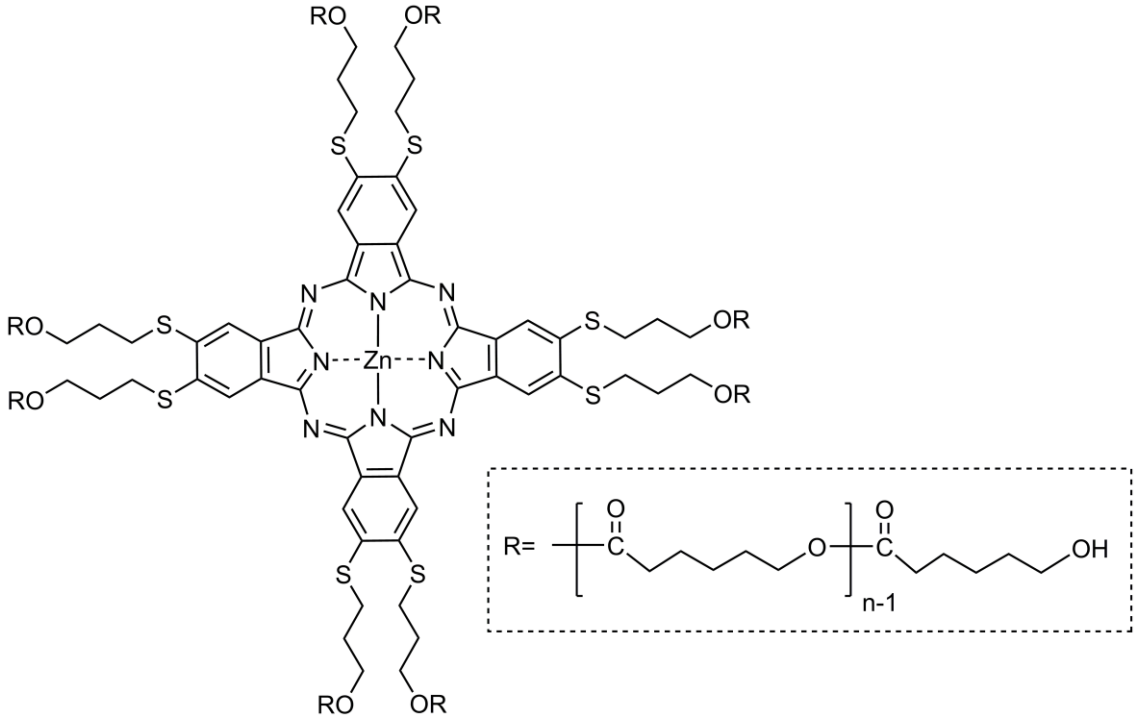

Figure 2.12 Structure of star-shaped PZnPc containing poly(ε-caprolactone)s in the arms [92]

3
EXPERIMENTAL PART

3.1 Materials

All reagents and solvents were obtained from commercial suppliers. 4-nitrophthalonitrile, 4-*tert*-butyl phthalonitrile, 1,3-diphenylisobenzofuran (DPBF), 9,10-anthracenediyl-bis(methylene)dimalonic acid (ADMA) were purchased from Sigma-Aldrich. Hydroxyl substituted oxanorbornene, hydroxy phenoxy substituted phthalonitrile (1), tosylated oxanorbornene (4), triphenyl phosphonium substituted oxanorbornene (M3) and triethyl phosphonium substituted oxanorbornene (M4) were synthesized according to the published procedures [7, 97, 98]. Phosphate-buffered saline (PBS) solution (pH 7.4) was prepared using Na_2HPO_4 and KH_2PO_4 in ultra-pure Millipore water. *B. subtilis* (DB104), *S. aureus* (ATCC 25923) and *E. coli* (ATCC 25922) were taken from Davies Diagnostics.

3.2 Instruments

Thermo Scientific iS10 FT-IR was used to record FT-IR spectra. Shimadzu UV-2450 was used to measure electronic spectra. Agilent VNMRS 500 MHz spectrometer was used to record NMR spectra. Mass spectra were measured on a Bruker Microflex LT MALDI TOF-MS. Varian Eclipse spectrofluorometer was used to measure fluorescence emission spectra. Time correlated single photon counting setup (TCSPC) was used to calculate fluorescence lifetimes. Laser flash photolysis system was utilized to obtain triplet quantum yield values. Niello LED Grow light (UFO) light source (150W and 300W) was used for photo-irradiations. Zeiss EVO MA 10 and Zeiss Axio Observer 7 were used to record SEM and fluorescence images, respectively.

3.3 Synthesis of Compounds

3.3.1 Unsymmetrical *tert*-butyl Substituted Zinc(II) Phthalocyanine (3)

In DMAE (4 mL), $Zn(CH_3COO)_2$ (97 mg, 0.529 mmol), 4-(4-hydroxyphenoxy)phthalonitrile (1) (100 mg, 0.423 mmol) and 4-*tert*-butyl phthalonitrile (2) (312 mg, 1.69 mmol) were stirred at reflux for 24 h. After cooling, the crude product was precipitated in water and filtrated. The purification was achieved by silica gel chromatography (Hexane/THF 4:1 to 2:1) yielding 3 as a blue solid. Yield: 70 mg (19%). **FT-IR** υ_{max} (cm^{-1}): 3255.51, 3069.45, 2955.01, 2864.96, 1714.68, 1660.01, 1610.72, 1505.96, 1487.49, 1390.80, 1362.46, 1331.19, 1282.10, 1256.44, 1218.49, 1198.99, 1150.60, 1087.08, 1045.60, 964.14, 939.49, 921.52, 872.68, 828.13, 762.50, 745.70, 690.88, 671.94. **UV/Vis** (THF): λ_{max}/nm = 673, 607, 349 nm.

3.3.2 PEG Substituted Phthalonitrile (5)

4-nitrophthalonitrile (0.400 g, 2.31 mmol) and tetraethyleneglycol monomethyl ether (0.962 g, 4.62 mmol) were taken into a 50 mL flask and dissolved with 8 mL of DMF. The reaction mixture was stirred at room temperature for 24 hours after K_2CO_3 (1.280 g, 9.24 mmol) was added under nitrogen atmosphere. The resulting mixture was poured into ice-water, and extracted with ethyl acetate. It was dried with Na_2SO_4, filtered and the organic phase was evaporated. The final substance was dried in a vacuum oven at 40 °C. An oily light green substance 5 was obtained. Yield: 0.56 g (73%). **FT-IR** υ_{max} (cm^{-1}): 3077.12, 2915.63, 2229.39, 1596.46, 1561.88, 1491.74, 1454.23, 1349.46, 1319.97, 1254.84, 1199.75, 1095.97, 1043.86, 966.07, 842.28, 729.36, 525.81. **MALDI-TOF MS**, dithranol: m/z calcd.: 334.370; found: 373.483 $[M+K]^+$, 357.518 $[M+Na]^+$. **^{1}H NMR** (500 MHz, $CDCl_3$): δ 7.71 (d, 1H), 7.31 (d, 1H), 7.24 (dd, 1H), 4.22 (t, 2H), 3.88 (t, 2H), 3.70 (t, 2 H), 3.65 (m, 8H), 3.54 (t, 2H), 3.37 (s, 3H) ppm. **^{13}C NMR** (126 MHz, $CDCl_3$): δ 162.02, 135.15, 119.84, 119.57, 117.32, 115.66, 115.25, 107.35, 70.59, 70.49, 69.21, 68.68, 59.00 ppm [99].

3.3.3 Oxanorbornene Substituted Phthalonitrile Monomer (M1)

Hydroxyl substituted oxanorbornene (0.2 g, 0.895 mmol) and 4-nitrophthalonitrile (0.129 g, 0.746 mmol) were taken up in a 50 mL flask and dissolved with 8 mL of DMF in a nitrogen atmosphere. The reaction mixture was stirred for 6 days at room temperature after the addition of K_2CO_3 (0.495 g, 3.58 mmol). The resulting yellow-brown mixture was poured into ice-water and filtered. Dried in a vacuum oven at 40 °C. The product was purified by column chromatography first using DCM followed by DCM:CH_3OH solvent mixture (80:1) yielding M1 as a yellow solid. Yield: 0.16 g (61%). **FT-IR** υ_{max} (cm^{-1}): 3060.51, 3040.63, 2958.57, 2231.37, 1769.09, 1690.59, 1598.93, 1560.72, 1489.53, 1469.94, 1435.28, 1400.39, 1367.33, 1347.99, 1308.91, 1286.11, 1255.98, 1235.83, 1219.59, 1182.50, 1156.31, 1125.79, 1093.13, 1017.30, 956.88, 918.38, 880.33, 853.78, 838.96, 812.38, 801.65, 771.16. **^{1}H NMR** (500 MHz, $CDCl_3$), δ 7.72 (d, 1H), 7.25 (d, 1H), 7.17 (dd, 1H), 6.53 (s, 2H), 5.23 (s, 2H), 4.03 (t, 2H), 3.73 (t, 2H), 2.87 (s, 2H), 2.15 (m, 2H) ppm. **^{13}C NMR** (126 MHz, $CDCl_3$), δ 176.19, 161.78, 136.48, 135.19, 119.59, 119.31, 117.44, 115.66, 115.23, 107.43, 81.03, 66.09, 47.39, 35.52, 26.87 ppm.

3.3.4 Unsymmetrical *tert*-butyl Substituted Zinc(II) Phthalocyanine Monomer (M2)

3 (160 mg, 0.187 mmol), tosylated oxanorbornene (4) (156 mg, 0.413 mmol), KI (68 mg, 0.413 mmol) and K_2CO_3 (103 mg, 0.749 mmol) were stirred in DMF (15 mL) at room temperature for 6 days. The crude product was precipitated in water. it was filtered and dried in vacuum yielding M2 as a blue solid. Yield: 170 mg (85%). **FT-IR** υ_{max} (cm^{-1}): 3065.15, 2953.07, 2864.90, 1772.27, 1692.43, 1611.82, 1502.19, 1487.66, 1391.87, 1362.50, 1331.33, 1281.86, 1255.21, 1215.87, 1199.34, 1181.31, 1150.47, 1086.22, 1045.03, 1025.42, 939.19, 919.57, 875.59, 854.18, 827.15, 762.23, 745.73, 691.61, 671.81. **UV/Vis** (THF): λ_{max}/nm = 673, 607, 349 nm. **MALDI-TOF MS**, α-cyano-4-hydroxycinnamic acid: m/z calcd.: 1059.54; found: 1059.066 $[M]^+$, 991.930 [M-furan]$^+$. **^{1}H NMR** (500 MHz, $CDCl_3$ + a few drops DMSO-d_6), δ 9.54-9.28 (m, 8H), 8.25-8.20 (m, 3H),

7.76 (m, 1H), 7.31 (d, 2H), 7.03 (d, 2H), 6.50 (s, 2 H), 5.28 (s, 2H), 4.04 (m, 2H), 3.77 (m, 2H), 2.87 (s, 2H), 2.14 (m, 2H), 1.75 (m, 27H) ppm.

3.3.5 Unsymmetrical Zinc(II) Phthalocyanine Monomer (M5)

4-(4-hydroxyphenoxy)phthalonitrile (19.31 mg, 0.081 mmol), 4-((2,5,8,11-tetraoxatridecan-13-yl)oxy)phthalonitrile (4) (246 mg, 0.735 mmol), $Zn(CH_3COO)_2$ (37.49 mg, 0.204 mmol) and a few drops of DBU were stirred at the reflux temperature of 3 mL hexanol for 4 hours. The reaction mixture was poured into hexane and the oily substance was separated by centrifugation. The purification was conducted by silica gel chromatography (chloroform:methanol 30:1). Symmetrical and unsymmetrical Pc mixture was obtained. The resulting residual (274 mg), tosylated oxanorbornene (175 mg, 0.464 mmol), KI (77 mg, 0.464 mmol) and K_2CO_3 (116 mg, 0.840 mmol) were stirred in 10 mL of DMF at room temperature for 7 days. The resulting mixture was poured into cold water and extracted with ethyl acetate. It was dried with Na_2SO_4, filtered and the organic phase was evaporated. The residue was dried in a vacuum oven at 30 °C. Column chromatography was made on the dried substance in a 25:1:1 mixture of dichloromethane, ethanol, and acetone on silica gel. An oily green substance M5 was obtained. Yield: 5 mg (5% in two steps). **FT-IR** υ_{max} (cm^{-1}): 3067.12, 2871.78, 1770.49, 1698.36, 1606.56, 1487.78, 1450.28, 1394.42, 1337.05, 1282.19, 1218.86, 1088.05, 1060.78, 953.42, 852.36, 773.76, 745.06, 729.10, 655.71, 588.74. **UV/Vis** (DMSO): λ_{max}/nm = 682, 615, 356 nm. **MALDI-TOF MS**, dithranol: m/z calcd.: 1507.520; found: 1507.707 $[M]^+$, 1439.201 $[M\text{-furan}]^+$. **^{1}H-NMR** (500 MHz, DMSO-d_6): δ 9.16-8.52 (m, 8H), 7.78-7.65 (m, 4H), 7.46 (d, 2H), 7.19 (d, 2H), 6.56 (s, 2H), 5.19 (s, 2H), 4.66 (m, 5H), 4.09 (m, 5H), 3.81-3.34 (m, 38H), 2.21 (m, 9H), 2.98 (s, 2H), 2.63 (m, 2H), 2.36 (m, 2H), 2.01 (m, 2H) ppm.

3.3.6 Homopolimer Bearing Phthalonitrile (P1)

M1 (75 mg, 0.214 mmol) was dissolved in 2 mL of DMF in a nitrogen atmosphere and Grubbs' catalyst (2nd gen) (6.36 mg, 0.0075 mmol) in 0.5 mL of DCM was added in one shot to the stirring monomer solution. The reaction was monitored by TLC and, after 135 minutes, 0.5 mL of 30% ethyl vinyl ether was added and

stirred for 30 minutes. It was then precipitated and washed with diethylether. After centrifugation, it was dried in a vacuum oven. A brown substance P1 was obtained (theoretical molecular weight = 10,000 g mol^{-1}). Yield: 60 mg (80%). **FT-IR** υ_{max} (cm^{-1}): 3077.12, 2948.07, 2229.59, 1775.61, 1695.02 1667.43, 1595.89, 1562.35, 1491.92, 1470.12, 1437.15, 1395.86, 1319.34, 1253.34, 1173.00, 1089.05, 1015.21, 966.81, 911.64, 836.71. **^{1}H NMR** (500 MHz, DMSO-d_6): δ 7.72 (br, 1H), 7.67 (br, 1H), 7.37 (br, 1H), 5.91 (br, 1H), 5.74 (br, 1H), 4.88 (br, 1H), 4.37 (br, 1H), 4.11 (br, 2H), 3.53 (br, 2H), 1.96 (br, 2H) ppm.

3.3.7 Homopolymer Bearing *tert*-butyl Substituted Zinc(II) Phthalocyanine (P2)

P1 (90 mg, Mn = 10,000), 4-*tert*-butyl phthalonitrile (538 mg, 2.92 mmol) and zinc(II) acetate (83 mg, 0.45 mmol) were stirred in a nitrogen atmosphere at 15 mL DMAC. The reaction mixture was heated to 80 °C, then 4 drops of DBU were added and the temperature was raised to 130 °C. The reaction was continued for 24 h, then precipitated and washed 5 times with diethylether. After centrifugation, it was dried in a vacuum oven. Soxhlet extraction with diethylether was applied to the dry product for five hours. A dark green color P2 was obtained. Yield: 55 mg (61%). **FT-IR** υ_{max} (cm^{-1}): 2952.95, 1778.35, 1699.05 1466.56, 1392.75, 1321.76, 1153.67, 1086.04, 1045.77, 919.23, 827.10, 749.02, 674.39. **UV/Vis** (DMF): λ_{max}/nm = 681, 617, 349 nm. **^{1}H NMR** (500 MHz, DMSO-d_6): δ 9.43, 8.36, 7.95, 7.81, 6.67, 5.30, 1.77, 1.34, 1.21, 0.84 ppm.

3.3.8 Homopolymer Bearing *tert*-butyl Substituted Zinc(II) Phthalocyanine (P3)

M2 (30 mg, 0.0283 mmol) was dissolved in 2 mL of DMF:$CHCl_3$ mixture in a nitrogen atmosphere and Grubbs' catalyst (2nd gen) (2.54 mg, 0.003 mmol) in 0.5 mL of DCM was added in one shot to the stirring monomer solution. The reaction was monitored by TLC and, after waited overnight, 0.5 mL of 30% ethyl vinyl ether was added and stirred for 30 minutes. It was then precipitated and washed with diethylether. After centrifugation, it was dried in a vacuum oven. A blue colored substance P3 was obtained (theoretical molecular weight = 10,000 g mol^{-1}). Yield: 0.015 g (50%). **FT-IR** υ_{max} (cm^{-1}): 2953.28, 2161.26, 2034.89,

1777.32, 1703.01, 1611.93, 1501.43, 1488.05, 1392.02, 1362.70, 1330.75, 1280.95, 1255.75, 1215.21, 1198.63, 1144.42, 1086.42, 1044.66, 962.47, 938.46, 920.25, 894.75, 828.15, 746.16, 691.42, 672.34. **UV/Vis** (DMSO): λ_{max}/nm = 678, 637, 344 nm. **^{1}H NMR** (500 MHz, DMSO-d_6): δ 8.13-7.09, 5.95, 5.76, 4.97, 4.44, 4.03, 3.54, 1.96, 1.75 ppm.

3.3.9 General Synthesis Procedure for Copolymers Bearing *tert*-butyl Substituted Zinc(II) Phthalocyanine (P4, P5, P6)

M2 and M3 were dissolved in 2 mL of DMF:$CHCl_3$ mixture in a nitrogen atmosphere and Grubbs' catalyst (2nd gen) in 0.5 mL of DCM was added in one shot to the stirring monomer solution. The reaction was monitored by TLC and, after waited overnight, 0.5 mL of 30% ethyl vinyl ether was added and stirred for 30 minutes. It was then precipitated and washed with diethylether. After centrifugation, it was dried in a vacuum oven.

3.3.9.1 Synthesis of P4

M2 (15 mg, 0.01416 mmol), M3 (15 mg, 0.0271 mmol) and Grubbs' catalyst (2nd gen) (2.53 mg, 0.00298 mmol) were used. A blue colored substance P4 was obtained (theoretical molecular weight = 10,000 g mol^{-1}). Yield: 25 mg (83%). **FT-IR** υ_{max} (cm^{-1}): 3391.54, 2954.81, 1775.51, 1698.94, 1613.02, 1488.32, 1437.71, 1396.81, 1363.60, 1329.17, 1281.04, 1255.20, 1216.62, 1152.31, 1111.71, 1086.11, 1044.52, 996.66, 938.28, 919.96, 831.38, 749.08, 723.33, 689.12. **UV/Vis** (DMSO): λ_{max}/nm = 680, 614, 349 nm. **^{1}H NMR** (500 MHz, DMSO-d_6): δ 9.26-7.08, 5.92, 5.70, 4.84, 4.39, 4.00, 3.50, 1.96, 1.73 ppm. **^{31}P NMR** (DMSO-d_6): δ 24.07 ppm.

3.3.9.2 Synthesis of P5

M2 (8.6 mg, 0.00812 mmol), M3 (20 mg, 0.0383 mmol) and Grubbs' catalyst (2nd gen) (2.57 mg, 0.003 mmol) were used. A blue colored substance P5 was obtained (theoretical molecular weight = 10,000 g mol^{-1}). Yield: 0.024 g (84%). **FT-IR** υ_{max} (cm^{-1}): 3381.84, 2953.80, 1774.84, 1697.97, 1587.57, 1487.53, 1437.49, 1397.80, 1363.51, 1328.97, 1216.24, 1152.70, 1111.75, 1086.41, 1044.18, 996.26, 938.24, 919.63, 832.25, 748.47, 722.94, 688.90. **UV/Vis** (DMSO):

λ_{max}/nm = 680, 613, 352 nm. **^{1}H NMR** (500 MHz, DMSO-d_6): δ 9.26-7.09, 5.93, 5.74, 4.86, 4.43, 4.01, 3.53, 1.99, 1.73 ppm. **^{31}P NMR** (DMSO-d_6): δ 24.16 ppm.

3.3.9.3 Synthesis of P6

M2 (20 mg, 0.0188 mmol), M3 (8.51 mg, 0.0155 mmol) and Grubbs' catalyst (2nd gen) (2.41 mg, 0.00284 mmol) were used. A blue colored substance P6 was obtained (theoretical molecular weight = 10,000 g mol^{-1}). Yield: 0.020 g (70%). **FT-IR** υ_{max} (cm^{-1}): 3391.08, 2954.19, 1776.46, 1701.49, 1612.06, 1488.30, 1437.83, 1393.57, 1363.41, 1329.11, 1280.72, 1255.34, 1216.25, 1197.94, 1151.23, 1085.70, 1044.48, 963.56, 938.15, 919.92, 830.23, 748.91, 723.62, 689.37, 674.24. **UV/Vis** (DMSO): λ_{max}/nm = 679, 613, 346 nm. **^{1}H NMR** (500 MHz, DMSO-d_6): δ 8.96-7.09, 5.93, 5.71, 4.84, 4.38, 4.01, 3.45, 2.03, 1.75 ppm. **^{31}P NMR** (DMSO-d_6): δ 24.00 ppm.

3.3.10 Copolymer Bearing *tert*-butyl Substituted Zinc(II) Phthalocyanine (P7)

M2 (8.46 mg, 0.00798 mmol) and M4 (19.6 mg, 0.0486 mmol) were dissolved in 2 mL of DMF in a nitrogen atmosphere and Grubbs' catalyst (2nd gen) (2.39 mg, 0.00281 mmol) in 0.5 mL of DCM was added in one shot to the stirring monomer solution. The reaction was monitored by TLC and, after waited overnight, 0.5 mL of 30% ethyl vinyl ether was added and stirred for 30 minutes. It was then precipitated and washed with diethylether. After centrifugation, it was dried in a vacuum oven. A blue colored substance P7 was obtained (theoretical molecular weight = 10,000 g mol^{-1}). Yield: 0.025 g (87%). **FT-IR** υ_{max} (cm^{-1}): 3339.73, 2943.36, 1774.23, 1694.62, 1489.66, 1440.09, 1399.39, 1361.28, 1330.21, 1215.58, 1154.61, 1086.83, 1043.46, 918.90, 877.37, 770.12, 750.64. **UV/Vis** (DMSO): λ_{max}/nm = 680, 613, 353 nm. **^{1}H NMR** (500 MHz, DMSO-d_6): δ 9.41-7.16, 5.97, 5.76, 4.94, 4.47, 4.09, 3.48, 2.28, 1.75, 1.10 ppm. **^{31}P NMR** (DMSO-d_6): δ 39.25 ppm.

3.3.11 Homopolymer Bearing PEG Substituted Zinc(II) Phthalocyanine (P8)

M5 (41 mg, 0.0271 mmol) was dissolved in 1.5 mL of $CHCl_3$ in a nitrogen atmosphere and Grubbs' catalyst (3rd gen) (3.61 mg, 0.00408 mmol) in 0.5 mL of DCM was added in one shot to the stirring monomer solution. The reaction was monitored by TLC and, after 3 hours, 0.5 mL of 30% ethyl vinyl ether was added and stirred for 30 minutes. It was then precipitated and washed with diethyl ether. After centrifugation, it was dried in a vacuum oven. A blue colored substance P8 was obtained (theoretical molecular weight = 10,000 g mol^{-1}). Yield: 20 mg (48%). **FT-IR** υ_{max} (cm^{-1}): 3068.32, 2921.73, 2870.19, 1772.93, 1702.51, 1606.59, 1503.15, 1487.61, 1470.24, 1450.36, 1394.22, 1336.86, 1280.58, 1219.77, 1198.18, 1178.23, 1088.90, 1058.52, 1040.58, 952.46, 825.74, 774.12, 746.16, 729.99, 686.19, 656.84. **UV/Vis** (DMF): λ_{max}/nm = 677, 615, 350. **^{1}H NMR** (500 MHz, DMSO-d_6): δ 9.18-7.07, 5.99, 5.84, 5.00, 4.54, 4.05, 3.78-3.42, 3.21, 2.06 ppm.

3.3.12 General Synthesis Procedure for Copolymers Bearing PEG Substituted Zinc(II) Phthalocyanine (P9, P10, P11)

M5 and M3 were dissolved in 1.5 mL of $CHCl_3$ in a nitrogen atmosphere and Grubbs' catalyst (3rd gen) in 0.5 mL of DCM was added in one shot to the stirring monomers' solution. The reaction was monitored by TLC and, after 3 hours, 0.5 mL of 30% ethyl vinyl ether was added and stirred for 30 minutes. It was then precipitated and washed with diethyl ether. After centrifugation, it was dried in a vacuum oven.

3.3.12.1 Synthesis of P9

M5 (30.4 mg, 0.02 mmol), M3 (12.9 mg, 0.0235 mmol) and Grubbs' catalyst (3rd gen) (3.8 mg, 0.0043 mmol) were used. A blue colored substance P9 was obtained (theoretical molecular weight = 10,000 g mol^{-1}). Yield: 25 mg (57%). **FT-IR** υ_{max} (cm^{-1}): 3060.16, 2870.18, 1775.18, 1701.26, 1606.15, 1487.90, 1470.33, 1438.67, 1394.51, 1371.40, 1334.69, 1280.00, 1218.77, 1197.66, 1111.81, 1087.50, 1058.07, 1039.71, 996.62, 951.24, 828.65, 773.24, 747.75, 724.07, 689.31, 659.02. **UV/Vis** (DMSO): λ_{max}/nm = 679, 613, 356. **^{1}H NMR** (500 MHz,

DMSO-d_6): δ 9.21-7.08, 5.93, 5.73, 4.87, 4.42, 4.05, 3.77-3.41, 3.21, 2.01, 1.77, 1.61 ppm. **^{31}P NMR** (DMSO-d_6): δ 24.11 ppm.

3.3.12.2 Synthesis of P10

M5 (31 mg, 0.02 mmol), M3 (31 mg, 0.0565 mmol) and Grubbs' catalyst (3rd gen) (5.4 mg, 0.0062 mmol) were used. A blue colored substance P10 was obtained (theoretical molecular weight = 10,000 g mol^{-1}). Yield: 40 mg (64%). **FT-IR** υ_{max} (cm^{-1}): 3057.23, 2869.78, 1775.23, 1699.25, 1607.19, 1588.66, 1487.86, 1438.06, 1396.55, 1369.70, 1335.31, 1280.68, 1219.63, 1111.95, 1089.31, 1057.88, 1040.07, 996.56, 956.25, 848.55, 747.59, 736.11, 723.77, 689.98. **UV/Vis** (DMSO): λ_{max}/nm = 680, 612, 359 nm. **^{1}H NMR** (500 MHz, DMSO-d_6): δ 9.25-7.08, 5.92, 5.75, 4.86, 4.42, 4.03, 3.76-3.39, 3.20, 2.01, 1.80, 1.60 ppm. **^{31}P NMR** (DMSO-d_6): δ 24.14 ppm.

3.3.12.3 Synthesis of P11

M5 (33.4 mg, 0.022 mmol), M3 (77.8 mg, 0.14 mmol) and Grubbs' catalyst (3rd gen) (9.8 mg, 0.011 mmol) were used. A blue colored substance P11 was obtained (theoretical molecular weight = 10,000 g mol^{-1}). Yield: 80 mg (71%). **FT-IR** υ_{max} (cm^{-1}): 3055.89, 2923.93, 2869.01, 1774.55, 1698.46, 1667.76, 1607.09, 1587.56, 1487.19, 1437.47, 1397.55, 1369.11, 1335.42, 1238.18, 1219.78, 1151.50, 1111.82, 1037.45, 996.16, 969.81, 848.76, 806.15, 747.34, 736.98, 723.05, 689.38, 660.34. **UV/Vis** (DMSO): λ_{max}/nm = 680, 612, 359. **^{1}H NMR** (500 MHz, DMSO-d_6): δ 9.29-7.09, 5.92, 5.73, 4.84, 4.44, 4.03, 3.77-3.40, 3.20, 2.02, 1.81, 1.62 ppm. **^{31}P NMR** (DMSO-d_6): δ 24.17 ppm.

3.4 Antimicrobial Photodynamic Activities

Bacterial strains were multiplied on lysogeny broth (LB; Miller) agar and stored at 4 °C. One single isolated colony was taken from this plate, transferred to LB broth, and incubated aerobically overnight at 37 °C at 180 rpm. Bacteria were then suspended in fresh LB medium to an optical density $OD_{600} \approx 0.1$ and grown to attenuation of $OD_{600} \approx 0.4$. The bacterial suspensions were then centrifuged at 4000 rpm and PBS was added to achieve the concentration of approximately 1 x 10^{-8} cells per mL. This suspension was used for the irradiation experiments.

1 mL bacterial suspension containing a certain amount of PS was incubated in the dark at 37 °C in 24-well plate. Irradiation was performed with an LED lamp (660 ± 24 nm). After the incubation overnight at 37 °C, the number of CFU/mL was counted using an automated colony counter “ProtoCOL2” from Synbiosis.

4
RESULTS AND DISCUSSION

4.1 Synthesis of Monomers and Polymers

There are three methods for the incorporation of Pcs into polymers as pendant groups (see Chapter 2.5.4). In this thesis, firstly the desired polymers have been tried to obtain via post-polymerization modification of the dinitrile substituted polymer precursor (Route A). However, since characteristic peaks couldn't be seen in the ^{1}H NMR spectrum of P2, the study has continued with other approach which involves the polymerization of ZnPc-containing monomer (Route B).

4.1.1 Synthesis of First Series Monomers and Polymers: Route A

In route A, phthalonitrile derivative M1 was obtained by aromatic nucleophilic substitution reaction between 4-nitrophthalonitrile and hydroxy substituted oxanorbornene. Phthalonitrile-containing homopolymer P1 was synthesized via ROMP, which was carried out in DMF at room temperature using Grubbs' Catalyst (2nd gen). Subsequently, P1 reacted with excess phthalonitrile derivative 4-*tert*-butylphthalonitrile to synthesize polymer P2 (Figure 4.1). Although different spectroscopic techniques were approved the formation of desired homopolymer P2, unfortunately, it was not characterized in the ^{1}H NMR spectrum. The typical polymer double bond peaks at around 5.7-5.9 ppm have fully disappeared which strongly suggests that the polymeric backbone was damaged during the formation of Pc ring (Figure 4.6).

4.1.2 Synthesis of First Series Monomers and Polymers: Route B

In route B, ZnPc with a phenolic moiety (3) was synthesized by statistical reaction of 4-(4-hydroxyphenoxy)phthalonitrile (1) and 4-*tert*-butylphthalonitrile (2). Later, the reaction between the tosylated oxanorbornene derivative 4 and unsymmetrical ZnPc 3 resulted in the desired macrocyclic monomer M2 (Figure 4.2). Homopolymer (P3) and copolymers with different compositions (P4-P7) were obtained by using M2, M3 and M4 monomers (Figure 4.3). Polymerizations

of monomers were conducted in DMF:$CHCl_3$ solvent mixture in the presence of Grubbs' Catalyst (2nd gen) at room temperature.

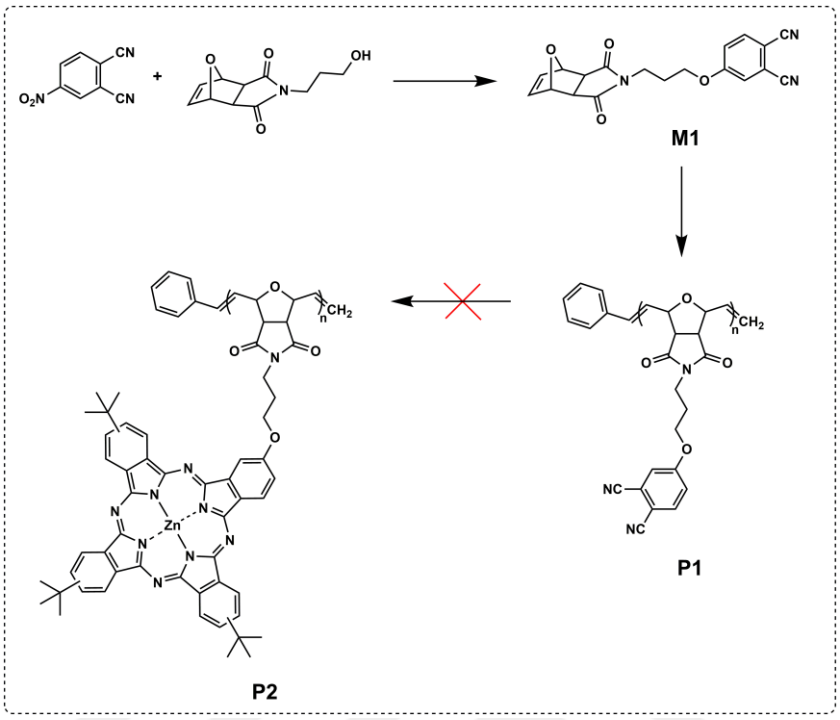

Figure 4.1 The synthetic route A

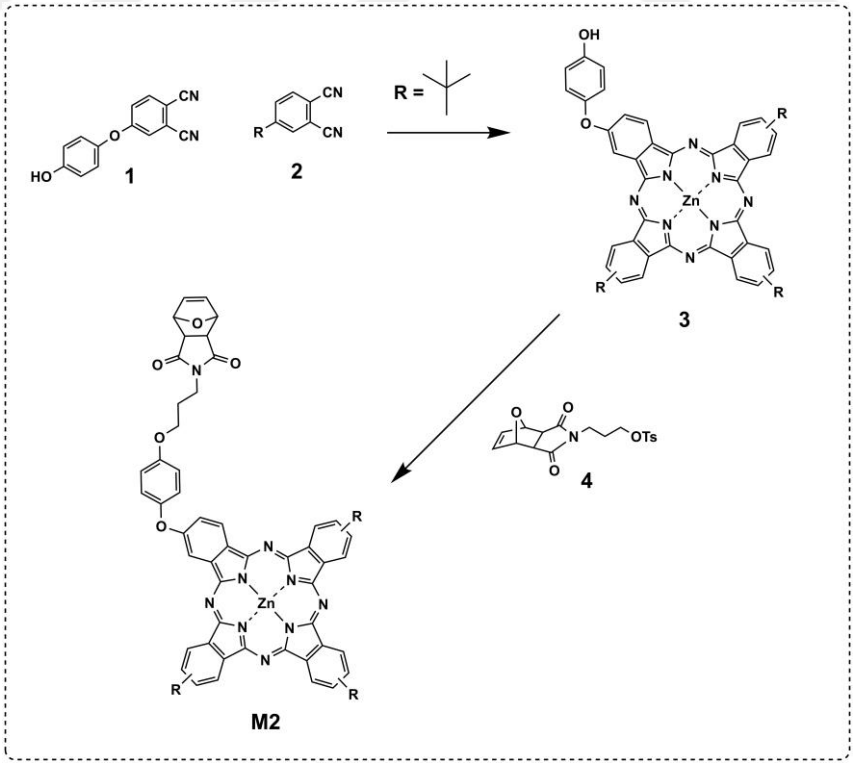

Figure 4.2 The synthetic route B for monomer synthesis

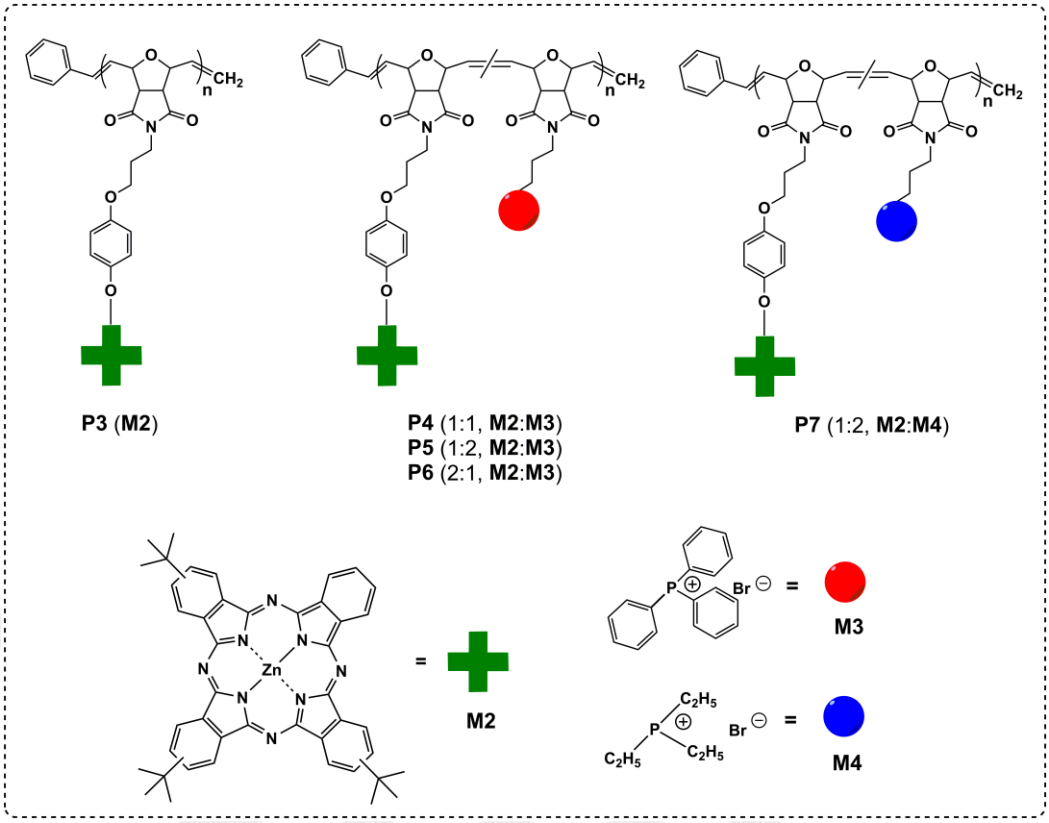

Figure 4.3 The structures of first series polymers

4.1.3 Synthesis of Second Series Monomers and Polymers

Firstly, PEG substituted phthalonitrile (5) was obtained by the reaction of 4-nitrophthalonitrile with tetraethyleneglycol monomethyl ether. Subsequently, an intermediate unsymmetrical and symmetrical ZnPc mixture was prepared by statistical reaction of 4-(4-hydroxyphenoxy) phthalonitrile (1) and excess amount of PEG substituted phthalonitrile (5). Finally, the mixture was used to synthesize AB_3-type unsymmetrical ZnPc (M5) by reacting with excess tosylated oxanorbornene derivative (Figure 4.4). Homopolymer (P8) and copolymers with varying compositions (P9-P11) were synthesized by using M5 and M3 (Figure 4.5). Polymerizations of monomers were carried out in $CHCl_3$ in the presence of Grubbs' Catalyst (3rd gen) at room temperature.

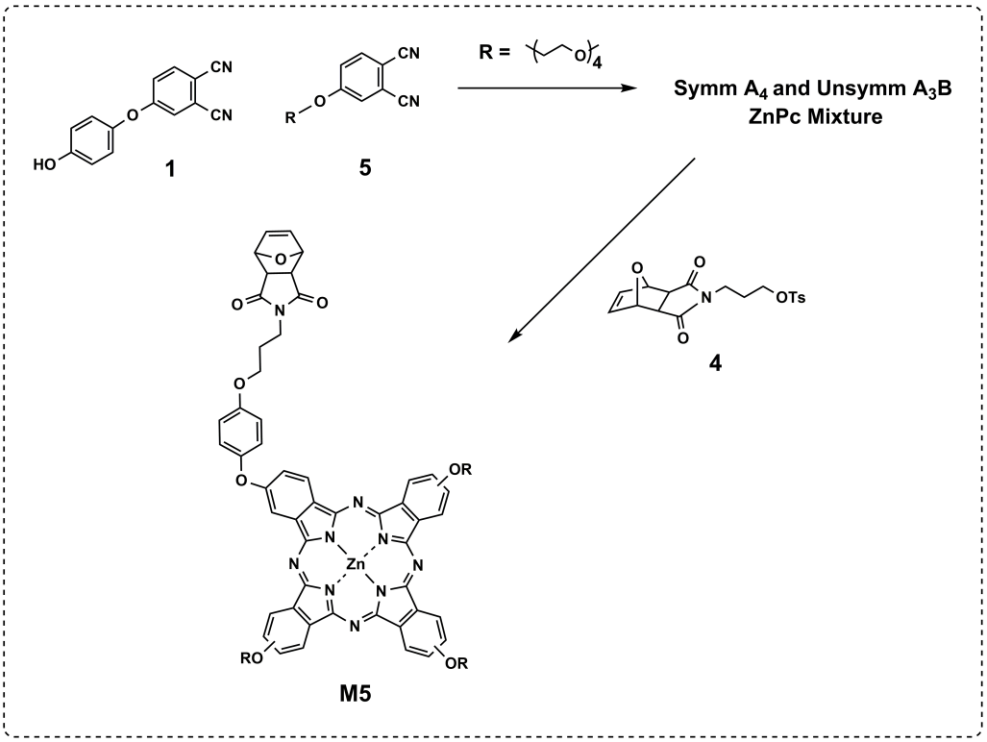

Figure 4.4 Synthesis of monomer M5

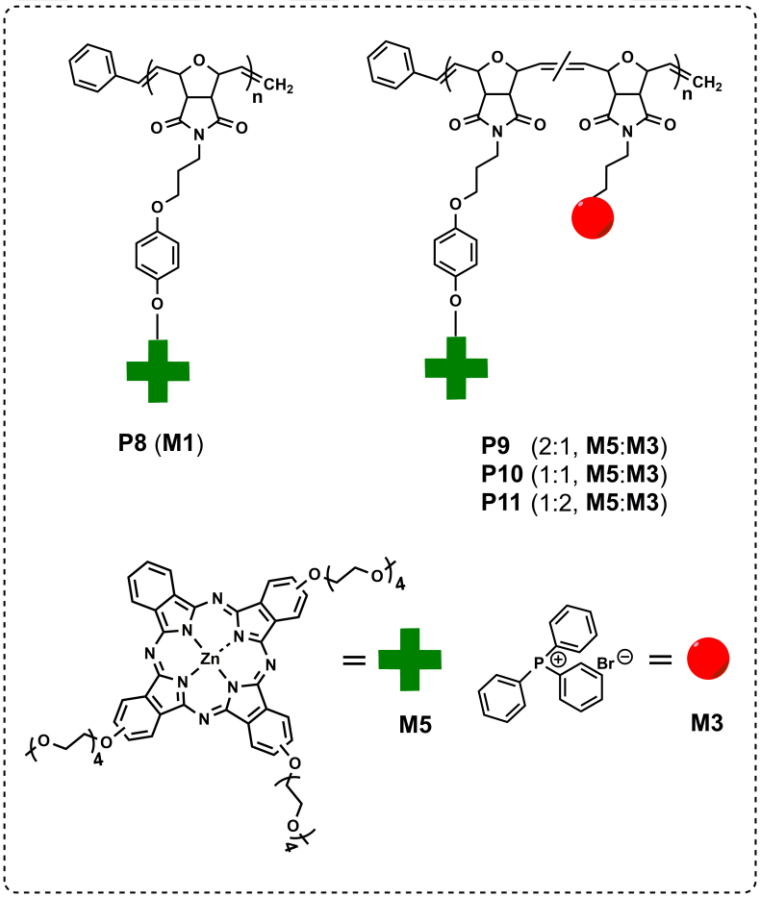

Figure 4.5 The structures of second series polymers

4.2 Characterization of Monomers and Polymers

The structure of the new compounds characterized by FT-IR, ICP-MS, MALDI-TOF MS, UV-vis, NMR and GPC techniques.

4.2.1 Characterization of First Series Monomers and Polymers

In the FT-IR spectra of M1 and P1, the presence of the aliphatic C-H stretching vibrations at 2958 and 2948 cm^{-1}, the aromatic C-H stretching vibrations at 3060 and 3077 cm^{-1}, with the protection of the -C≡N vibration at around 2230 cm^{-1}, showed that the monomer M1 was converted to polymer P1 (Figure S1 and S2). Meanwhile, in the FT-IR spectrum of P2, the disappearance of the -C≡N vibration indicated the formation of Pc ring. The UV-vis absorption spectra of P1 and P2 were recorded in DMF (Figure S4). P2 showed a typical Pc UV-vis absorption spectrum with bands at ~349 nm, ~617 and ~681 nm while P1 didn't show any absorption band. Thus, formation of Pc were proved thanks to the comparison with spectra. ^{1}H and ^{13}C NMR spectral characterization of compounds were achieved in $CDCl_3$ for M1 and DMSO-d_6 for P1 and P2 (Figure S5-S8). In the ^{1}H and ^{13}C NMR spectra of M1, the characteristic signals of oxanorbornene's hydrogen and carbon atoms appeared at 6.53, 5.23, 2.87 ppm and 176.19, 136.48, 81.03, 47.39 ppm, respectively. In the ^{1}H NMR spectrum of P1, complete conversion was observed by the disappearance of the monomer's olefin proton peaks at 5.0–6.5 ppm and the appearance of the polymer's backbone double bond protons as cis or trans signals at 5.74–5.91 ppm. Conversely, these double bond protons could not be seen in ^{1}H NMR spectrum of P2. Although we observed the formation of Pc moiety at P2 via UV-vis and FT-IR spectroscopy analyses, NMR analysis showed that the polymeric backbone was damaged and the target polymer P2 could not be successfully obtained (Figure 4.6).

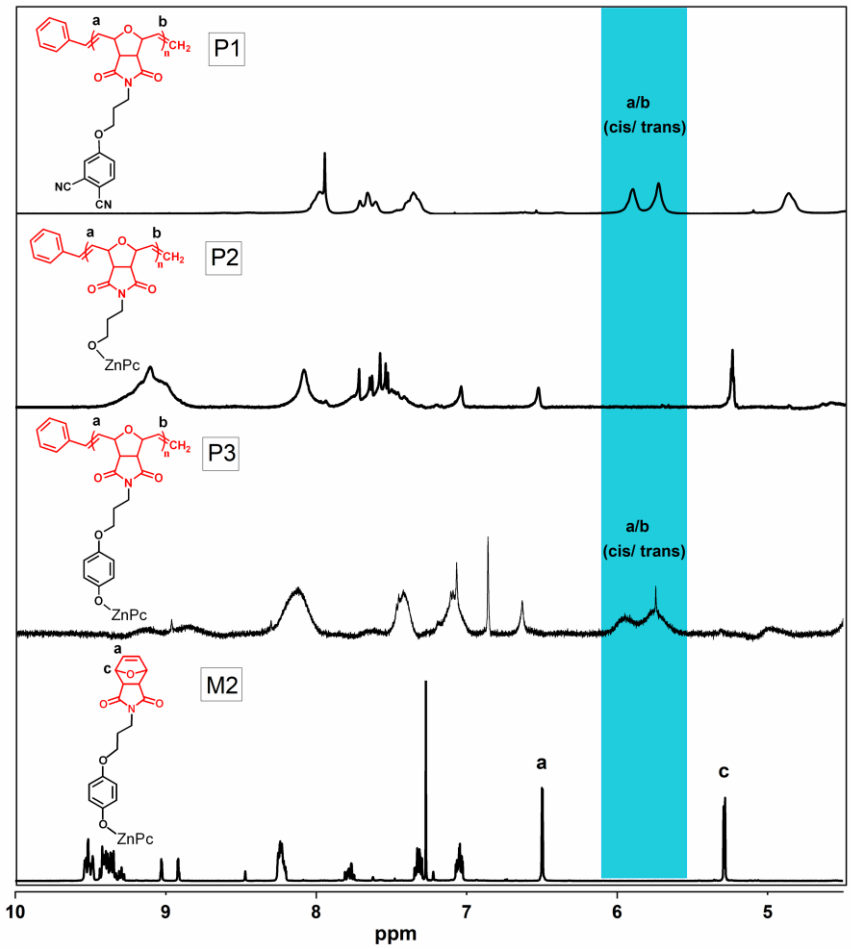

Figure 4.6 ^{1}H NMR spectra of M2 and P1-P3

In the FT-IR spectra, aliphatic C-H bands at around 2864-2955 cm^{-1} and the aromatic C-H bands at 3069 and 3065 cm^{-1} were both observed for 3 and M2, whereas -O-H band at 3250 cm^{-1} was only seen for M2. In the FT-IR spectra of M2, the appearance of the C=O stretching vibrations at 1692 cm^{-1} and the absence of the -O-H band indicated the conversion of 3 to M2 (Figure S9 and S10). In the MALDI-TOF MS spectrum of M2, the molecular ion peak was observed at 1059.066 m/z (Figure S12). The UV-vis spectra of 3 and M2 showed almost the same absorption and shape in THF. Their spectra showed a typical Pc Soret band at ~349 nm and a Q-band at ~673 nm (Figure S11). The UV-vis spectra of P3, P4, P5, P6 and P7 were recorded at the same concentration in DMF and all first series polymers showed the same absorption bands approximately at 349, 614 and 680 nm. The results showed that the Q band absorption value increased in parallel with the Pc content. (Figure S19 and S20). ^{1}H and ^{31}P NMR spectral characterization of compounds were achieved in $CDCl_3$ for M2 and DMSO-d_6 for

P3, P4, P5, P6 and P7. In the ^{1}H NMR spectrum of M2, *tert*-butyl groups were assigned at 1.79 ppm. Two peaks at 7.31 and 7.05 ppm showed the presence of the phenyl group, while peaks between 9.55 and 7.76 pointed out Pc ring in the structure. Moreover, the characteristic signals of oxanorbornene protons appeared at 6.50, 5.29, 2.87 ppm (Figure S13). In the ^{1}H NMR spectra of all polymers (P3-P7), it was seen that the polymerization successfully occurred, monomer peaks belong M2, M3 and M4 at 5.0–6.5 ppm disappeared and double bond protons' signals representing polymer backbone came out at ~5.92–5.70 ppm (Figure S21-S25). ^{1}H NMR spectra of all polymers with the same theoretical molecular weights were taken at the same concentration (10.000 g mol^{-1}). It is fact that there is a linear correlation between the amount of triphenyl groups in the polymer backbone and the signal intensity. The peaks belonging to the triphenyl groups at ~7.7 ppm differ according to the polymer composition (P3-P6). In the ^{1}H NMR spectra of P7, two new peaks at 1.10 and 2.28 ppm derived from triethyl groups were seen as expected (Figure 4.7). On the other hand, in the ^{31}P NMR spectra of polymers, one peak was observed at 24 ppm for triphenyl groups in P4-P6, at 39 ppm for triethyl groups in P7 (Figure S26). In addition, the linear correlation for the triphenyl signal intensity in the ^{1}H NMR followed the same trend in the ^{31}P NMR.

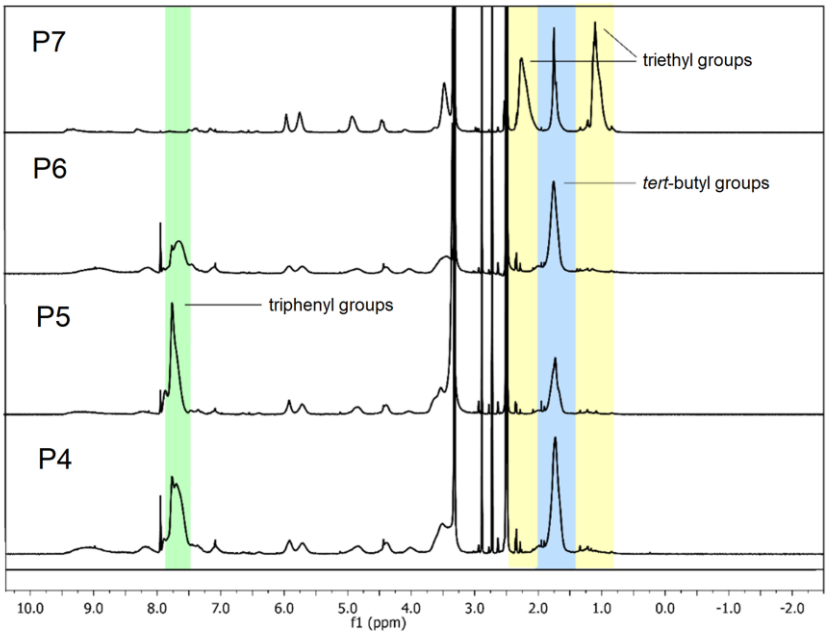

Figure 4.7 ^{1}H NMR spectra of P4-P7 in DMSO-d_6

4.2.2 Characterization of Second Series Monomers and Polymers

In the FT-IR spectrum of monomer M5, stretching vibrations of aromatic C-H (3067 cm^{-1}), aliphatic C-H (2871 cm^{-1}), and C=O (1698 cm^{-1}) appeared at expected frequencies (Figure S31). In the MALDI-TOF MS spectrum, $[M]^+$ and [M-furan]$^+$ peaks were observed at *m/z* 1507.707 and 1439.201 for M5, respectively (Figure S33). The UV-vis spectrum of M5 showed a typical Pc Q-band at 682 nm and a B-band at 356 nm in THF (Figure S32). UV-vis spectra of polymers P8-P11 were recorded in DMF at the same concentration. Polymers showed the same absorption bands approximately at ~ 350, ~ 615, and ~ 680 nm. UV-vis spectra also showed that the increase in Pc molar ratio in the polymer structures resulted in the rise of the Q-band absorption (Figure S39 and S40). The ^{1}H-NMR spectrum of monomer M5 exhibited aromatic protons in the range of 9.16-7.19 ppm, integrating 16 protons for M5 as expected. The characteristic peaks of oxanorbornene protons appeared at 6.56 (olefin proton), 5.19 (cyclic ether proton) and 2.98 ppm. Also, the -OCH_2 protons of PEG chains were observed between 4.66-3.39 ppm. The rest of the aliphatic CH_3 and CH_2 protons were observed at 3.21, 2.63, 2.36 and 2.01 ppm (Figure S34). The formation of polymers was proved with the appearance of polymer double bond protons peaks at around 5.73-5.99 ppm and the disappearance of the olefinic peaks belonging to monomers at around 5.19 and 6.56 ppm in the ^{1}H-NMR spectra of P8-P11 and these changes are in harmony with the reported values for PONs (Figure S41-S44) (Figure 4.8). In the ^{31}P-NMR spectra of copolymers P8-P11, one peak was observed at 24 ppm for triphenylphosphonium groups (Figure S45). The spectrum showed that the peak intensity value increased in parallel with the triphenyl content. Polymers (P8-P11) were analyzed by gel-permeation chromatography (GPC, in DMAC). In the GPC elugram, homopolymer and copolymers had a ranging polydispersity index (M_w/M_n) from 1.22 to 1.05. While the target molecular mass for polymers P8-P11 was 10,000 g/mol, the calculated masses were significantly lower or higher (4213, 4102, 4013, 18695 g/mol, respectively) (Figure S46-S49). ICP-MS technique was also used to determine Zn in copolymers (P8-P11). The Zn% in the same amount of copolymers (P8-P11) was found to be 2.39 ± 0.07,

1.62 ± 0.05 and 1.15 ± 0.03, respectively. This result is consistent with the ZnPc molar ratio in the copolymers.

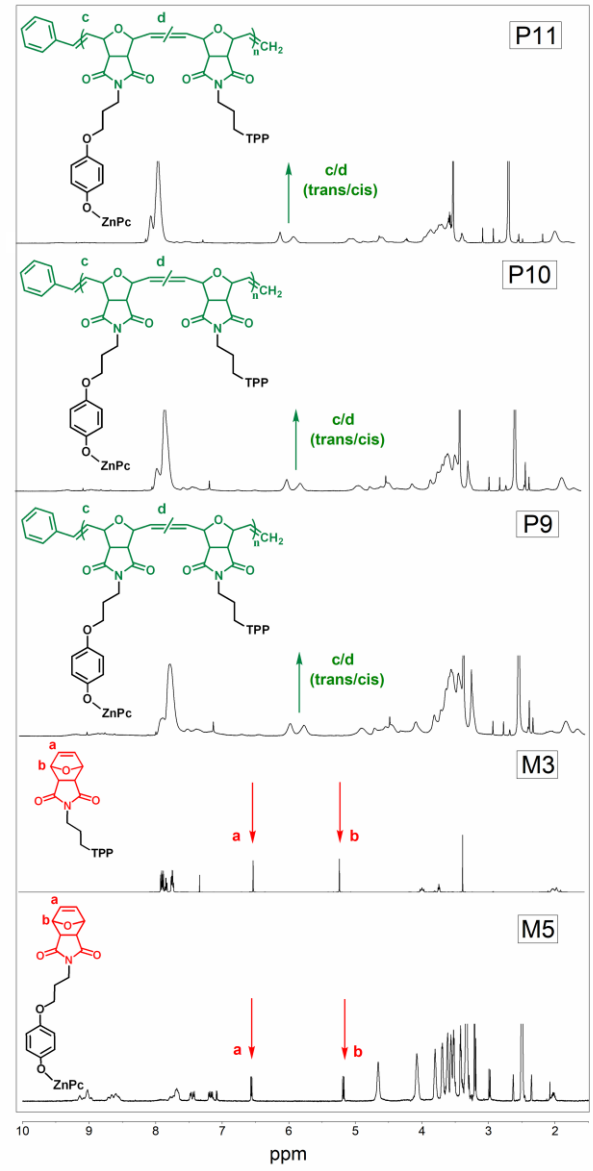

Figure 4.8 ^{1}H-NMR spectra of M5, M3 and P8-P11 in DMSO-d_6

4.3 Photophysical Studies

The fluorescence behavior of the first series polymer (P3-P7) was studied in DMSO and 5% DMSO-water. Figure 4.9 belongs to absorption, emission and excitation spectra of P5 and it represents all polymers. While excitation values of the polymers (P3-P7) are 677 nm, 680 nm, 681 nm, 680 nm, and 682 nm, their absorption wavelength were determined at 677 nm, 678 nm, 679 nm, 678 nm, and 679 nm, respectively, in DMSO. While the absorption and excitation spectra

of P3 are the same, which means all fluorescence features result from a single molecule, the excitation spectrum of compounds P4-P7 is slightly red-shifted up to 3 nm (Figure 4.9). In addition, the observed Stokes shifts were 6 nm for P3, 10 nm for P4, 10 nm for P5, 3 nm for P6, and 6 nm for P7. The fluorescence quantum yield (Φ_F) is the number of the transform of absorbed light into radiated light. To obtain the fluorescence quantum yields of the polymers, unsubstituted ZnPc and the comparative method were used [100]. The fluorescence quantum yields (Φ_F) of first series polymers (P3-P7) were measured in DMSO and 5% DMSO-water. The Φ_F values were found in DMSO 0.033 for P3 and 0.032 for P4, 0.059 for P5, 0.047 for P6 and 0.032 for P7. All polymers (P3-P7) showed weaker fluorescence quantum yield than standard in DMSO. In aqueous media, copolymers (P4-P7) didn't show fluorescent behavior. The fluorescence spectra for these polymers were not observed since the water increased the aggregation which lead to decrease the photoactivity of compounds [101]. Fluorescence lifetime values (τ_F) express the time that the absorbed photon spends in the excited state before going back to the ground state. The lifetime values of the studied polymers were determined as 2.97 ns for P3, 2.76 ns for P4, 2.71 ns for P5, 2.84 ns for P6 and 2.71 ns for P7 in DMSO by TCSPC (time correlated single photon counting) method (Table 4.1). Figure 4.10 represent the fluorescence decay curve of P3 in DMSO.

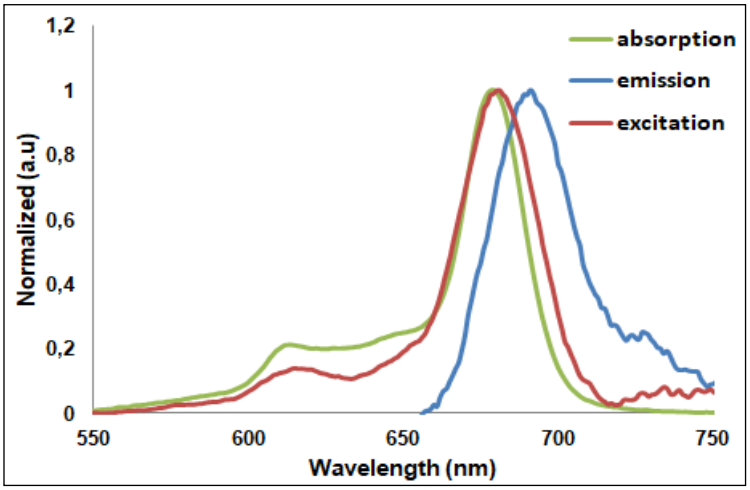

Figure 4.9 Absorption, excitation and emission spectra of P5 (excitation wavelength: 617 nm)

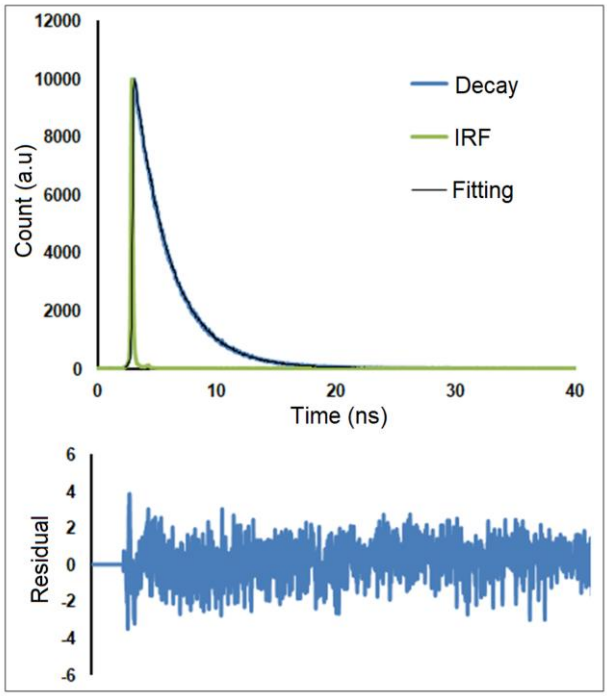

Figure 4.10 Fluorescence decay (blue), χ2 fitting (black) and IRF (green) curves for P3 in DMSO

The fluorescence behaviour of the second series polymers (P8-P11) were studied in DMF and water. In fluorescence measurements in DMF, an increase in ZnPc content clearly correlates with the emission intensity, while the emission intensity of P11 is significantly higher in aqueous media, indicating the role of monomerization in improving photophysical properties. Nevertheless, quenching of fluorescence in aqueous solutions for all polymers studied here further supports the presence of exciton coupling associated with Pc aggregation.

The fluorescence quantum yields for P9-P11 determined in DMF at room temperature ranged from 0.11 to 0.39, while quantum yields in water were < 0.01 (Table 4.2). Moreover, aggregation study of the second series polymers (P8-P11) was carried out. In DMF, all compounds showed strong and sharp absorption maxima at about 680 nm associated with the S_0-S_1 transition of the monomeric ZnPc core (Figure 4.11a). Interesting insights arise from the comparison of the UV-vis spectra of the obtained copolymers in water. ZnPc residue tends to aggregate in an aqueous solution, leading to a decrease in the overall absorption coefficient and an increase in the peak characteristic of the formation of inactive H-aggregates. As could be seen from Figure 4.11b a blue-shifted peak at ca. 630

nm appears in the UV-vis spectra of all copolymers. A comparison of the individual components clearly shows that P11 contains less PS, but it is present in a markedly non-aggregated form. Increasing the ZnPc content in the polymer leads to increased aggregate formation. It can be derived that the relatively large and positively charged TPP units not only increase the solubility of the polymers in water but also interfere with the stacking of the ZnPc macrocycle.

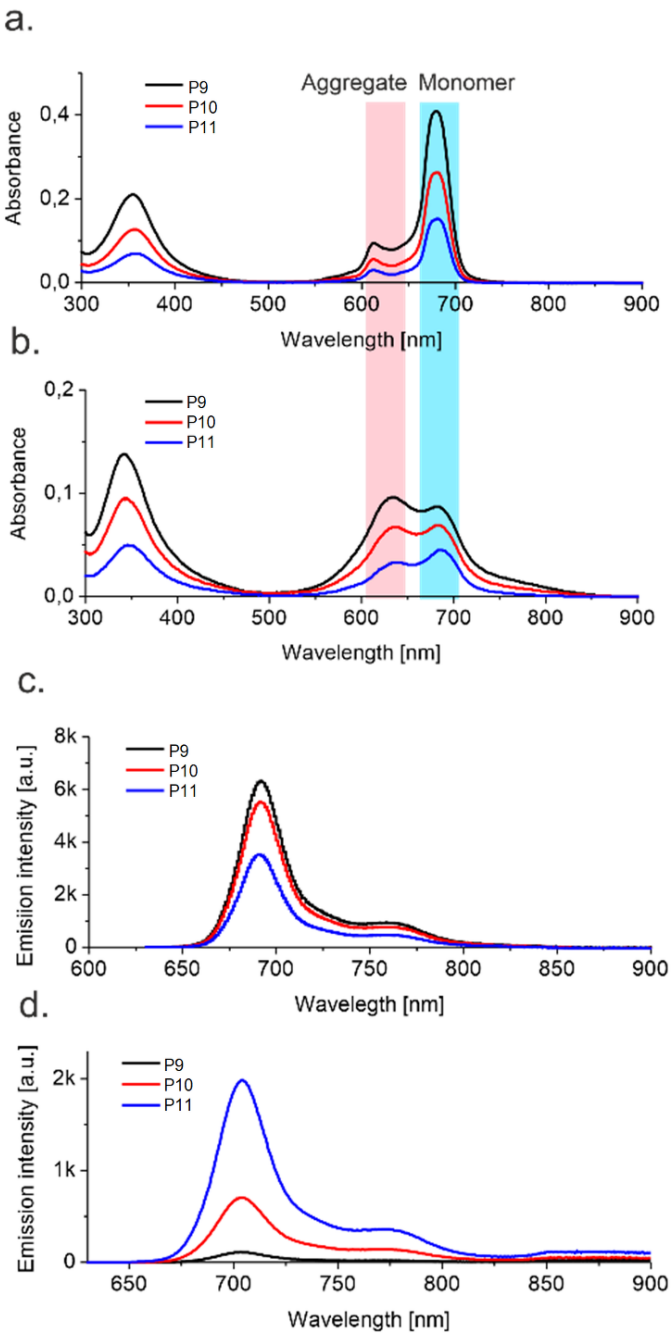

Figure 4.11 (a),(b) UV-vis spectra (c),(d) fluorescence spectra of copolymers (P9-P11) in DMF and H_2O (concentration: 10 µg/mL)

4.4 Singlet Oxygen Quantum Yields (Φ_Δ)

The success of the photodynamic process is dependent on the generation of highly reactive and cytotoxic singlet oxygen ($^1O_2$). Singlet oxygen quantum yield (Φ_Δ) reflects the ability of the PSs to transform the molecular oxygen into singlet oxygen [102, 103]. The measurement of $^1O_2$ of the first series polymers was performed using the UV-vis spectroscopic method. While DPBF and ADMA were utilized as singlet oxygen quenchers, unsubstituted ZnPc and AlPcSmix were used as standard in DMSO and 5% DMSO-water, respectively. Figure 4.12 belongs to the absorbance changes of quenchers for compound P5 and represents the singlet oxygen generation for all the first series polymers. The intensities and shapes of the Q bands did not show any changes and this is indicating that the PSs did not degrade during the singlet oxygen studies by the light irradiation [104-107]. While P3 displayed the lowest singlet oxygen generation (Φ_Δ =0.09), P5 and P7 have the highest values (Φ_Δ=0.22, 0.41) in DMSO. It seems that the introduction of the cationic charge on the copolymers gave rise to more singlet oxygen production [108]. The lowest value in 5% DMSO-water arises from the aggregation tendency of copolymers (P4-P7) and the quenching of singlet oxygen in water (Table 4.1).

The measurement of $^1O_2$ of second series polymers was performed using the UV-vis spectroscopic method and fluorescence spectroscopy method. While DPBF and ADMA were utilized as singlet oxygen quenchers, unsubstituted ZnPc and methylene blue were used as standard in DMF and water, respectively [109, 110]. Figure 4.13a and S50 show the degradation rate of DPBF upon irradiation in the presence of polymers and reference ZnPc in the time range of 0-45 s. The results show that P11 has the highest value of singlet oxygen generation Φ_Δ = 0.80 despite the lower amount of ZnPc in the structure, while Φ_Δ of P9 and P10 can also be considered very high with values of 0.36 and 0.46, respectively, in DMF. P8 appears to have a lower singlet oxygen production efficiency, although it is completely soluble in DMF, and the amount of ZnPc is comparable with P9.

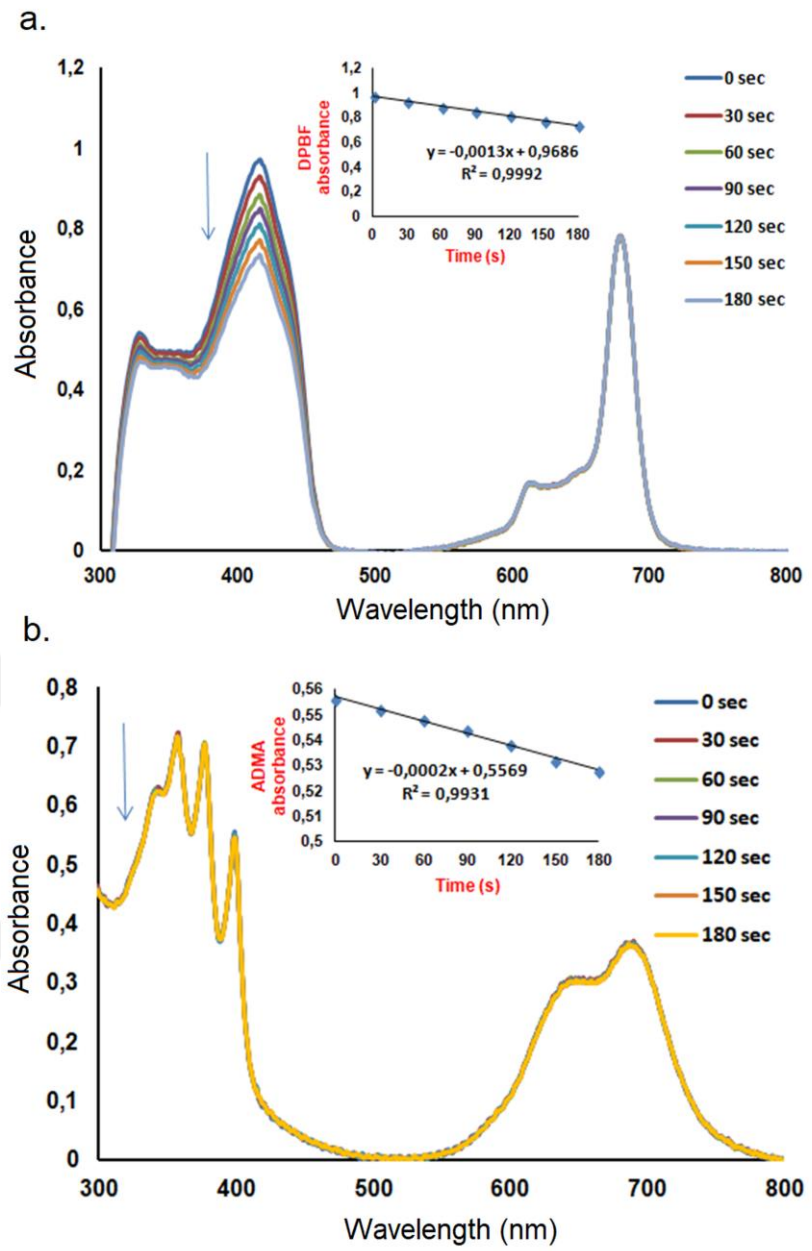

Figure 4.12 Determination of singlet oxygen quantum yield of P5 (a) in DMSO using DPBF (b) in 5% DMSO-water using ADMA

These differences are even more pronounced in water, where the aggregation tendency has considerable influence. As shown in Figure 4.13b and S51, the fluorescence emission intensity of ADMA incubated with copolymers P9-P11 continuously decreased with increasing duration of red light irradiation, the P10 and P11 copolymers with the values of 0.74 and 0.93 showed much higher ADMA degradation rates than the commercially available methylene blue ($\Phi_\Delta = 0.52$),

while the $^1O_2$ yield for P9 with 0.45 was slightly lower. Singlet oxygen generation was even almost completely quenched in the case of the homopolymer P8. A comparison of the obtained values with the results of first series clearly shows that not only the amount but also the bulk of the positively charged groups as well as presence of PEG chains on ZnPc contributes to the disaggregation of PS and increase the efficiency of the polymers in generating ROS (Table 4.2).

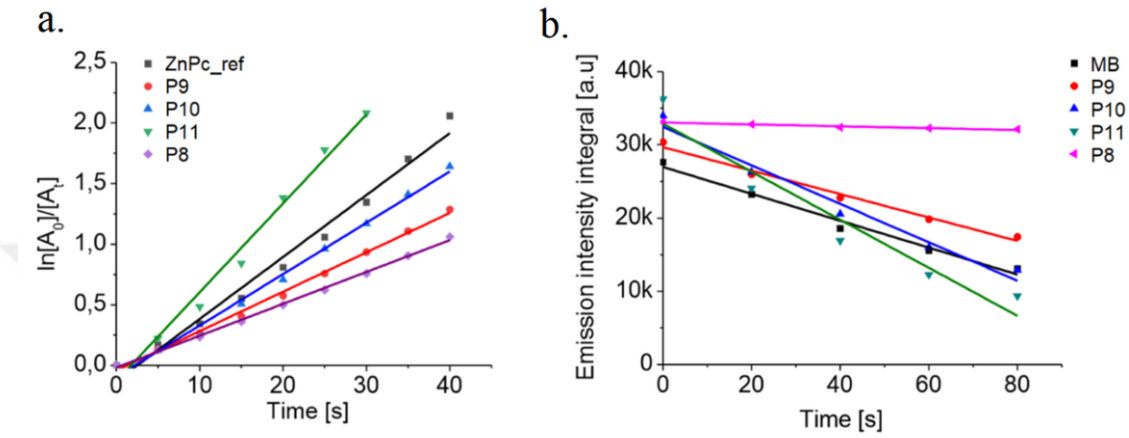

Figure 4.13 (a) Decay curves of DPBF (b) Decay curves of ADMA in presence of corresponding PSs

4.5 Triplet Quantum Yield (Φ_T) and Lifetimes (τ_T)

The determination of triplet quantum yield (Φ_T) and its lifetime (τ_T) during the photochemical reactions play significant role in the photodynamic process because the generation of singlet oxygen takes place triplet excited state. The triplet quantum yield (Φ_T) and triplet lifetimes values of the first series polymers (P3-P7) were measured using unsubstituted ZnPc and comparative method in DMSO [104]. The copolymers (P4-P7) displayed lower triplet quantum yield (Φ_T) (0.31, 0.35, 0.29, and 0.50) than homopolymer (P3) (0.89). The highest values belong to P5 and P7 between copolymers and these results are compatible with the singlet oxygen quantum yields. On the other hand, triplet lifetime values express the time that the PS spends in the triplet excited state and these values are directly proportional to the triplet quantum yields [111]. The triplet lifetime values of first series polymers have ranged from 87 to 183 μs (Table 4.1). Triplet decay curve of P3 is seen in Figure 4.14 and represents all first series polymers.

Table 4.1 Photodynamic parameters of P3-P7 in DMSO and 5% DMSO-water

PS	Solvent	Abs.	Exc.	Em.	Φ_F	Stokes shift Δ_{Stokes}, nm	Φ_Δ	τ_F (ns)	Φ_T	τ_T (μs)
P3	DMSO	677	677	683	0.033	6	0.09	2.9	0.89	183
P4	DMSO	678	680	690	0.032	10	0.25	2.7	0.31	119
P4	H_2O	637	-	-	<0.01	-	0.06	-	-	-
P5	DMSO	679	681	691	0.059	10	0.29	2.7	0.35	120
P5	H_2O	636	-	-	<0.01	-	0.09	-	-	-
P6	DMSO	678	680	683	0.047	3	0.22	2.8	0.29	87
P6	H_2O	638	-	-	<0.01	-	0.04	-	-	-
P7	DMSO	679	682	688	0.032	6	0.41	2.7	0.50	130
P7	H_2O	636	-	-	<0.01	-	0.16		-	-

Table 4.2 Photodynamic parameters of P8-P11 in DMF and Water

PS	Solvent	λ_{abs}/nm	λ_{em}/nm	$\Phi_F \pm 0.02$[a]	$\Phi_\Delta \pm 0.03$[a]
P8	DMF	355, 628, 695	694	0.02	0.28
P8	H_2O	347, 637, 687	n.d.	< 0.01	0.04
P9	DMF	356, 612, 680	694	0.39	0.36
P9	H_2O	343, 631, 684	704	< 0.01	0.45
P10	DMF	357, 612, 680	694	0.14	0.46
P10	H_2O	344, 636, 684	705	< 0.01	0.74
P11	DMF	357, 612, 680	694	0.11	0.80
P11	H_2O	346, 637, 687	705	< 0.01	0.93

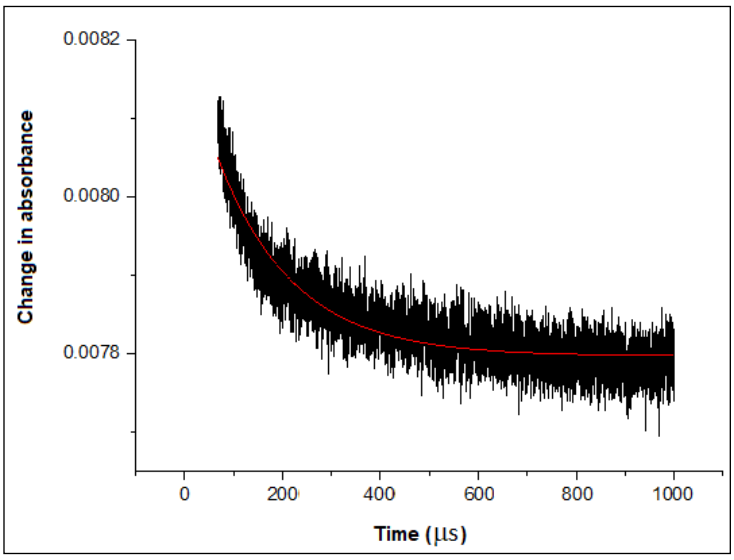

Figure 4.14 Triplet absorption decay (black) and fitting (red) curve for P3 in DMSO

4.6 Antimicrobial Photodynamic Activities in the Planktonic Phase

The photobactericidal activity of first series polymers (P3-P7) was investigated against gram-positive *S. aureus* and gram-negative *E. coli*. Figure 4.15 represents the survival percentage of *S. aureus* and *E. coli* in the presence of polymers (P4-P7). P3 did not show considerable activity against the studied bacteria cells because of the highly hydrophobic structure of the compound preventing make it soluble in studied media and affecting the penetration ability of it into the cell wall and membrane [112]. P5 which has 1:2 ZnPc and triphenylphosphonium moiety in the backbone showed the highest activity against *S. aureus and E. coli* after irradiation for 20 min intervals up to 80 min with the log reduction value of 9.67 against *S. aureus* and 10.42 against *E. coli*. (Table 4.3). Introducing lower triphenyl phosphonium units in the backbone (P4 and P6) resulted in drops in activity against both types of bacteria. The activity of the first series polymers was in the order P5>P4>P6 and it follows the overall cationic units. While copolymer P5 showed complete loss of *S. aureus* and *E. coli* with a concentration of 1 μg/mL and 10 μg/mL after 80 min irradiation, the *S. aureus* cell viability reduced to 0.12% with P4, and 0.72% for P6. The *E. coli* cell viability reduced to 1.9% with P4, and 6.21% with P6. It can be concluded that the presence of triphenylphoshonium based cationic polyelectrolyte units activate the action

through the π-π and rigid aromatic functional groups with the negatively charged bacteria cell membrane. Further to confirm this hypothesis, triethylphosphonium and ZnPc based copolymer (P7) with the same molecular weight and ratio of each repeating unit was synthesized and compared to P5. Surprisingly, P7 indicated the complete loss of *S. aureus* cells under light condition like P5, however killing efficiency against *E. coli* was low (52.25%). These results showed that aromatic phosphonium side chains in P5 provided better antimicrobial activity compared to alkyl phosphonium side chains in P7 which is in agreement with previous studies.

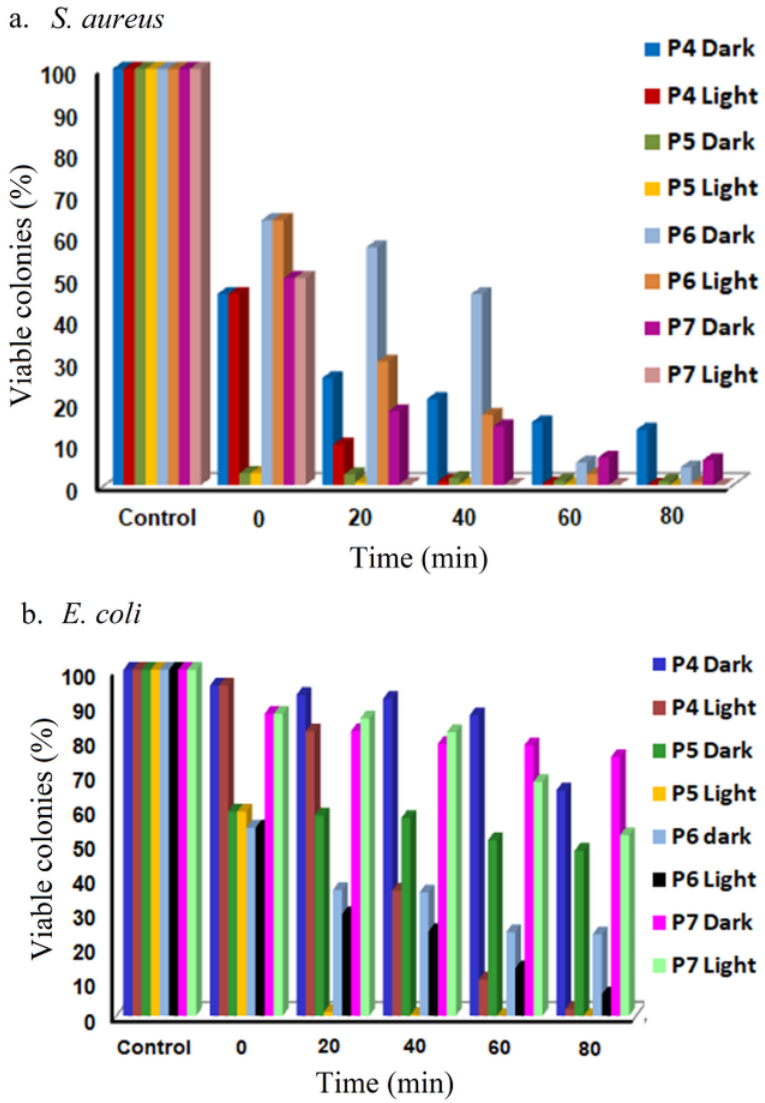

Figure 4.15 Antimicrobial activities of copolymers (P4-P7) (a) against *S. aureus* (b) against *E. coli*

Table 4.3 Log reduction and percentage cell survival (% survival) values of *S. aureus* and *E. coli* after 80 min irradiation in the presence of first series polymers (P3-P7)

Polymers	*S. aureus*					*E. coli*				
	Conc. (μg/mL)	Log reduction		Cell Survival (%)		Conc. (μg/mL)	Log reduction		Cell Survival (%)	
		D	L	D	L		D	L	D	L
P4	10	0.88	2.92	13,35	0,12	100	0.19	1.72	65.15	1.92
P5	1	2.02	9.67	0.97	0	10	0.32	10.42	47.72	0
P6	20	1.37	2.14	4.30	0.72	200	0.63	1.21	23.6	6.21
P7	2.5	1.22	9.67	6.05	0	25	0.13	0.29	74.81	52.27

The photobactericidal activity of the second series polymers (P8-P11) was investigated against gram-positive *B. subtilis* and gram-negative *E. coli*. Bacteria were incubated with different amounts of the polymers pre-dissolved in DMSO and diluted with water (< 0.1% final concentration of DMSO and 1-10 μg/mL P8-P11) and then irradiated with red light or kept in the dark for the same duration. Cells were irradiated with a very low light intensity of 10 mW/cm^2, corresponding to a total light dose of 18 J/cm^2 (Figure 4.16). P11 showed complete inactivation of *B. subtilis* at a concentration of 10 μg/mL and enhanced activity even at a lower concentration with a $\log_{10}$ reduction value of 5.3 and 3.3 for 5 and 1 μg/mL, respectively, while polymer P10 with higher content of ZnPc gave $\log_{10}$ reduction values of 6.8, 4.1 and 1.1 for 10, 5 and 1 μg/mL final concentrations, respectively. A significantly lower effect was observed for P9 (2.4 at 10 μg/mL), while P8 was found to be inactive. The highest activity against *E. coli* was obtained with P10 and P11 at a concentration of 10 μg/mL, achieving a reduction of 5.7 and 4.2 $\log_{10}$, respectively. These results clearly indicate that the increased activity of the polymers is due to the generation of ROS. The higher activity of P11 and P10 in the presence of light compared to P9 and P8 supports the idea of better binding of these polymers to bacteria due to the higher number of positive charges present

in the structure, leading also to activity in the dark. The presence of a larger number of bulky and charged TPPs as well as the presence of PEG chains on the Pc macrocycle also contributes to ZnPc being in a more monomeric form and generating more singlet oxygen.

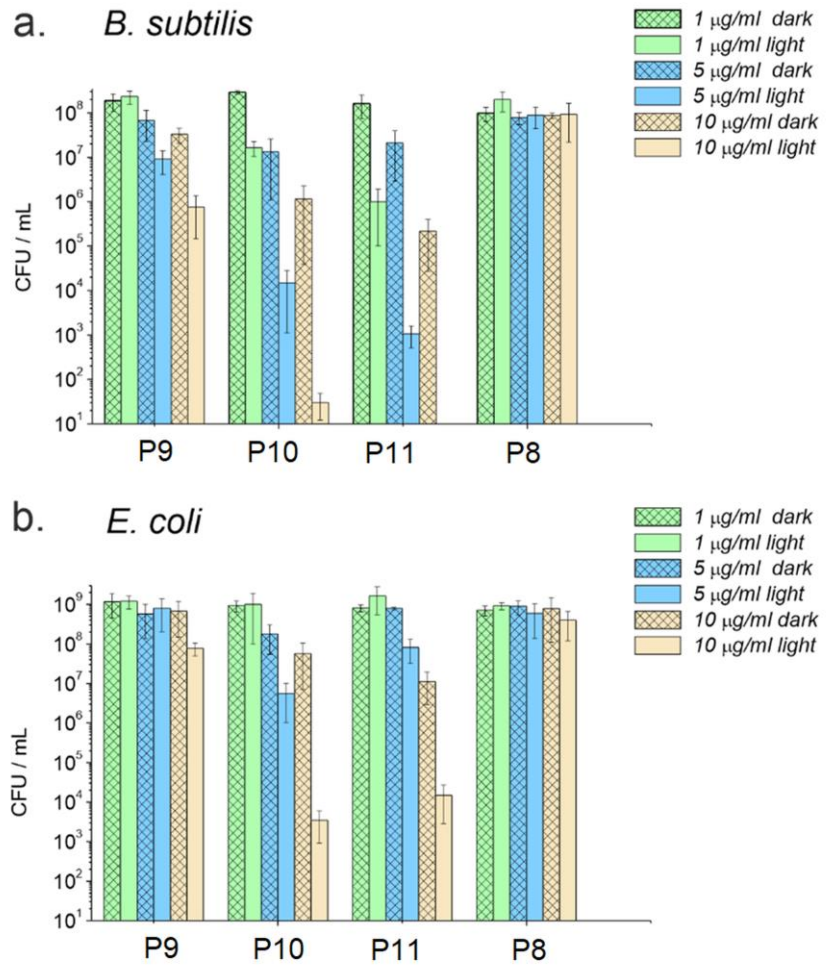

Figure 4.16 (a) Viability of *B. subtilis* (b) Viability of *E. coli* in dark and after irradiation in the presence of P8-P11. Overall light dose 18 J/cm^2

4.7 Antimicrobial Photodynamic Activities in Biofilms

As many as 65% of infectious diseases in humans are estimated to be caused by biofilms [113] that are characterized by rapidly evolving resistance to available antibacterial agents and are extremely difficult to treat [114]. This is due to the ability of bacteria to form densely packed, multicellular communities encapsulated in extracellular polymeric substances (EPS) that protect them from ambient environmental stresses leading to increased resistance to known antibacterial

agents [115]. Therefore, new strategies for the effective elimination of biofilms are urgently needed. The cationic photoactive polymers not only bind efficiently to bacteria, improving the efficacy of the photodynamic effect but also have the potential to increase the effectiveness of the PS in penetrating and eliminating bacterial biofilms [116].

The viability of bacteria in the biofilm was investigated using the 2,3-bis (2-methoxy-4-nitro-5-sulfophenyl)-5-[(phenylamino) carbonyl]- 2H-tetrazolium hydroxide (XTT) assay, which measures the reduction of water-soluble formazan in viable cells. The results allow read-out of the absorbance measurement to be made straight away, which makes the method efficient and quite easy to use [117]. To test the destructive effect of the second series polymers (P8-P11) on biofilms, a corresponding amount of polymer (1 - 50 μg/mL) was incubated with 72 hours grown biomass of *B. subtilis* or *E. coli* and irradiated using the same irradiation scheme as for planktonic cultures (30 minutes, total light dose 18 J/cm^2). Remarkable activity in reducing the viability of bacteria in biofilms was observed for P10 and P11. The viability of bacteria in *B. subtilis* biofilms is reduced by 78% and 88% after treatment with 50 μg/mL of P10 and P11, respectively. The reduction in viability of *E. coli* in biofilms using the same concentration was even higher - 91% and 90% for P10 and P11, respectively. It is worth noting that to achieve higher values for bacteria viability reduction in biofilms, higher concentrated polymer solutions were used. While P10 and P11 at 10 μg /mL were found to be sufficient to achieve an antibacterial effect in planktonic cultures, at this concentration the viability of *B. subtilis* in the biofilm was reduced by about 33% and 44%, and for *E. coli* by 68% and 62%, respectively (Figure 4.17). The contrasting inactivation profiles for gram-positive and gram-negative bacteria in planktonic culture and biofilm may be related to the ability of *B. subtilis* to form a more robust biofilm than *E. coli*.

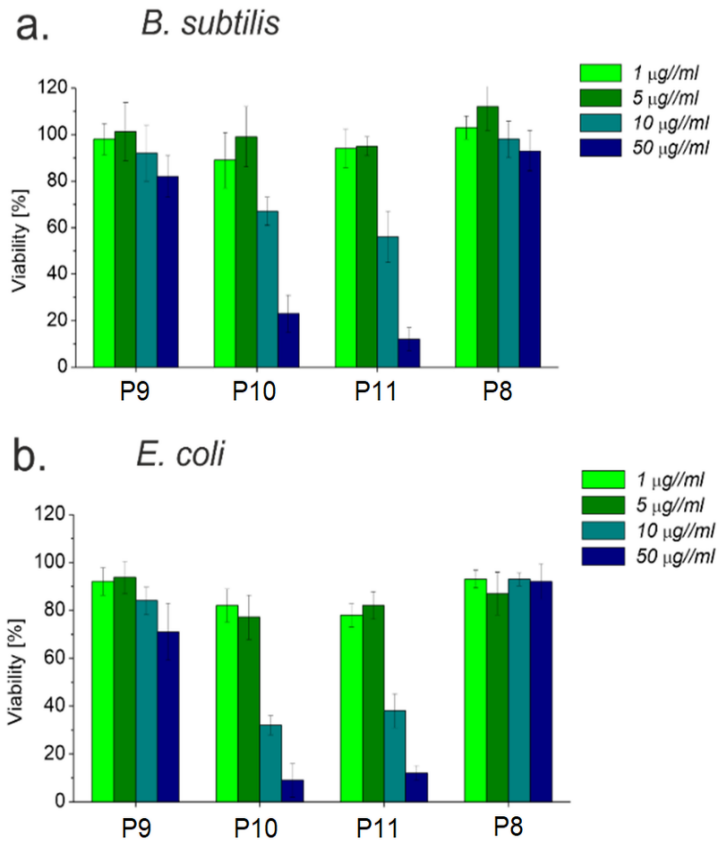

Figure 4.17 (a) Viability of *B. subtilis* (b) Viability of *E. coli* in biofilms

4.8 Bacteria Imaging Studies

The polymer-bacteria interaction of P5 on *S. aureus* was confirmed by SEM. In Figure 4.18a, we can see the characteristic grape shape of *S. aureus* because of applying subMIC concentration. At a concentration of MIC value (Figure 4.18b), significant morphological changes were clearly seen and it has been observed that bacteria damage especially at the supraMIC concentration. (Figure 4.18c).

The SYTO9-PI live/dead assay was used concomitantly to qualitatively assess cell viability after incubation with the second series polymers (P8-P11) at 10 µg/mL concentration and under irradiation. While SYTO9 can stain the nucleic acid of live and dead gram-positive and gram-negative bacteria, PI only labels dead cells, owing to the ability of this dye to penetrate the cell membrane of dead cells but being excluded from live cells. As shown in Figure 4.19 and 4.20, the P10 and P11 treatment groups had a large amount of red-stained dead cells. In groups P9 and

P8, there were almost no dead bacterial cells. This result is consistent with the results of the colony counting method. Overall, these results confirmed that P10 and P11 are promising PSs with excellent antibacterial properties.

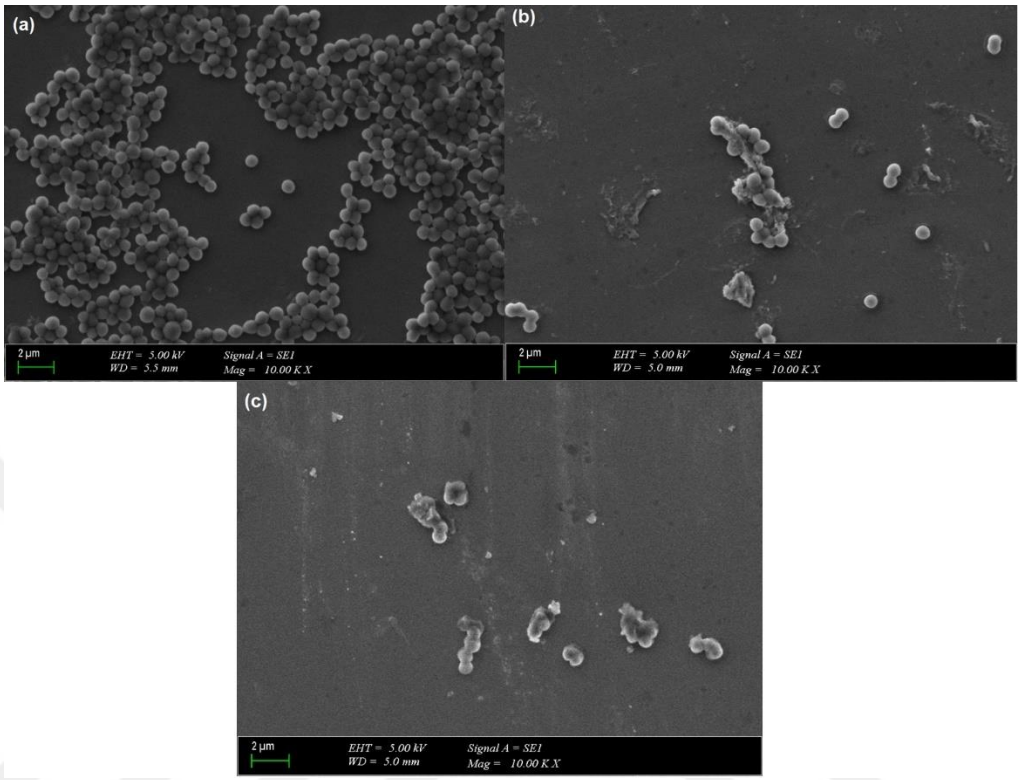

Figure 4.18 SEM micrographs of (a) *S. aureus* untreated (b) *S. aureus* treated by P5 at MIC value (c) *S. aureus* treated by P5 at supra-MIC value

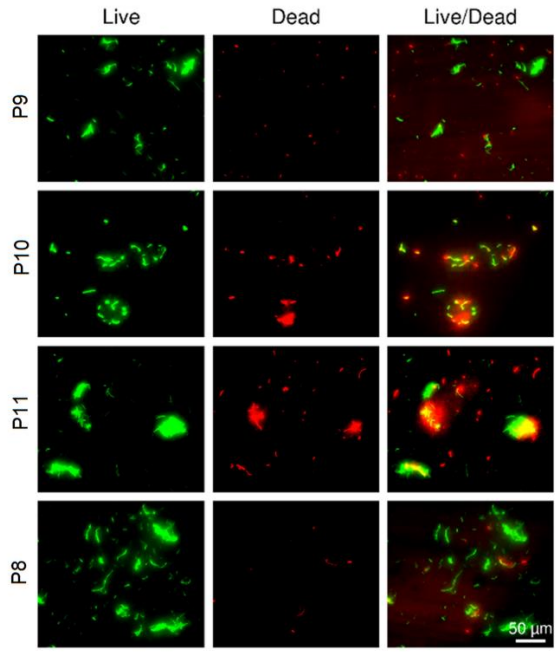

Figure 4.19 Fluorescence microscopy images of Live/Dead stained *B. subtilis* after incubation with 10 μg/mL of corresponding polymers and irradiation with red light of 18 J/cm^2 doses

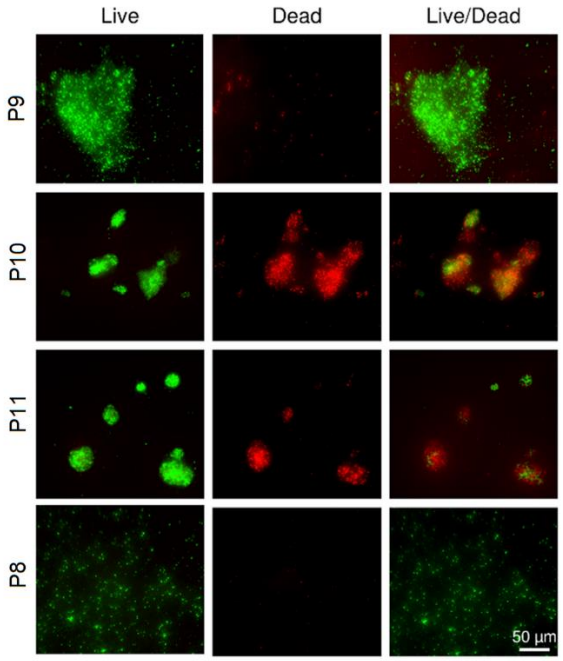

Figure 4.20 Fluorescence microscopy images of Live/Dead stained *E. coli* after incubation with 10 μg/mL of corresponding polymers and irradiation with red light of 18 J/cm^2 doses

4.9 Conclusion

In this thesis, ZnPc-PON conjugates with varying compositions were synthesized by ROMP in order to study their photophysical, photochemical and aPDT activities. In the first section, homopolimer and copolymers containing ZnPc with hydrophobic *tert*-butyl groups and cationic phosphonium groups were synthesized and characterized. The photophysicochemical studies showed that P5 and P7 containing mostly triphenyl units in their backbone have the highest singlet oxygen quantum and triplet quantum yield values. In addition, it seemed that the same increase in the amount of cationic triphenylphosphonium moiety in the copolymers lead to higher antibacterial activity. P5 exhibited the highest activity against *S. aureus* and *E. coli*. On the other hand, enhanced biocidal activity was achieved with P5 and P7 under irradiation. while P5 accomplished complete inactivation of *S. aureus* and *E. coli* at 1 μg/mL and 10 μg/mL respectively, P7 had the same success *S. aureus* at 2.5 μg/mL. In the second section, the synthesis and characterization of the homopolymer and copolymers bearing ZnPc with PEG groups and cationic phosphonium groups were carried out. The photophysicochemical measurements indicated that rather than the amount of PS in the polymer chain, the proper balance between the cationic TPP and ZnPc with PEG units played a crucial role in the huge increase in singlet oxygen quantum yield reaching 0.93 in water. Furthermore, these values showed themselves in biocidal activity, and excellent results were obtained with polymers where the ratio between ZnPc and TPP units was 1:1 (P10) or 1:2 (P11). Especially, P11 achieved complete inactivation of *B. subtilis* at 10 μg/mL irradiated with very low light intensity. It is clearly seen that the synergistic effect of ZnPc-triphenyl phosphonium-based copolymers caused complete damage of bacterial strain with multifunctional interaction; electrostatic interaction, hydrophobic interaction and formation of ROS.

REFERENCES

[1] C. Deusenbery, Y. Wang, and A. Shukla, "Recent innovations in bacterial infection detection and treatment, "*ACS Infectious Diseases,* vol. 7, no. 4, pp. 695-720, 2021.

[2] T. R. McCulloch, T. J. Wells, and F. Souza-Fonseca-Guimaraes, "Towards efficient immunotherapy for bacterial infection," *Trends in Microbiology,* vol. 30, no. 2, pp. 158-169, 2022.

[3] A. E. Madkour, J. M. Dabkowski, K. Nüsslein, and G. N. Tew, "Fast disinfecting antimicrobial surfaces," *Langmuir,* vol. 25, no. 2, pp. 1060-1067, 2009.

[4] R. Namivandi-Zangeneh, E. H. Wong, and C. Boyer, "Synthetic antimicrobial polymers in combination therapy: tackling antibiotic resistance," *ACS Infectious Diseases,* vol. 7, no. 2, pp. 215-253, 2021.

[5] A. S. Akalın, "Dairy-derived antimicrobial peptides: Action mechanisms, pharmaceutical uses and production proposals," *Trends in Food Science & Technology,* vol. 36, no. 2, pp. 79-95, 2014.

[6] M. F. Ilker, K. Nüsslein, G. N. Tew, and E. B. Coughlin, "Tuning the hemolytic and antibacterial activities of amphiphilic polynorbornene derivatives," *Journal of the American Chemical Society,* vol. 126, no. 48, pp. 15870-15875, 2004.

[7] N. C. Süer, C. Demir, N. A. Ünübol, Ö. Yalçın, T. Kocagöz, and T. Eren, "Antimicrobial activities of phosphonium containing polynorbornenes," *RSC Advances,* vol. 6, no. 89, pp. 86151-86157, 2016.

[8] S. Colak, C. F. Nelson, K. Nüsslein, and G. N. Tew, "Hydrophilic modifications of an amphiphilic polynorbornene and the effects on its hemolytic and antibacterial activity," *Biomacromolecules,* vol. 10, no. 2, pp. 353-359, 2009.

[9] F. Cieplik, D. Deng, W. Crielaard, W. Buchalla, E. Hellwig, A. Al-Ahmad and T. Maisch, "Antimicrobial photodynamic therapy–what we know and what we don't," *Critical Reviews in Microbiology,* vol. 44, no. 5, pp. 571-589, 2018.

[10] M. B. Spesia and E. N. Durantini, "Evolution of Phthalocyanine Structures as Photodynamic Agents for Bacteria Inactivation," *The Chemical Record,* vol. 22, no. 4, p. e202100292, 2022.

[11] E. T. Carrera, H. B. Dias, S. C. T. Corbi, R. A. C. Marcantonio, A. C. A. Bernardi, V. S. Bagnato, M. R. Hamblin and A. N. S. Rastelli, "The application of antimicrobial photodynamic therapy (aPDT) in dentistry: a critical review," *Laser Physics,* vol. 26, no. 12, p. 123001, 2016.

[12] S. N. Nyamu, L. Ombaka, E. Masika, and M. Ng'ang'a, "Antimicrobial photodynamic activity of phthalocyanine derivatives," *Advances in Chemistry,* vol. 2018, 2018.

[13] L. B. d. O. de Siqueira, A. P. dos Santos Matos, M. R. M. da Silva, S. R. Pinto, R. Santos-Oliveira and E. Ricci-Júnior, "Pharmaceutical Nanotechnology Applied to Phthalocyanines for the Promotion of the Antimicrobial Photodynamic Therapy: A Literature Review," *Photodiagnosis and Photodynamic Therapy,* p. 102896, 2022.

[14] H. Lin, J. Chen, Y. Zhang, A. Ulla, J. Liu, F. Lin, L. Jiang and M. Huang, "Enhanced anti-microbial effect through cationization of a mono-triazatricyclodecane substituted asymmetric phthalocyanine," *Journal of Inorganic Biochemistry,* vol. 189, pp. 192-198, 2018.

[15] V. Kussovski, V. Mantareva, I. Angelov, P. Orozova, D. Wöhrle, G. Schnurpfeil, E. Borisova and L. Avramov, "Photodynamic inactivation of Aeromonas hydrophila by cationic phthalocyanines with different hydrophobicity," *FEMS Microbiology Letters,* vol. 294, no. 2, pp. 133-140, 2009.

[16] N. B. McKeown, "Phthalocyanine-containing polymers," *Journal of Materials Chemistry,* vol. 10, no. 9, pp. 1979-1995, 2000.

[17] D. Wöhrle, "Porphyrins, phthalocyanines and related systems in polymer phases," *Journal of Porphyrins and Phthalocyanines,* vol. 4, no. 4, pp. 418-424, 2000.

[18] D. Wöhrle, "Phthalocyanines in macromolecular phases–methods of synthesis and properties of the materials," *Macromolecular Rapid Communications,* vol. 22, no. 2, pp. 68-97, 2001.

[19] J. Zhang, L. Wang, C. Li, Y. Li, J. Liu, Y. Tu, W. Zhang, N. Zhou and X. Zhu, "Preparation and characterization of solution processable phthalocyanine-containing polymers via a combination of RAFT polymerization and post-polymerization modification techniques," *Journal of Polymer Science Part A: Polymer Chemistry,* vol. 52, no. 5, pp. 691-698, 2014.

[20] C. W. Bielawski and R. H. Grubbs, "Living ring-opening metathesis polymerization," *Progress in Polymer Science,* vol. 32, no. 1, pp. 1-29, 2007.

[21] S. Sutthasupa, M. Shiotsuki, and F. Sanda, "Recent advances in ring-opening metathesis polymerization, and application to synthesis of functional materials," *Polymer Journal,* vol. 42, no. 12, pp. 905-915, 2010.

[22] M. Kimura, H. Ueki, K. Ohta, K. Hanabusa, H. Shirai and N. Kobayashi, "Aggregation behavior of amphiphilic phthalocyanine block copolymers," *Langmuir,* vol. 18, no. 20, pp. 7683-7687, 2002.

[23] A. de la Escosura, M. V. Martínez-Díaz, T. Torres, R. H. Grubbs, D. M. Guldi, H. Neugebauer, C. Winder, M. Drees and N. S. Sariciftci, "New donor–acceptor materials based on random polynorbornenes bearing pendant phthalocyanine and fullerene units," *Chemistry–An Asian Journal,* vol. 1, no. 1-2, pp. 148-154, 2006.

[24] X. Chen, I. Salmon, Thaddeus R and D. V. McGrath, "Asymmetric phthalocyanine synthesis by ROMP-capture-release," *Organic Letters,* vol. 11, no. 10, pp. 2061-2064, 2009.

[25] A. Dag, E. Cakilkaya, P. S. O. Ozgen, S. Atasoy, G. Y. Erdem, B. Cetin, A. Ç. Kokuroğlu and A. G.Gürek, "Phthalocyanine-conjugated glyconanoparticles for chemo-photodynamic combination therapy," *Biomacromolecules,* vol. 22, no. 4, pp. 1555-1567, 2021.

[26] Z. Lu, X. Zhang, Y. Zhao, Y. Xue, T. Zhai, Z. Wu and C. Li, "BODIPY-based macromolecular photosensitizer with cation-enhanced antibacterial activity," *Polymer Chemistry,* vol. 6, no. 2, pp. 302-310, 2015.

[27] P. R. Judzewitsch, N. Corrigan, E. H. Wong and C. Boyer, "Photo-Enhanced Antimicrobial Activity of Polymers Containing an Embedded Photosensitiser," *Angewandte Chemie,* vol. 133, no. 45, pp. 24450-24458, 2021.

[28] Z. Xu, L. Mei, Y. Shi, M. Yun, Y. Luan, Z. Miao, Z. Liu, X. Li and M. Jiao, "Multivalent Phthalocyanine-Based Cationic Polymers with Enhanced Photodynamic Activity for the Bacterial Capture and Bacteria-Infected Wound Healing," *Biomacromolecules,* vol. 23, pp. 2778−2784, 2022.

[29] K. Strokov and A. Galstyan, "Chitosan-Silicon Phthalocyanine Conjugate as Effective Photo-Functional Hydrogel for Tracking and Killing of Bacteria," *European Journal of Organic Chemistry,* vol. 2020, no. 47, pp. 7327-7332, 2020.

[30] W. Tong, Y. Xiong, S. Duan, X. Ding, and F.-J. Xu, "Phthalocyanine functionalized poly (glycidyl methacrylate) nano-assemblies for photodynamic inactivation of bacteria," *Biomaterials Science,* vol. 7, no. 5, pp. 1905-1918, 2019.

[31] L. R. Johnson and M. Mangel, "Life histories and the evolution of aging in bacteria and other single-celled organisms," *Mechanisms of Ageing and Development,* vol. 127, no. 10, pp. 786-793, 2006.

[32] K. H. Schleifer, "Classification of Bacteria and Archaea: past, present and future," *Systematic and Applied Microbiology,* vol. 32, no. 8, pp. 533-542, 2009.

[33] B. Biswas, P. Basu and M. Pal, "Gram staining and its molecular mechanism," *International Review of Cytology,* vol. 29, pp. 1-27, 1970.

[34] T. Gregersen, "Rapid method for distinction of Gram-negative from Gram-positive bacteria," *European Journal of Applied Microbiology and Biotechnology,* vol. 5, no. 2, pp. 123-127, 1978.

[35] Y. Tang, T. S. Corbitt, A. Parthasarathy, Z. Zhou, K. S. Schanze and D. G. Whitten, "Light-induced antibacterial activity of symmetrical and asymmetrical oligophenylene ethynylenes," *Langmuir,* vol. 27, no. 8, pp. 4956-4962, 2011.

[36] R. C. James, J. G. Pierce, A. Okano, J. Xie and D. L. Boger, "Redesign of glycopeptide antibiotics: back to the future," *ACS Chemical Biology*, vol. 7, pp. 797-804, 2012.

[37] G. Taubes, "The bacteria fight back," *American Association for the Advancement of Science*, 2008.

[38] G. Cope and A. Cope, "Antibiotic resistance and how to act on it," *Dental Nursing,* vol. 9, no. 12, pp. 706-709, 2013.

[39] L.-j. Zhang and R. L. Gallo, "Antimicrobial peptides," *Current Biology,* vol. 26, no. 1, pp. R14-R19, 2016.

[40] A. Kaymaz, "1,4-Diazabisiklo[2.2.2] Oktan Esasli Katyonik Polimerlerin Halka Açilma Metatez Polimerizasyonu Metodu İle Sentezi Ve Antibakteriyel Etkinliklerinin İncelenmesi," Master Thesis, 2017.

[41] A. R. Koczulla and R. Bals, "Antimicrobial peptides," *Drugs,* vol. 63, no. 4, pp. 389-406, 2003.

[42] A. Izadpanah and R. L. Gallo, "Antimicrobial peptides," *Journal of the American Academy of Dermatology,* vol. 52, no. 3, pp. 381-390, 2005.

[43] A. A. Bahar and D. Ren, "Antimicrobial peptides," *Pharmaceuticals,* vol. 6, no. 12, pp. 1543-1575, 2013.

[44] C. D. Fjell, J. A. Hiss, R. E. Hancock and G. Schneider, "Designing antimicrobial peptides: form follows function," *Nature Reviews Drug Discovery,* vol. 11, no. 1, pp. 37-51, 2012.

[45] K. Lienkamp, A. E. Madkour, A. Musante, C. F. Nelson, K. Nusslein and G. N. Tew, "Antimicrobial polymers prepared by ROMP with unprecedented selectivity: a molecular construction kit approach," *Journal of the American Chemical Society,* vol. 130, no. 30, pp. 9836-9843, 2008.

[46] P. Jean-Louis Hérisson and Y. Chauvin, "Catalyse de transformation des oléfines par les complexes du tungstène. II. Télomérisation des oléfines cycliques en présence d'oléfines acycliques," *Die Makromolekulare Chemie: Macromolecular Chemistry and Physics,* vol. 141, no. 1, pp. 161-176, 1971.

[47] D. H. McConville, J. R. Wolf and R. R. Schrock, "Synthesis of chiral molybdenum ROMP initiators and all-cis highly tactic poly (2, 3-(R) 2norbornadiene)(R= CF_3 or CO_2Me)," *Journal of the American Chemical Society,* vol. 115, no. 10, pp. 4413-4414, 1993.

[48] P. Schwab, M. B. France, J. W. Ziller and R. H. Grubbs, "A Series of Well-Defined Metathesis Catalysts–Synthesis of [RuCl2 (=CHR′)(PR_3)$_2$] and Its Reactions," *Angewandte Chemie International Edition in English,* vol. 34, no. 18, pp. 2039-2041, 1995.

[49] N. C. Süer, "Fosfonyum Gruplari İçeren Romp Polimerlerinin Sentezi, Karakterizasyonu Ve Antibakteriyel Etkinliklerinin İncelenmesi," Master Thesis, 2015.

[50] T. Matsuo, "Functionalization of Ruthenium Olefin-Metathesis Catalysts for Interdisciplinary Studies in Chemistry and Biology," *Catalysts,* vol. 11, no. 3, p. 359, 2021.

[51] N. C. Süer, "Biyosensör Ve Antibakteriyel Özellik Gösteren Polimerlerin Sentezi Ve Uygulaması," Doctorate Thesis, 2021.

[52] R. Bonnett, "Chemical Aspects of Photodynamic Therapy," vol. 1, 2000.

[53] I. J. Macdonald and T. J. Dougherty, "Basic principles of photodynamic therapy," *Journal of Porphyrins and Phthalocyanines,* vol. 5, no. 02, pp. 105-129, 2001.

[54] A. Galstyan, "Turning Photons into Drugs: Phthalocyanine-Based Photosensitizers as Efficient Photoantimicrobials," *Chemistry–A European Journal,* vol. 27, no. 6, pp. 1903-1920, 2021.

[55] C. P. McCoy, E. J. O'Neil, J. F. Cowley, L. Carson, A. T. De Baroid, G. T. Gdowski, S. P. Gorman and D. S. Jones, "Photodynamic antimicrobial polymers for infection control," *PloS one,* vol. 9, no. 9, p. e108500, 2014.

[56] M. R. Hamblin and H. Abrahamse, "Oxygen-independent antimicrobial photoinactivation: Type III photochemical mechanism?," *Antibiotics,* vol. 9, no. 2, p. 53, 2020.

[57] R. Youf, M. Müller, A. Balasini, F. Thétiot, M. Müller, A. Hascoët, U. Jonas, H. Schönherr, G. Lemercier, T. Montier and T. Le Gall, "Antimicrobial photodynamic therapy: Latest developments with a focus on combinatory strategies," *Pharmaceutics,* vol. 13, no. 12, p. 1995, 2021.

[58] E. N. Kaya, "Fotodinamik Terapi İle Kanser Tedavisine Yönelik Çok Fonksiyonlu Fotosensitizerlerin Sentezi Ve Özelliklerinin İncelenmesi," Doctorate Thesis, 2020.

[59] C. Leznoff and A. Lever, *Properties and Applications*. VCH, New York, 1989.

[60] N. B. McKeown, *Phthalocyanine materials: synthesis, structure and function* (no. 6). Cambridge university press, 1998.

[61] A. Lever, "The phthalocyanines," *Advances in Inorganic Chemistry and Radiochemistry,* vol. 7, pp. 27-114, 1965.

[62] A. Atsay, "Hekzadeka Sübstitüe Ftalosiyaninlerin X-Işını Kristallografisi ve Nmr Spektroskopisi ile Yapısal Özelliklerinin İncelenmesi," Doctorate Thesis, 2015.

[63] N. Kobayashi, "Phthalocyanines," *Current opinion in solid state and materials science,* vol. 4, no. 4, pp. 345-353, 1999.

[64] A. Kalkan, "Bifenil Sübstitüentler İçeren Ftalosiyaninler," Doctorate Thesis, 2007.

[65] E. Ahmetali, "3,5-Bis(Triflorometil)Fenoksi Gruplari İçeren Simetrik Ve Asimetrik Çinko Ftalosiyaninlerin Sentezi Ve Karakterizasyonu," Master Thesis, 2017.

[66] T. C. Canak, D. Yeşildağ, I. Nar, E. Hamuryudan and I. E. Serhatli, "Synthesis of tetrakis bromine terminated phthalocyanine and its methyl methacrylate polymers via ATRP," *Turkish Journal of Chemistry,* vol. 43, no. 3, pp. 911-925, 2019.

[67] P. M. Budd, S. M. Makhseed, B. S. Ghanem, K. J. Msayib, C. E. Tattershall and N. B. McKeown, "Microporous polymeric materials," *Materials Today,* vol. 7, no. 4, pp. 40-46, 2004.

[68] N. B. McKeown, S. Makhseed and P. M. Budd, "Phthalocyanine-based nanoporous network polymers," *Chemical Communications,* no. 23, pp. 2780-2781, 2002.

[69] M. Nemakal and L. K. Sannegowda, "Biocompatible polymeric pyrazolopyrimidinium cobalt (II) phthalocyanine: An efficient electroanalytical platform for the detection of l-arginine," *Sensors and Actuators A: Physical,* vol. 324, p. 112690, 2021.

[70] K. N. Long, "The mechanics of network polymers with thermally reversible linkages," *Journal of the Mechanics and Physics of Solids,* vol. 63, pp. 386-411, 2014.

[71] R. J. Young and P. A. Lovell, *Introduction to polymers*. CRC press, 2011.

[72] S. Akiyama, "Molecular Design of Network Polymers," *Macromolecular Design of Polymeric Materials,* vol. 40, p. 393, 1997.

[73] V. Ahsen, E. Yilmazer and Ö. Bekâroğlu, "Synthesis and properties of (18-crown-6)-bridged phthalocyanine network polymers," *Die Makromolekulare Chemie: Macromolecular Chemistry and Physics,* vol. 189, no. 11, pp. 2533-2543, 1988.

[74] Giddaerappa, N. Manjunatha, Shantharaja, M. Hojamberdiev and L. K. Sannegowda, "Tetraphenolphthalein Cobalt (II) Phthalocyanine Polymer Modified with Multiwalled Carbon Nanotubes as an Efficient Catalyst for the Oxygen Reduction Reaction," *ACS Omega,* vol. 7, no. 16, pp. 14291-14304, 2022.

[75] S. Li, S. Dong, W. Xu, S. Tu, L. Yan, C. Zhao, J. Ding and Xuesi Chen, "Antibacterial hydrogels," *Advanced science,* vol. 5, no. 5, p. 1700527, 2018.

[76] E. M. Ahmed, "Hydrogel: Preparation, characterization, and applications: A review," *Journal of Advanced Research,* vol. 6, no. 2, pp. 105-121, 2015.

[77] F. Bayat, A. R. Karimi and T. Adimi, "Design of nanostructure chitosan hydrogels for carrying zinc phthalocyanine as a photosensitizer and difloxacin as an antibacterial agent," *International Journal of Biological Macromolecules,* vol. 159, pp. 598-606, 2020.

[78] A. R. Karimi, A. Khodadadi and M. Hadizadeh, "A nanoporous photosensitizing hydrogel based on chitosan cross-linked by zinc phthalocyanine: an injectable and pH-stimuli responsive system for effective cancer therapy," *RSC Advances,* vol. 6, no. 94, pp. 91445-91452, 2016.

[79] F. Bayat and A. R. Karimi, "Design of photodynamic chitosan hydrogels bearing phthalocyanine-colistin conjugate as an antibacterial agent," *International Journal of Biological Macromolecules,* vol. 129, pp. 927-935, 2019.

[80] S. K. Yang, A. V. Ambade and M. Weck, "Main-chain supramolecular block copolymers," *Chemical Society Reviews,* vol. 40, no. 1, pp. 129-137, 2011.

[81] K. A. Williams, A. J. Boydston and C. W. Bielawski, "Main-chain organometallic polymers: synthetic strategies, applications, and perspectives," *Chemical Society Reviews,* vol. 36, no. 5, pp. 729-744, 2007.

[82] Q. Yan, D. Han and Y. Zhao, "Main-chain photoresponsive polymers with controlled location of light-cleavable units: from synthetic strategies to structural engineering," *Polymer Chemistry,* vol. 4, no. 19, pp. 5026-5037, 2013.

[83] W. J. Youngblood, "Synthesis of a new trans-A2B2 phthalocyanine motif as a building block for rodlike phthalocyanine polymers," *The Journal of Organic Chemistry,* vol. 71, no. 9, pp. 3345-3356, 2006.

[84] G. Timothy, "Discotic liquid-crystal behaviour of some multinuclear phthalocyanine derivatives," *Journal of Materials Chemistry,* vol. 4, no. 2, pp. 209-216, 1994.

[85] J. L. G. Wade and J. W. Simek, *Organic Chemistry, 9e*. Pearson Education India, 2017.

[86] P. Kratochvil, R. Septo and U. Suter, "Glossary of basic terms in polymer science," *Pure and Applied Chemistry,* vol. 68, pp. 2287-2311, 1996.

[87] A. Bousquet, H. Awada, R. C. Hiorns, C. Dagron-Lartigau, and L. Billon, "Conjugated-polymer grafting on inorganic and organic substrates: A new trend in organic electronic materials," *Progress in Polymer Science,* vol. 39, no. 11, pp. 1847-1877, 2014.

[88] G. Ferraudi and A. Lappin, "Properties and chemical reactivity of metallo phthalocyanine and tetramethylbenzoannulene complexes grafted into a polymer backbone," *Journal of Coordination Chemistry,* vol. 67, no. 23-24, pp. 3822-3839, 2014.

[89] C. C. Leznoff and T. W. Hall, "The synthesis of a soluble, unsymmetrical phthalocyanine on a polymer support," *Tetrahedron Letters,* vol. 23, no. 30, pp. 3023-3026, 1982.

[90] J. M. Ren, T. G. McKenzie, Q. Fu, E. H. H. Wong, J. Xu, Z. An, S. Shanmugam, T. P. Davis, C. Boyer and G. G. Qiao, "Star polymers," *Chemical reviews,* vol. 116, no. 12, pp. 6743-6836, 2016.

[91] W. Wu, W. Wang and J. Li, "Star polymers: Advances in biomedical applications," *Progress in Polymer Science,* vol. 46, pp. 55-85, 2015.

[92] A. Bilgin and Ç. Yağcı, "Octa-armed star-shaped poly (ε-caprolactone) s with a phthalocyanine core by ring-opening polymerization: Synthesis and characterization," *European Polymer Journal,* vol. 61, pp. 240-252, 2014.

[93] J. Aimi, P. Wang, C. Shih, C. Huang, T. Nakanishi, M. Takeuchi, H. Hsuehe and W. Chen, "A star polymer with a metallo-phthalocyanine core as a tunable charge storage material for nonvolatile transistor memory devices," *Journal of Materials Chemistry C,* vol. 6, no. 11, pp. 2724-2732, 2018.

[94] Y. H. Gursel, B. F. Senkal, M. Kandaz and F. Yakuphanoglu, "Synthesis and liquid crystal properties of phthalocyanine bearing a star polytetrahydrofuran moiety," *Polyhedron,* vol. 28, no. 8, pp. 1490-1496, 2009.

[95] J. Wang, W. Dong, Q. Chen, Z. Si, X. Cui, D. Liu and Q. Duan, "Syntheses and nonlinear optical behavior of four-arm star-shaped phthalocyanine indium polymers containing azobenzene," *Dyes and Pigments,* vol. 194, p. 109632, 2021.

[96] H. Dinçer, H. Mert, B. N. Şen, A. Dağ and S. Bayraktar, "Synthesis and characterization of novel tetra terminal alkynyl-substituted phthalocyanines and their star polymers via click reaction," *Dyes and Pigments,* vol. 98, no. 2, pp. 246-254, 2013.

[97] F. He, Y. Tang, M. Yu, S. Wang, Y. Li and D. Zhu, "A strategy for the detection of Diels–Alder reactions using fluorescence quenching of conjugated polymers," *Advanced Functional Materials,* vol. 17, no. 6, pp. 996-1002, 2007.

[98] O. Tsaryova, A. Semioshkin, D. Wöhrle and V. I. Bregadze, "Synthesis of new carboran-based phthalocyanines and study of their activities in the photooxidation of citronellol," *Journal of Porphyrins and Phthalocyanines,* vol. 9, no. 04, pp. 268-274, 2005.

[99] Z. Q. Liu Tianjun, Cao Bo, C. Kangmin, "Bone-targeting zinc phthalocyanine and its preparation method and use," China, 2013.

[100] A. T. R. Williams, S. A. Winfield and J. N. Miller, "Relative fluorescence quantum yields using a computer-controlled luminescence spectrometer," *Analyst,* vol. 108, no. 1290, pp. 1067-1071, 1983.

[101] T. Nyokong, "Effects of substituents on the photochemical and photophysical properties of main group metal phthalocyanines," *Coordination Chemistry Reviews,* vol. 251, no. 13-14, pp. 1707-1722, 2007.

[102] R. Schmidt, "Photosensitized generation of singlet oxygen," *Photochemistry and Photobiology,* vol. 82, no. 5, pp. 1161-1177, 2006.

[103] M. C. DeRosa and R. J. Crutchley, "Photosensitized singlet oxygen and its applications," *Coordination Chemistry Reviews,* vol. 233, pp. 351-371, 2002.

[104] T. Nyokong and E. Antunes, "Photochemical and photophysical properties of metallophthalocyanines," in *Handbook of Porphyrin Science (Volume 7) with Applications to Chemistry, Physics, Materials Science, Engineering, Biology and Medicine*: World Scientific, 2010, pp. 247-357.

[105] M. D. Maree, N. Kuznetsova and T. Nyokong, "Silicon octaphenoxyphthalocyanines: photostability and singlet oxygen quantum yields," *Journal of Photochemistry and Photobiology A: Chemistry,* vol. 140, no. 2, pp. 117-125, 2001.

[106] I. Seotsanyana-Mokhosi, N. Kuznetsova and T. Nyokong, "Photochemical studies of tetra-2, 3-pyridinoporphyrazines," *Journal of Photochemistry and Photobiology A: Chemistry,* vol. 140, no. 3, pp. 215-222, 2001.

[107] D. Çakır, V. Çakır, Z. Bıyıklıoğlu, M. Durmuş and H. Kantekin, "New water soluble cationic zinc phthalocyanines as potential for photodynamic therapy of cancer," *Journal of Organometallic Chemistry,* vol. 745, pp. 423-431, 2013.

[108] L. Chen, Y. Zhao, X. Sun, J. Jiang, F. Wu and K. Wang, "Synthesis, singlet oxygen generation and DNA photocleavage of β, β′-conjugated polycationic porphyrins," *Journal of Porphyrins and Phthalocyanines,* vol. 23, no. 06, pp. 655-663, 2019.

[109] A. Galstyan and U. Dobrindt, "Breaching the wall: morphological control of efficacy of phthalocyanine-based photoantimicrobials," *Journal of Materials Chemistry B,* vol. 6, no. 28, pp. 4630-4637, 2018.

[110] K. Strokov, A. H. Schäfer, U. Dobrindt and A. Galstyan, "Facile fabrication of silicon (IV) phthalocyanine-embedded poly (vinyl alcohol)-based antibacterial and antifouling interfaces," *ACS Applied Bio Materials,* vol. 3, no. 6, pp. 3751-3760, 2020.

[111] C. Zhang, J. Zhao, S. Wu, Z. Wang, W. Wu, J. Ma, S. Guo and L. Huang, "Intramolecular RET enhanced visible light-absorbing bodipy organic triplet photosensitizers and application in photooxidation and triplet–triplet annihilation upconversion," *Journal of the American Chemical Society,* vol. 135, no. 28, pp. 10566-10578, 2013.

[112] D. Liua, L. Lic, J. Chena, Z. Chena, L. Jiangd, C. Yuand and M. Huang, "Dissociation of zinc phthalocyanine aggregation on bacterial surface is key for photodynamic antimicrobial effect," *Journal of Porphyrins and Phthalocyanines,* vol. 22, no. 09n10, pp. 925-934, 2018.

[113] H.-S. Joo and M. Otto, "Molecular basis of in vivo biofilm formation by bacterial pathogens," *Chemistry & Biology,* vol. 19, no. 12, pp. 1503-1513, 2012.

[114] N. Høiby, T. Bjarnsholt, M. Givskov, S. Molin and O. Ciofu, "Antibiotic resistance of bacterial biofilms," *International journal of antimicrobial agents,* vol. 35, no. 4, pp. 322-332, 2010.

[115] H.-C. Flemming and J. Wingender, "The biofilm matrix," *Nature Reviews Microbiology,* vol. 8, no. 9, pp. 623-633, 2010.

[116] A. Gupta, S. Mumtaz, C.-H. Li, I. Hussain and V. M. Rotello, "Combatting antibiotic-resistant bacteria using nanomaterials," *Chemical Society Reviews,* vol. 48, no. 2, pp. 415-427, 2019.

[117] D. A. Scudiere, R. H. Shoemaker, K. D. Paul, A. Monks, S. Tierney, T. H. Nofziger, M. J. Currens, D. Seniff and M. R. Boyd, "Evaluation of a soluble tetrazolium/formazan assay for cell growth and drug sensitivity in culture using human and other tumor cell lines," *Cancer Research,* vol. 48, no. 17, pp. 4827-4833, 1988.

A
SPECTRA

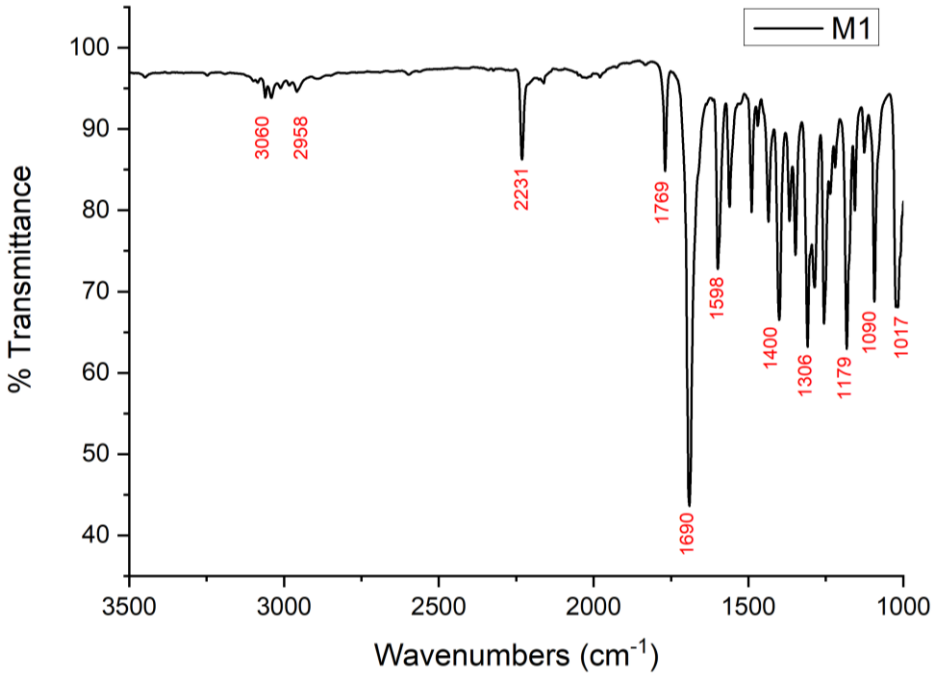

Figure A.1 Infrared spectrum of compound M1

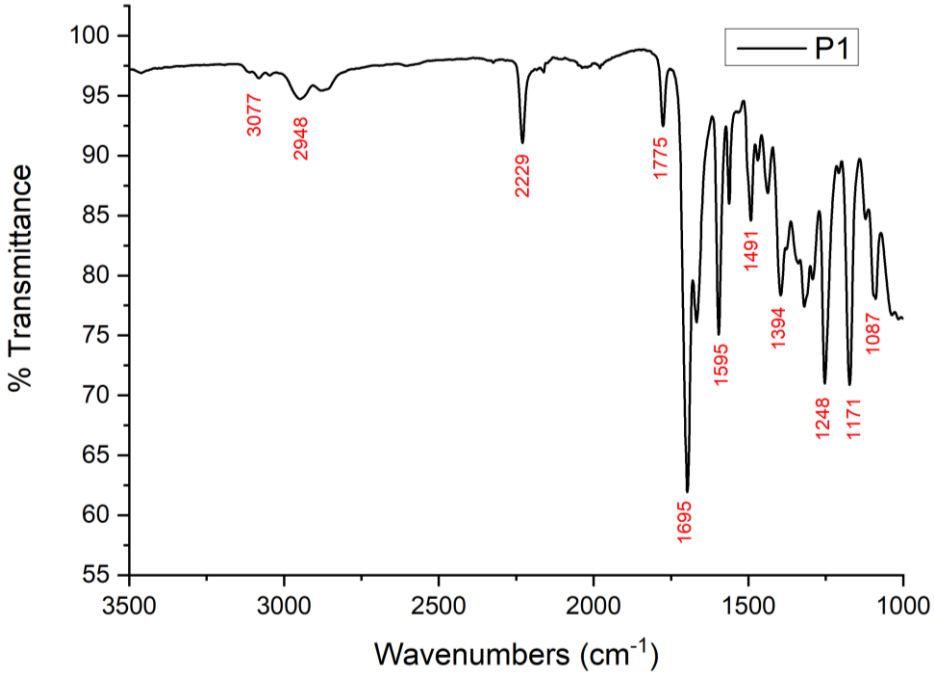

Figure A.2 Infrared spectrum of compound P1

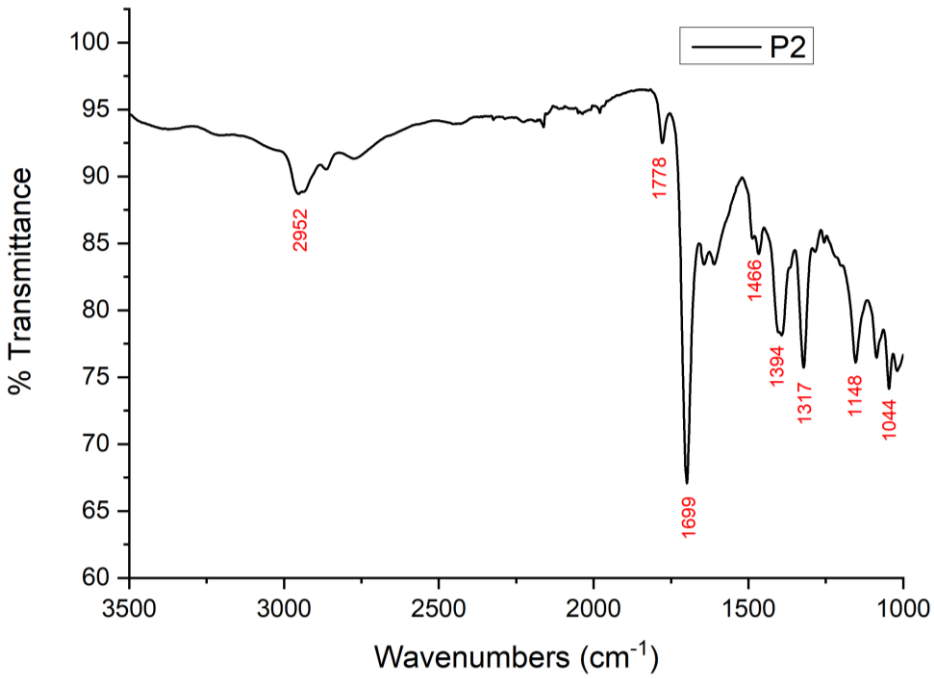

Figure A.3 Infrared spectrum of compound P2

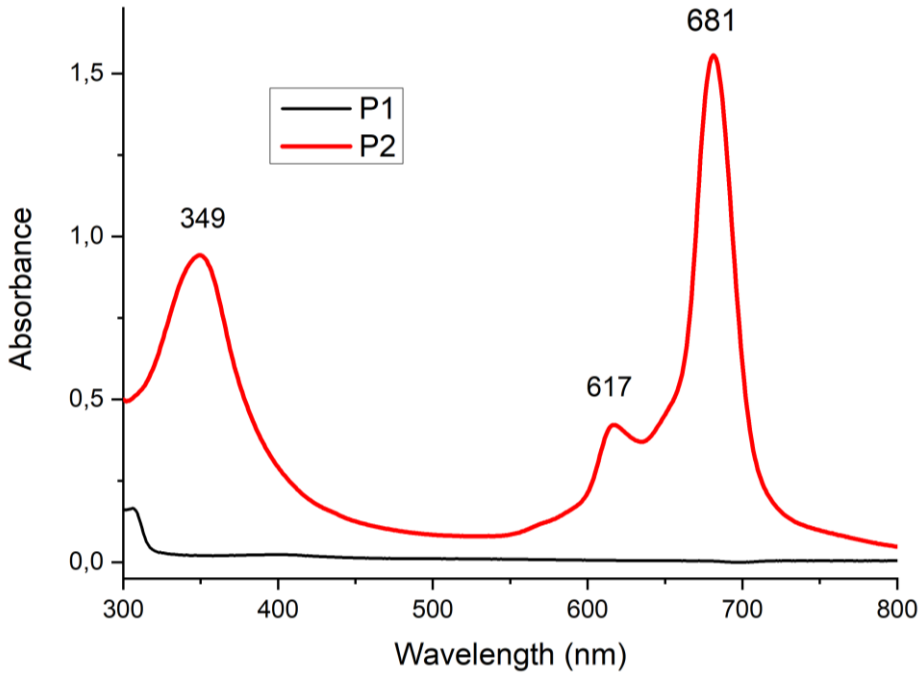

Figure A.4 UV-vis spectra of compound P1 and P2 at the same concentration in DMF

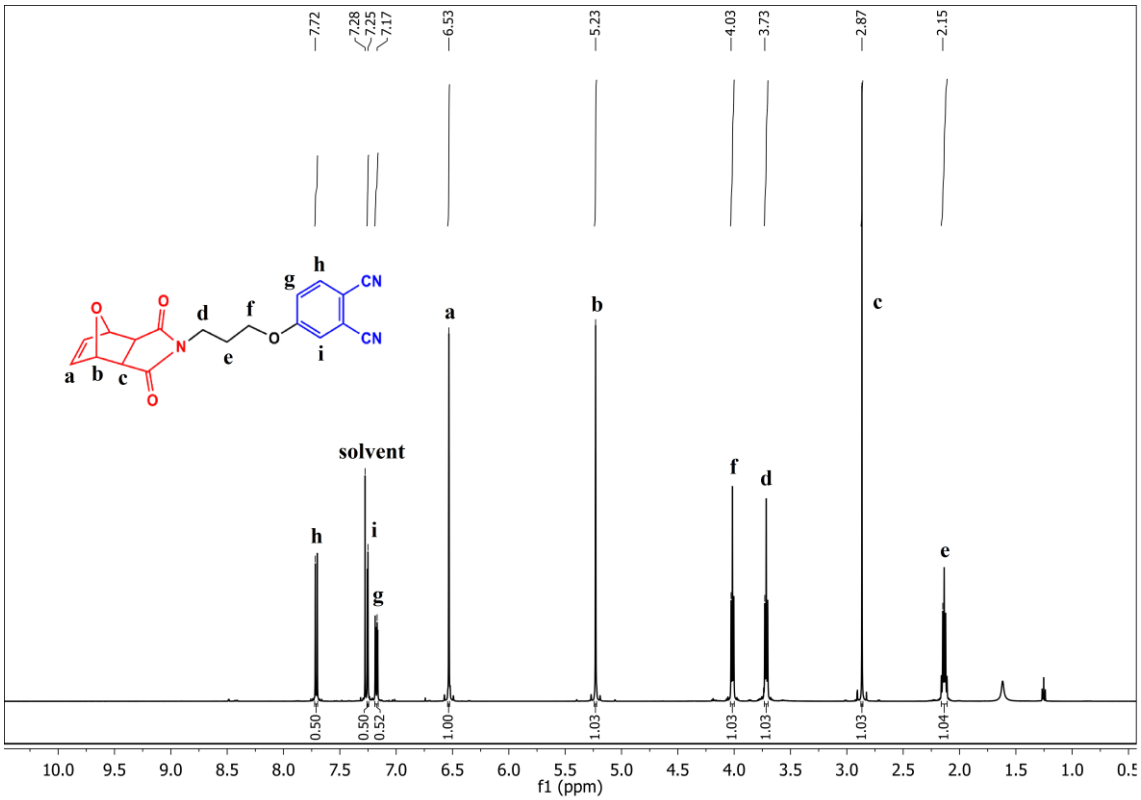

Figure A.5 ^{1}H NMR spectrum of compound M1 in $CDCl_3$

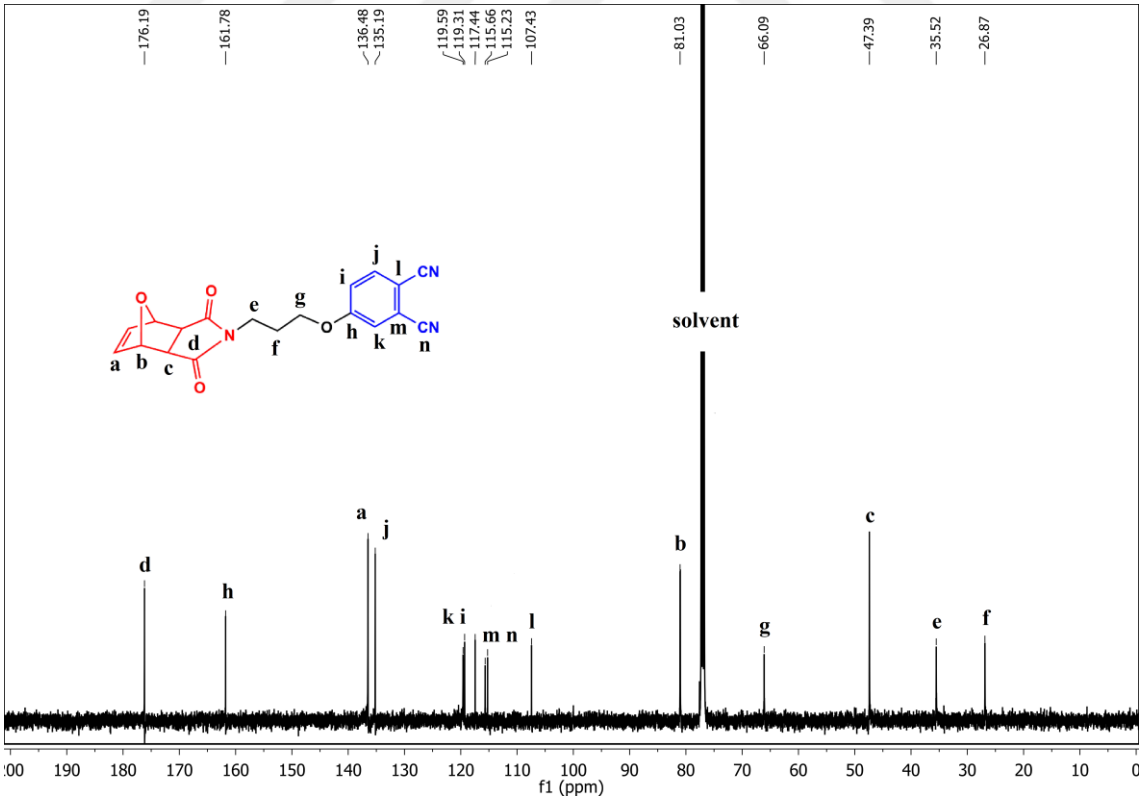

Figure A.6 ^{13}C NMR spectrum of compound M1 in $CDCl_3$

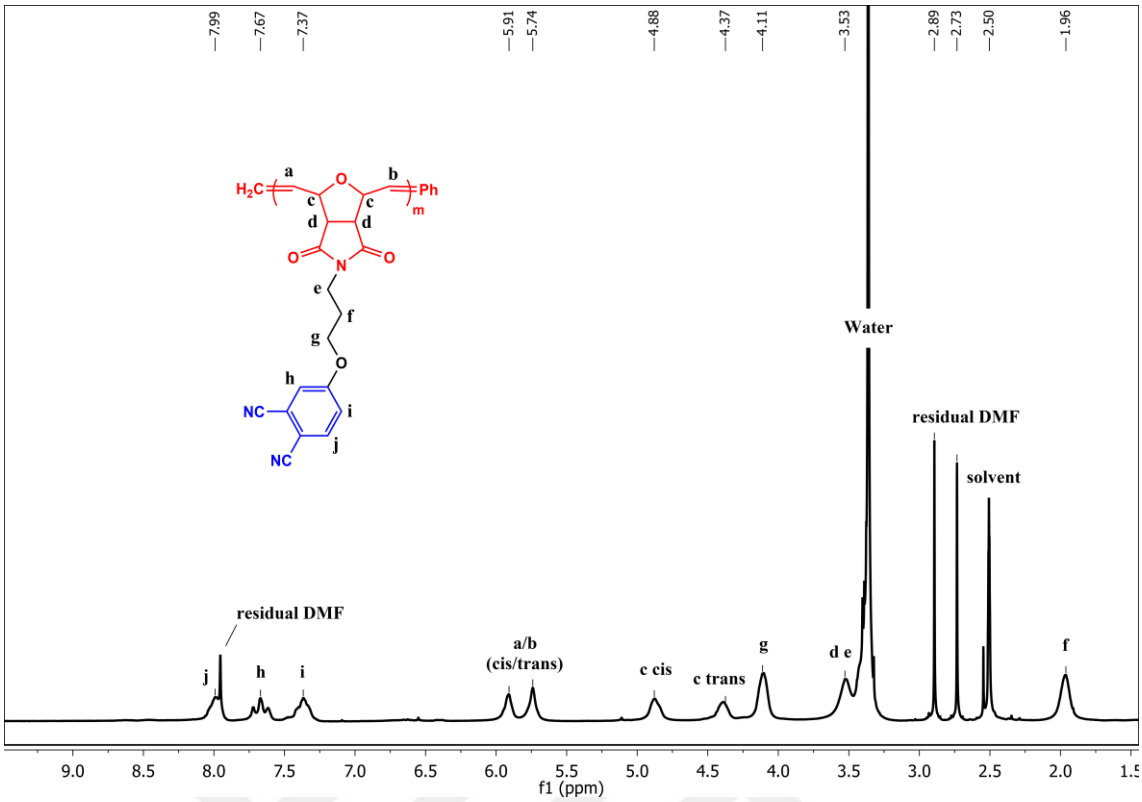

Figure A.7 ^{1}H NMR spectrum of compound P1 in *DMSO-d*$_6$

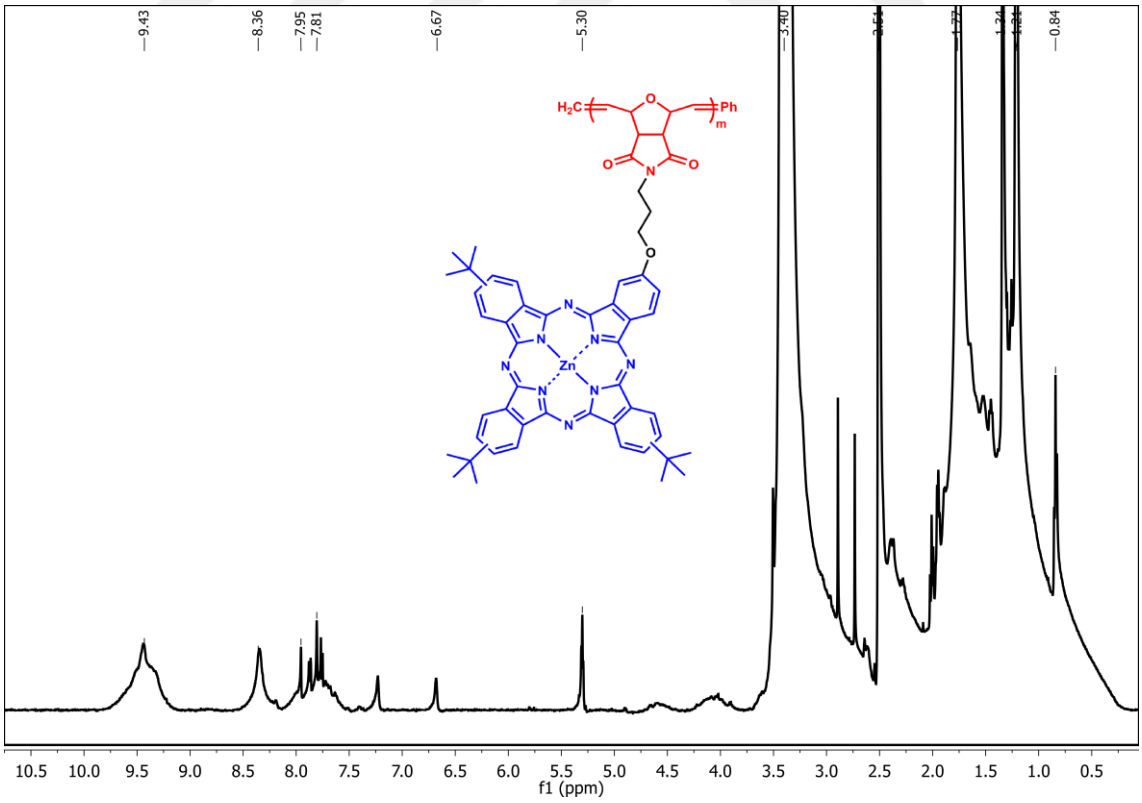

Figure A.8 ^{1}H NMR spectrum of compound P2 in *DMSO-d*$_6$

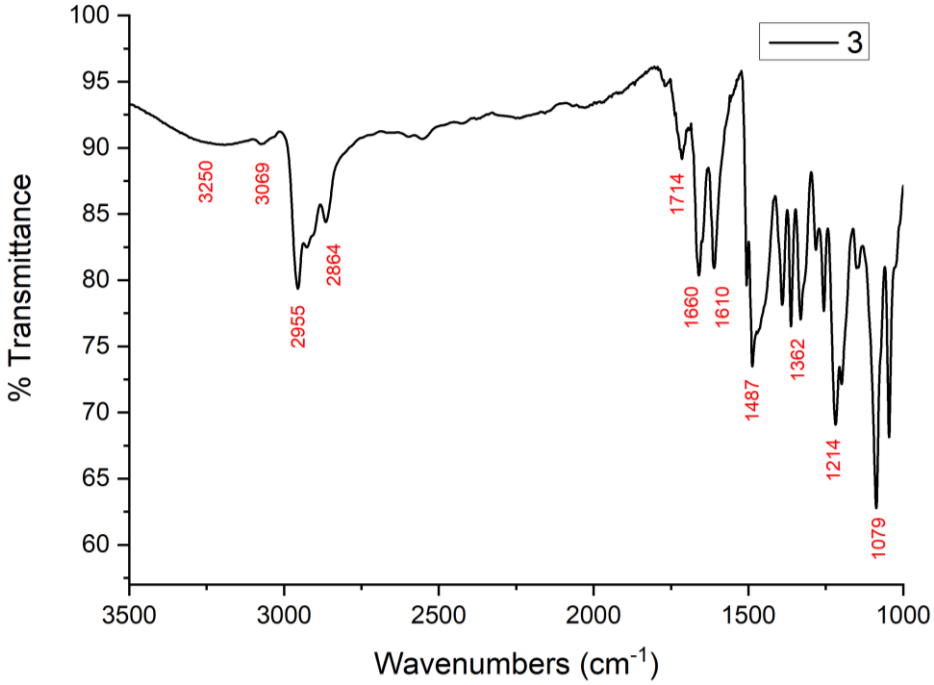

Figure A.9 Infrared spectrum of compound 3

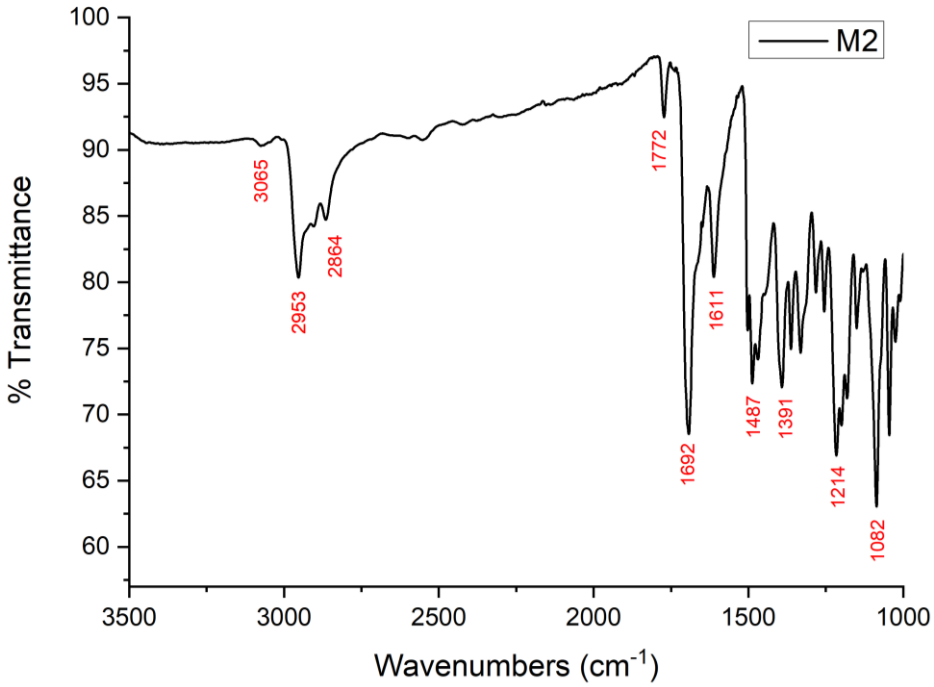

Figure A.10 Infrared spectrum of compound M2

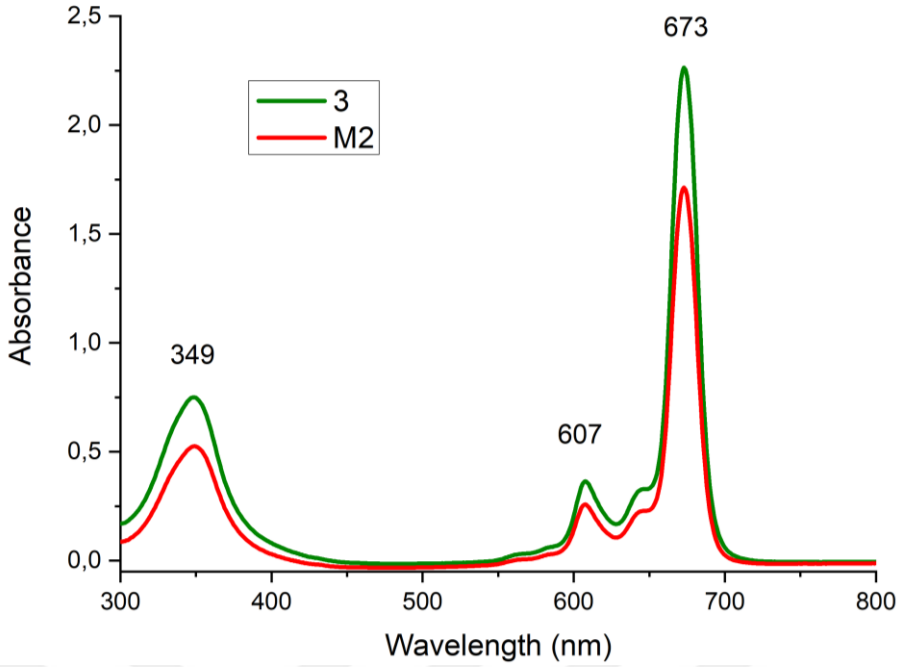

Figure A.11 UV-vis spectra of compound 3 and M2 at the same concentration in THF

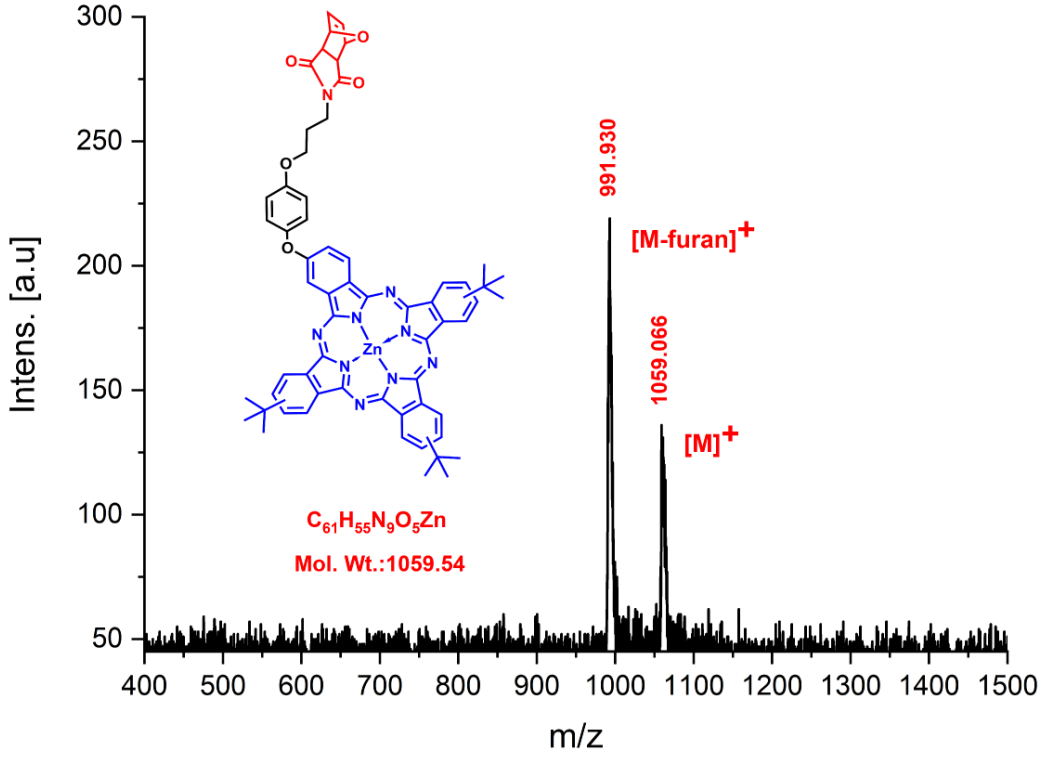

Figure A.12 MALDI-TOF MS spectrum of compound M2 (matrix: α-cyano-4-hydroxycinnamic acid)

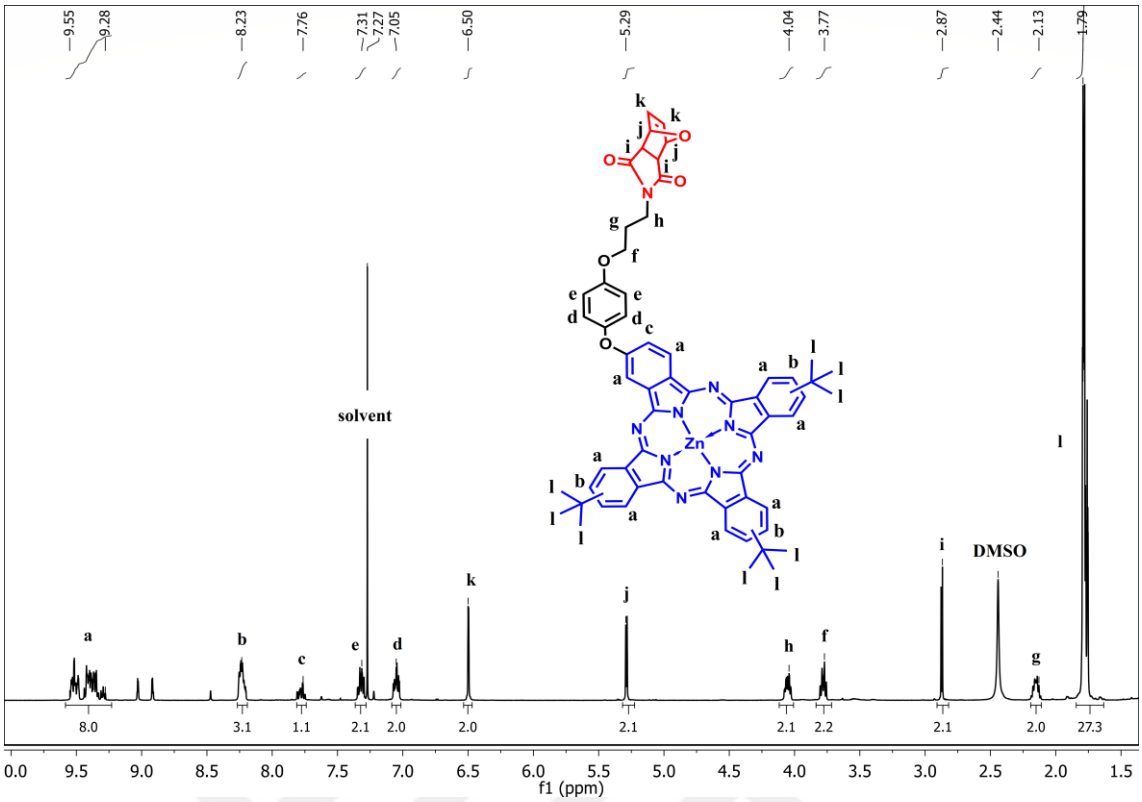

Figure A.13 ^{1}H NMR spectrum of compound M2 in $CDCl_3$ + a few drops DMSO-d_6

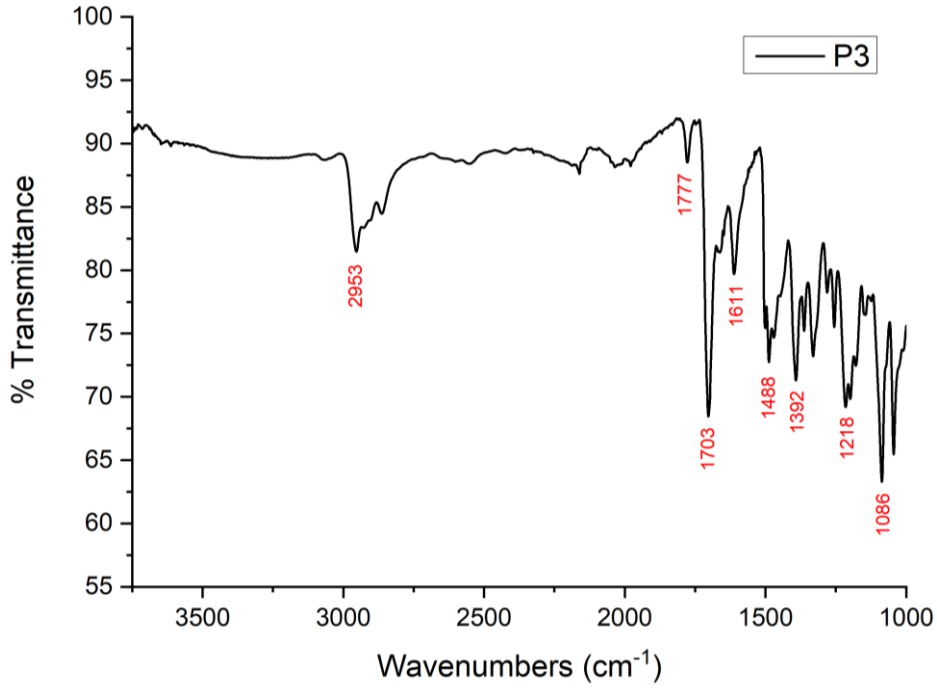

Figure A.14 Infrared spectrum of compound P3

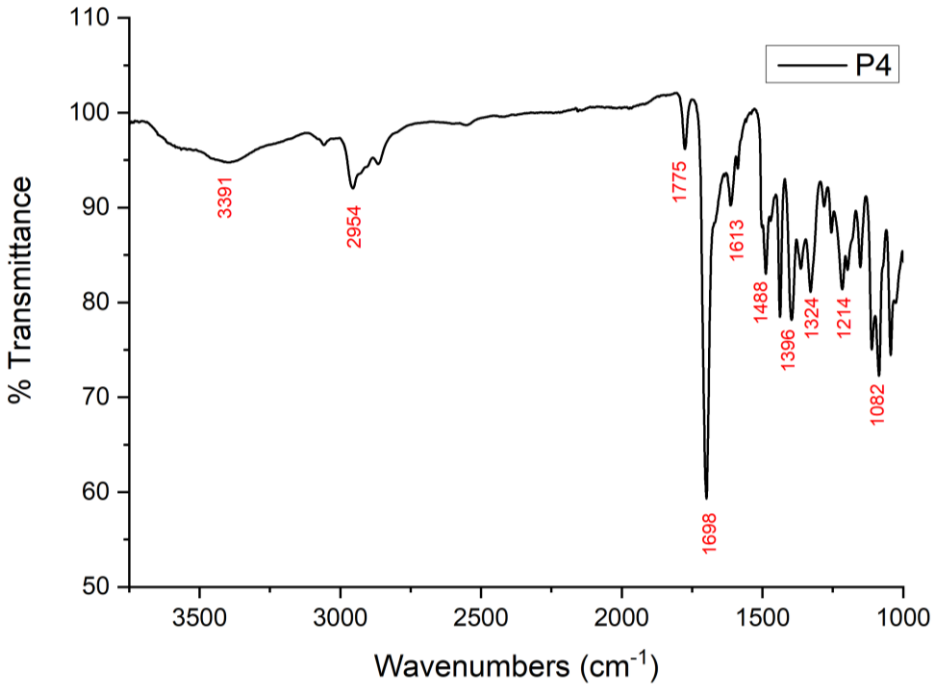

Figure A.15 Infrared spectrum of compound P4

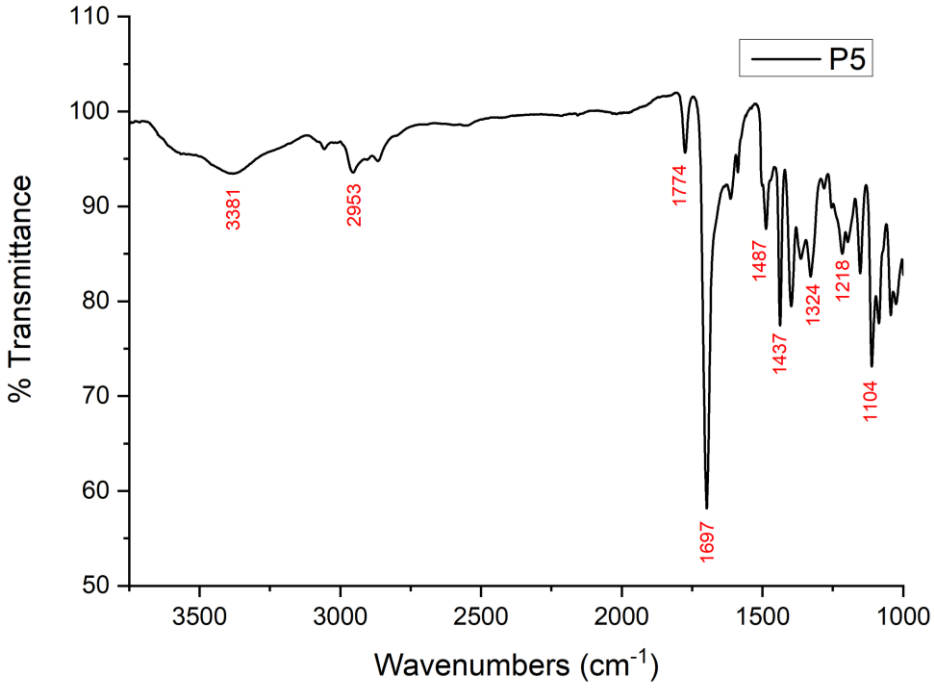

Figure A.16 Infrared spectrum of compound P5

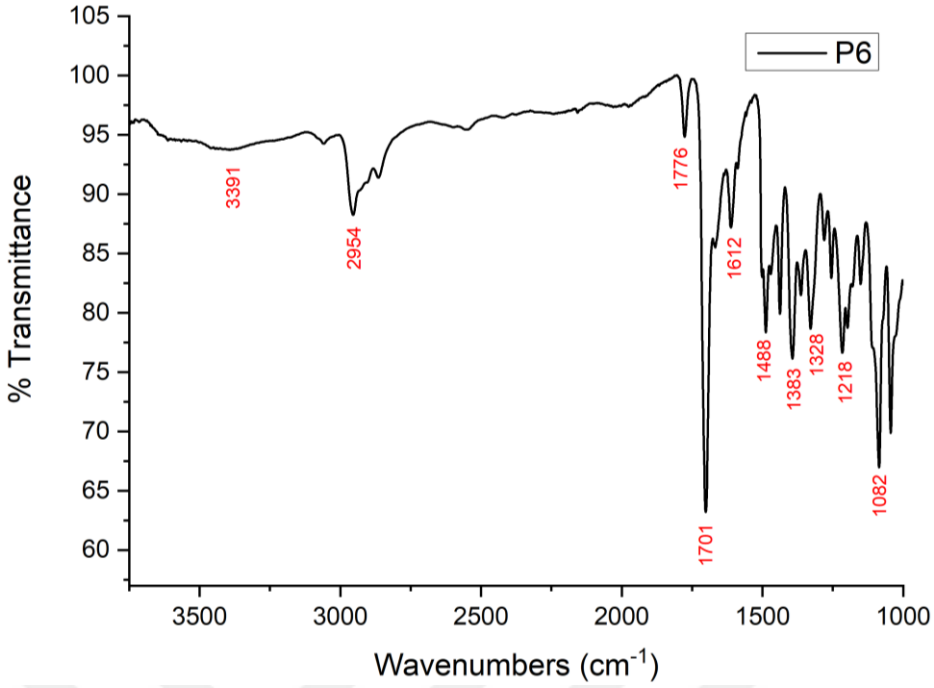

Figure A.17 Infrared spectrum of compound P6

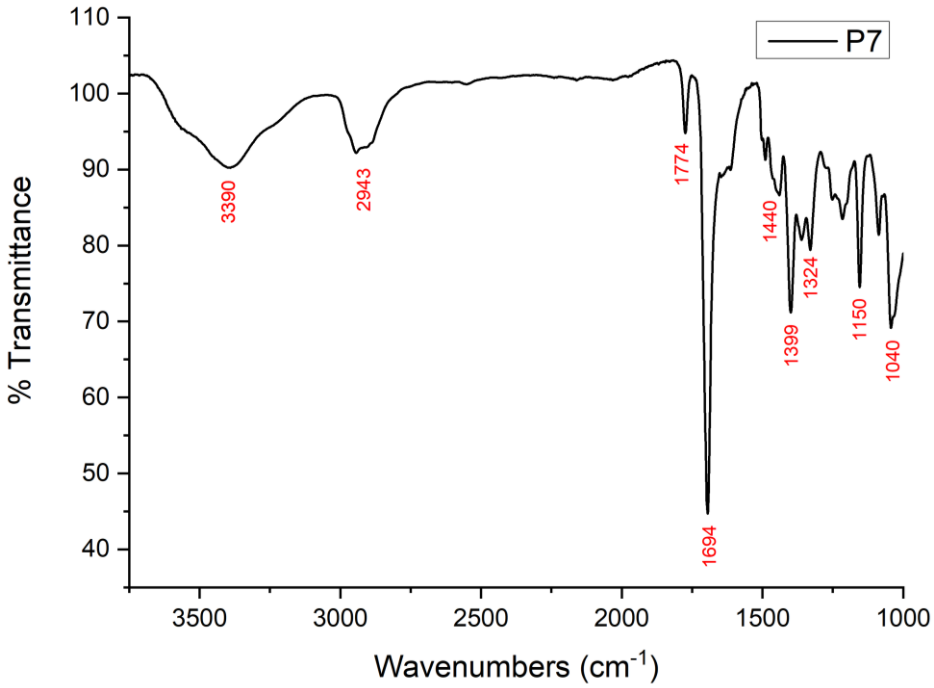

Figure A.18 Infrared spectrum of compound P7

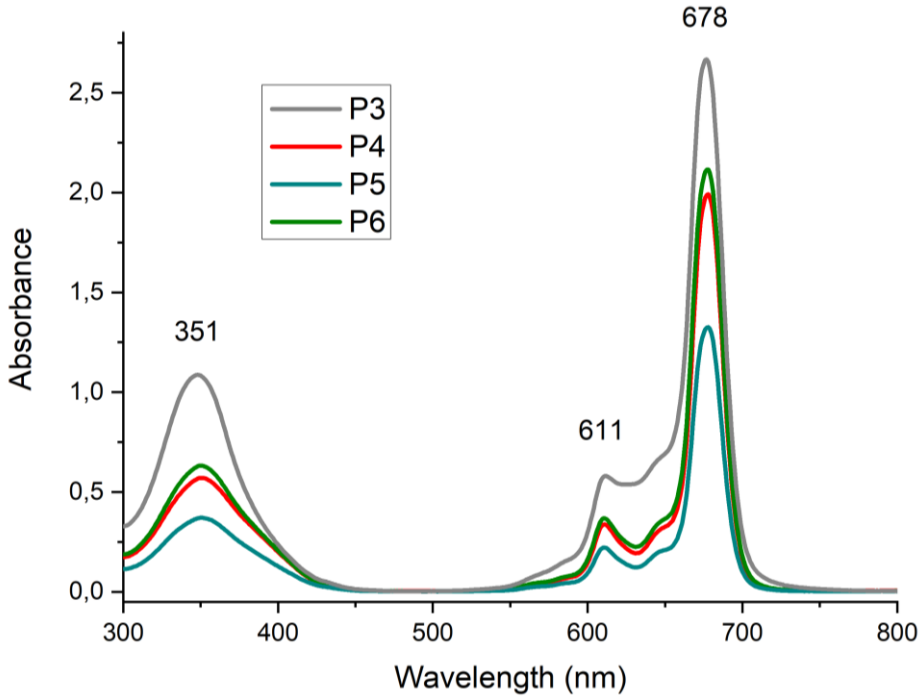

Figure A19. UV-vis spectra of polymers P3, P4, P5 and P6 at the same concentration in DMF

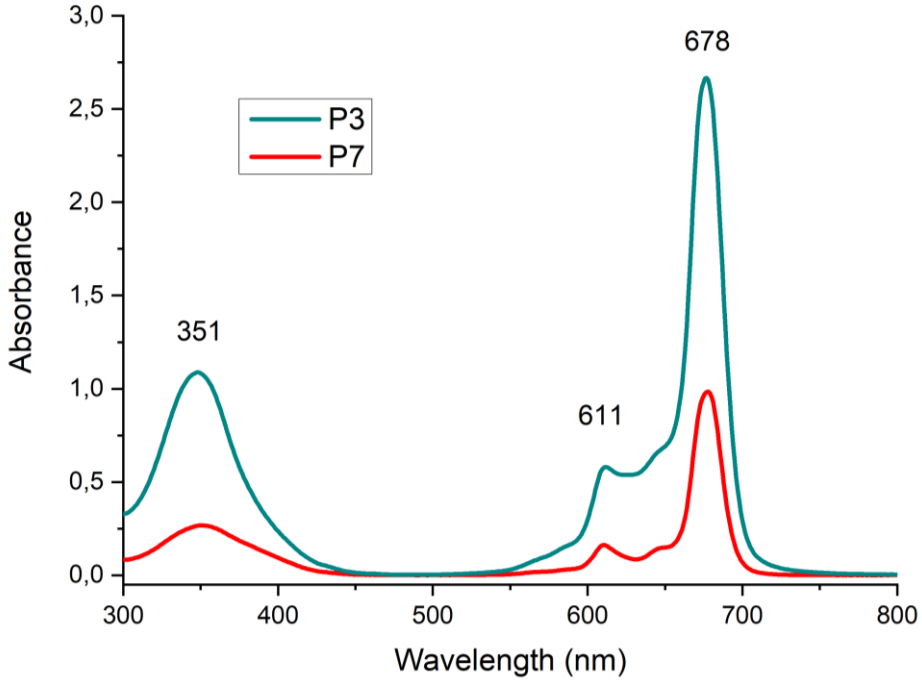

Figure A.20 UV-vis spectra of polymers P3 and P7 at the same concentration in DMF

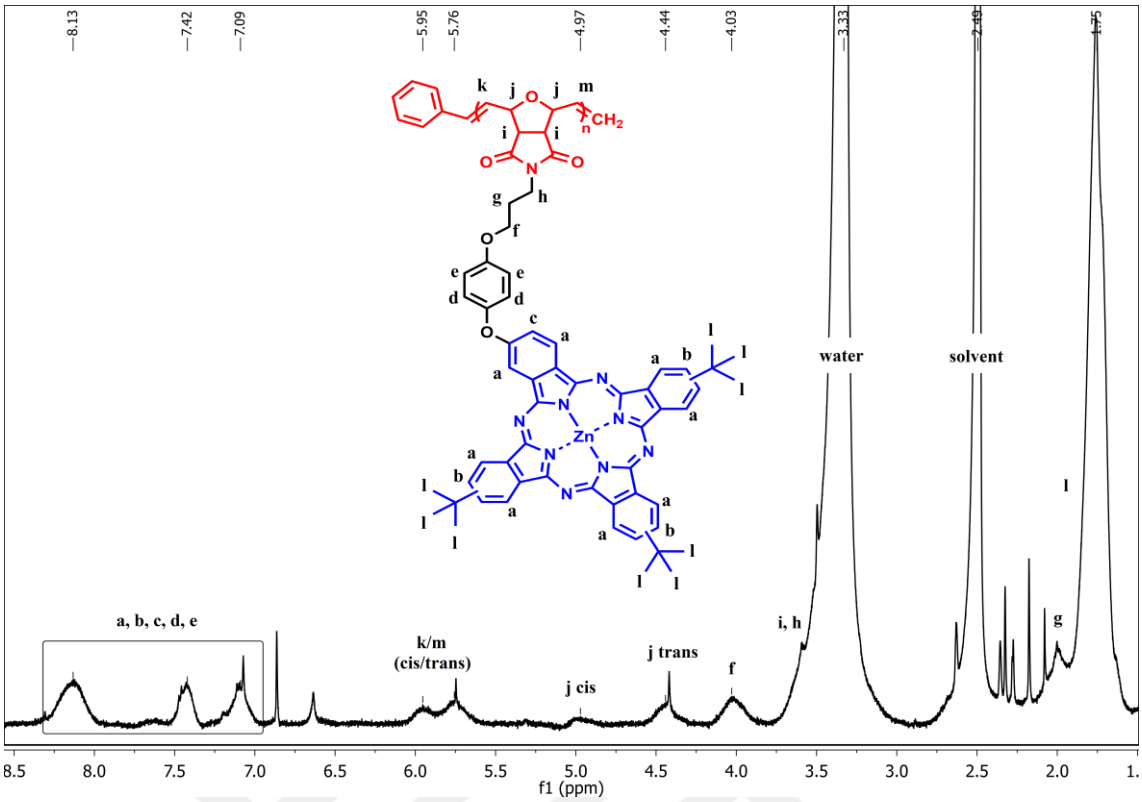

Figure A.21 ^{1}H NMR spectrum of compound P3 in *DMSO-d_6*

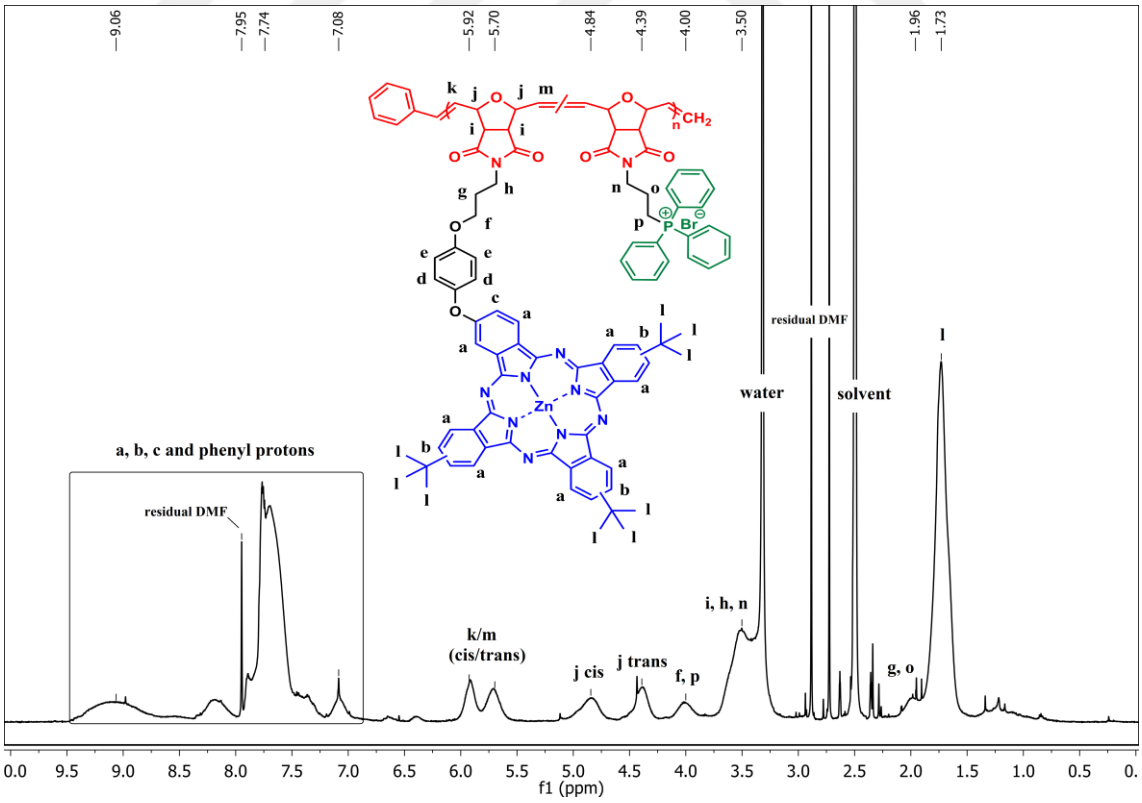

Figure A.22 ^{1}H NMR spectrum of compound P4 in *DMSO-d_6*

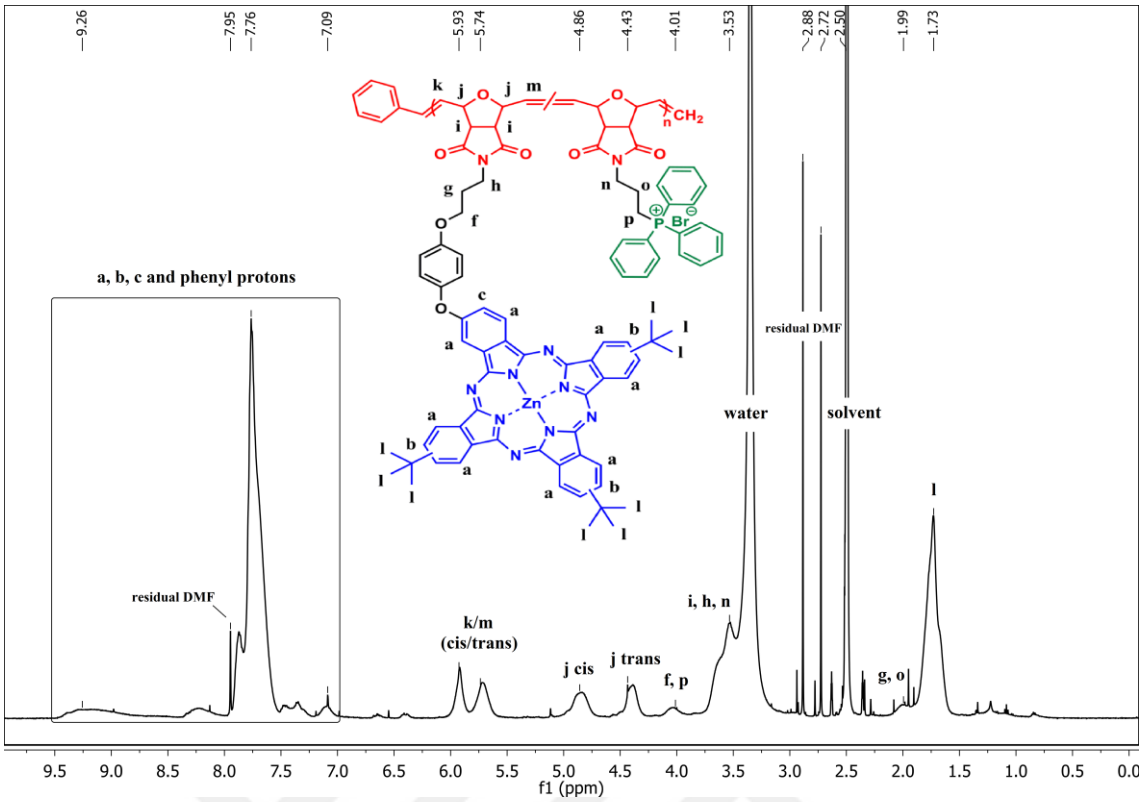

Figure A.23 ^{1}H NMR spectrum of compound P5 in *DMSO-d_6*

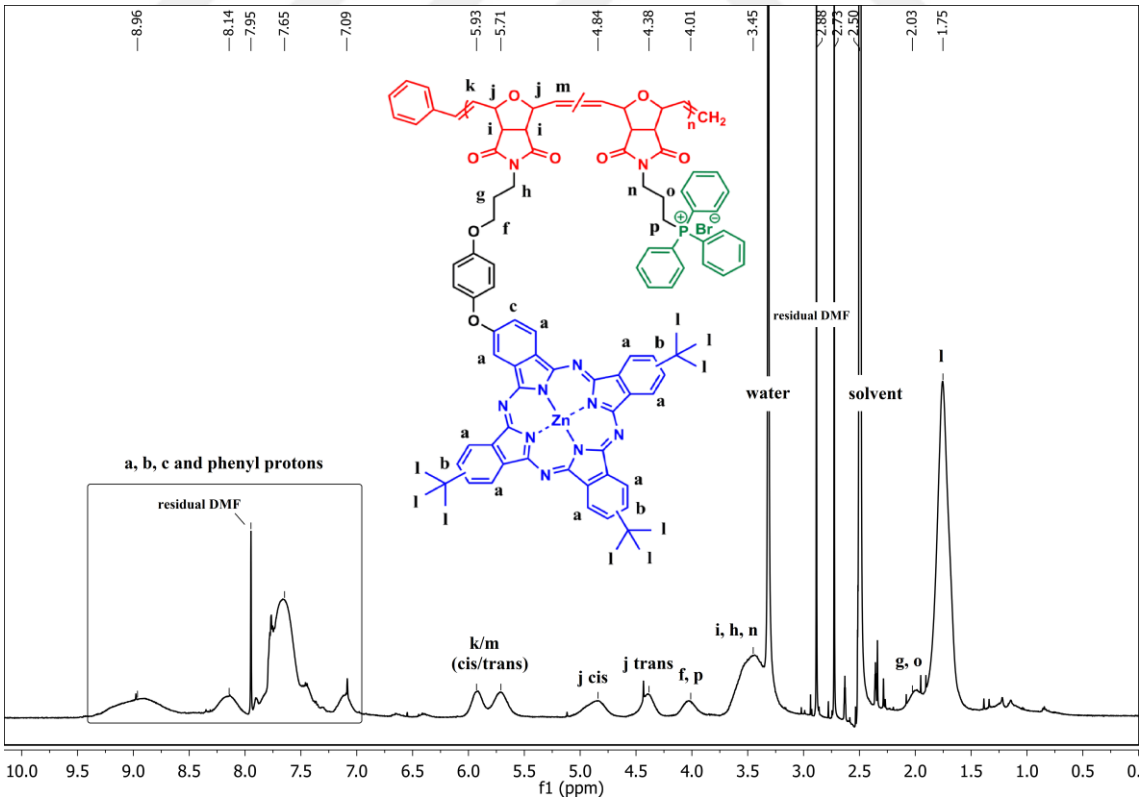

Figure A.24 ^{1}H NMR spectrum of compound P6 in *DMSO-d_6*

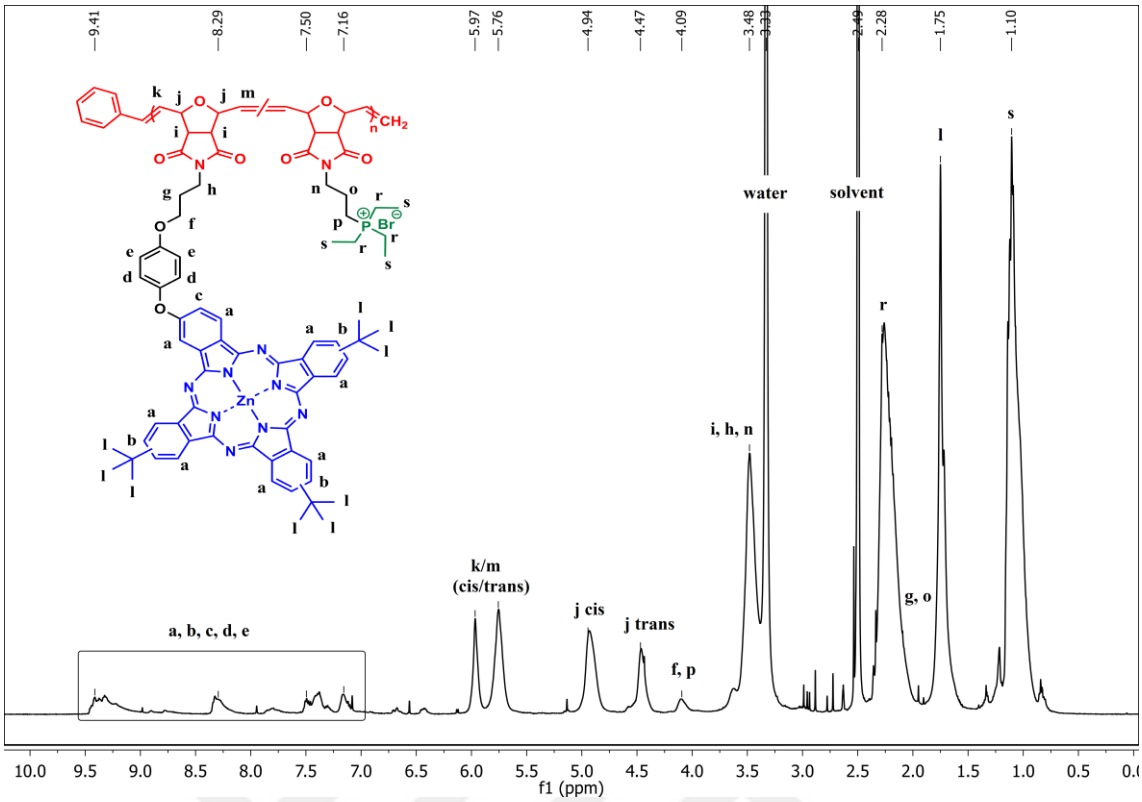

Figure A.25 ^{1}H NMR spectrum of compound P7 in *DMSO-d_6*

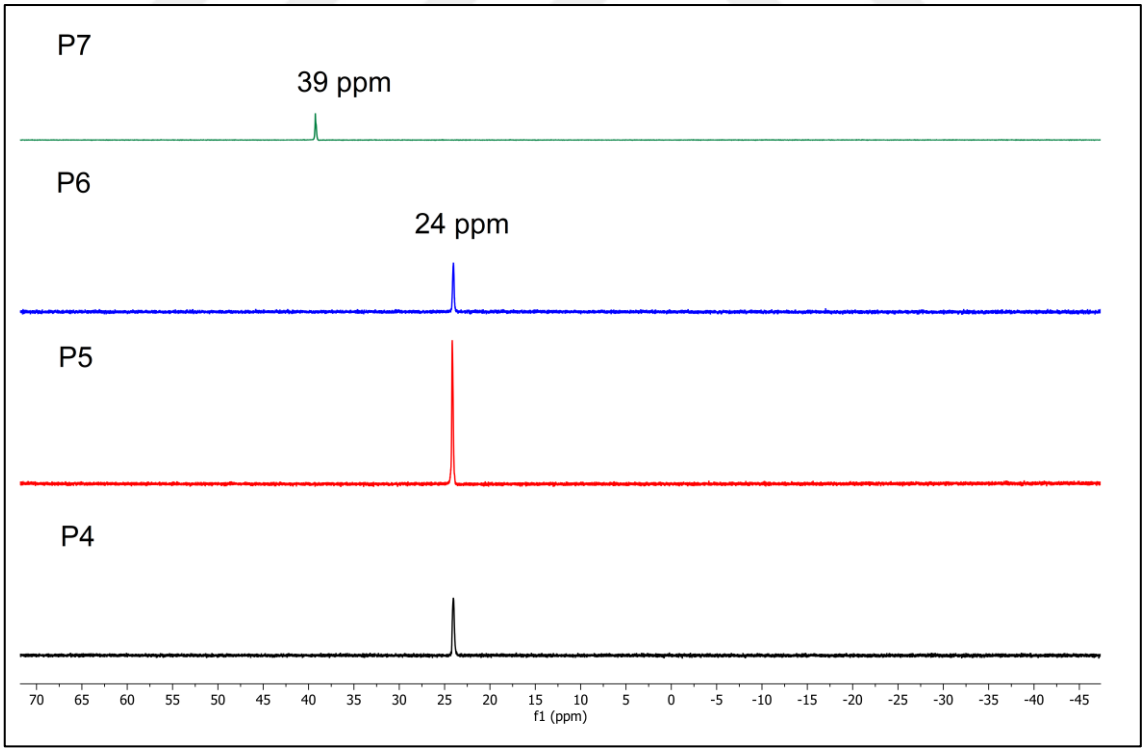

Figure A.26 ^{31}P NMR spectrum of compound P4-P7 in *DMSO-d_6*

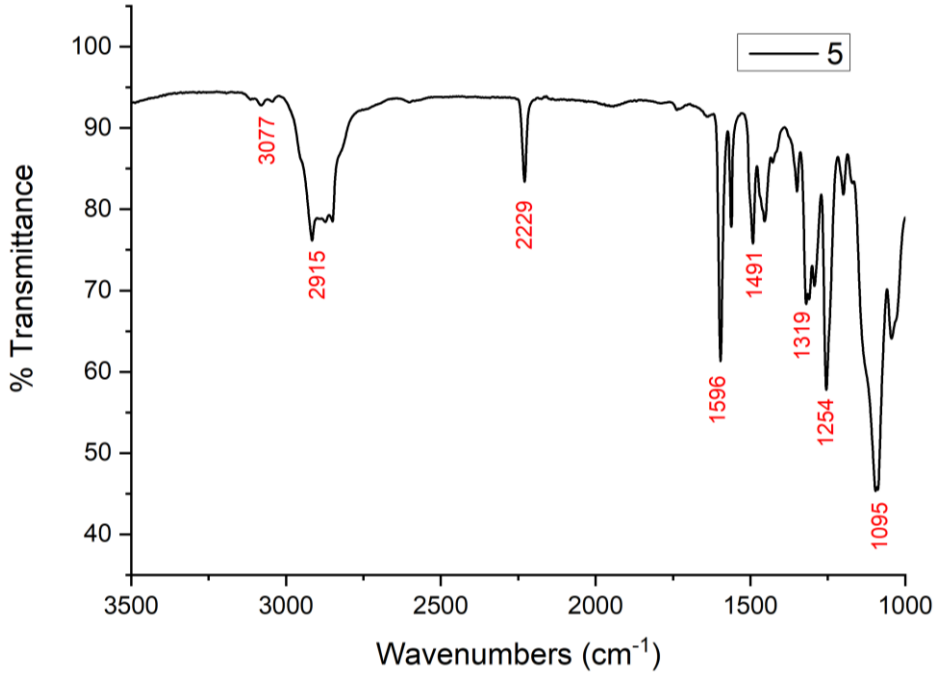

Figure A.27 FT-IR spectrum of compound 5

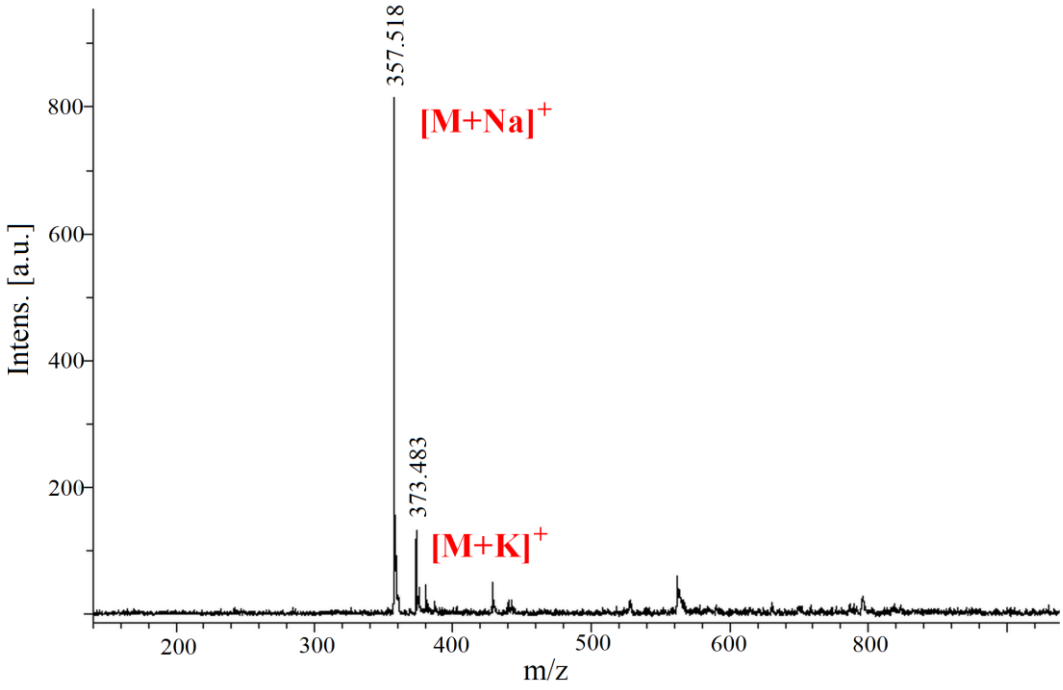

Figure A.28 MALDI-TOF MS spectrum of compound 5

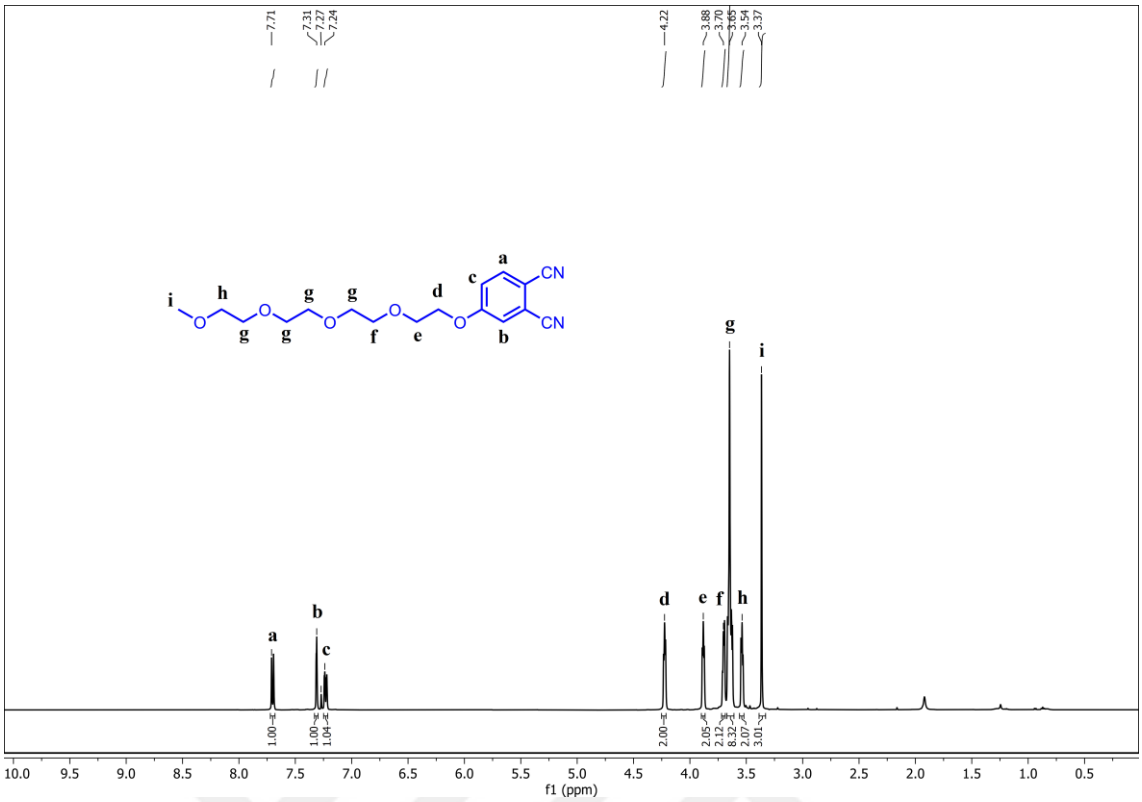

Figure A.29 ^{1}H-NMR spectrum of compound 5

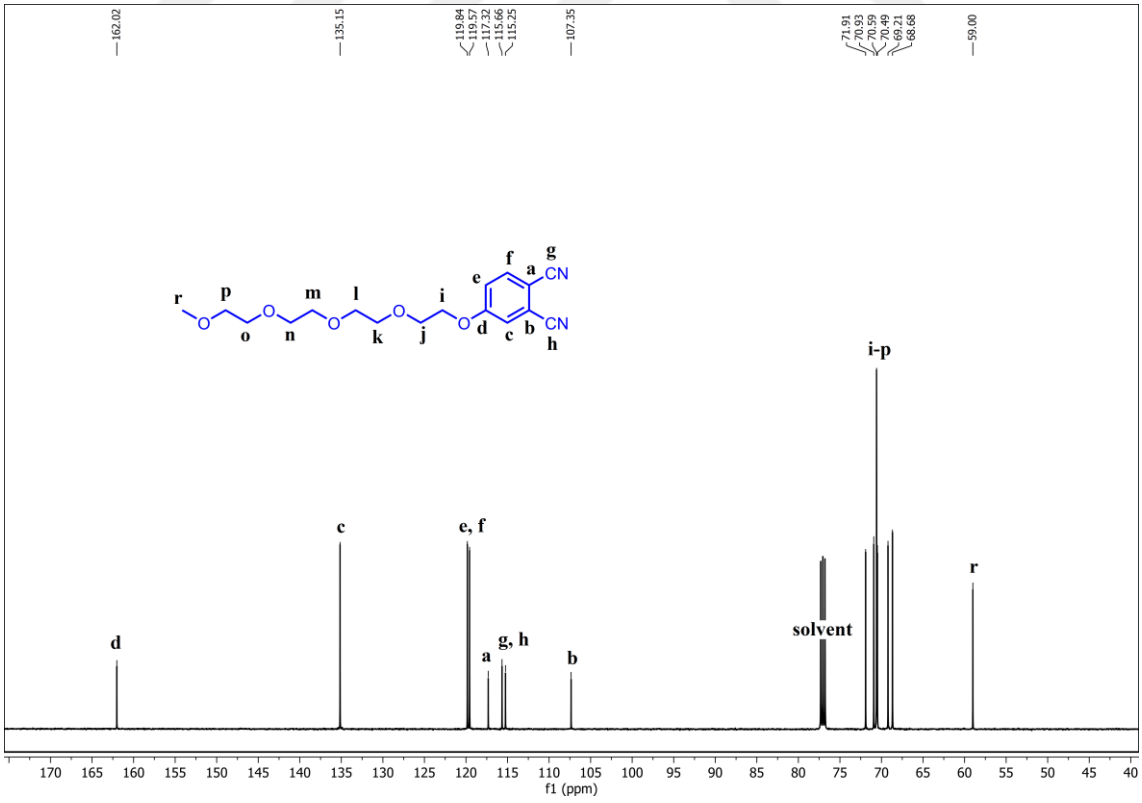

Figure A.30 ^{13}C-NMR spectrum of compound 5

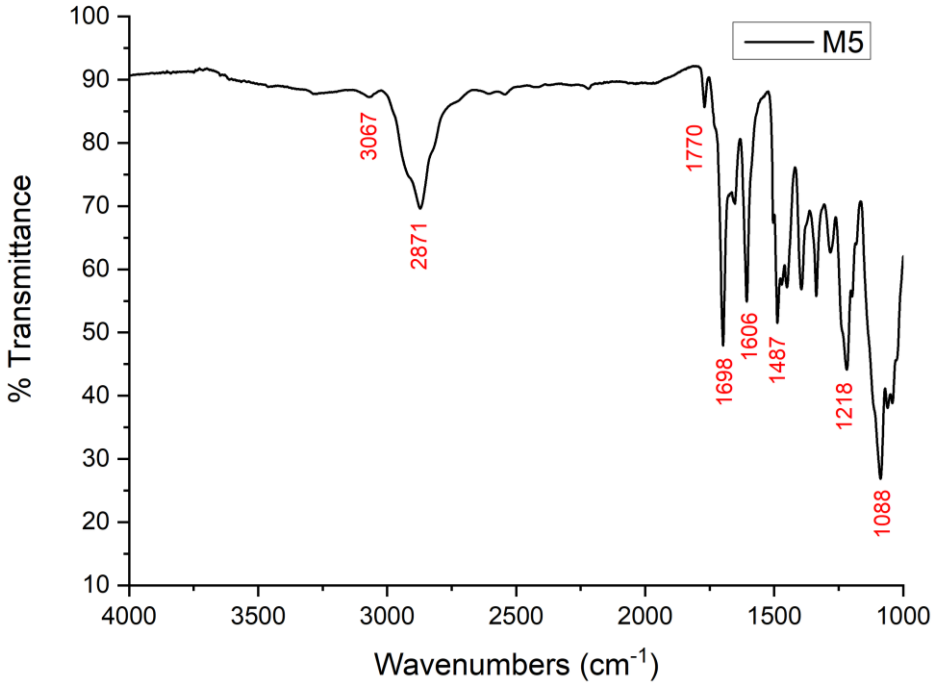

Figure A.31 FT-IR spectrum of M5

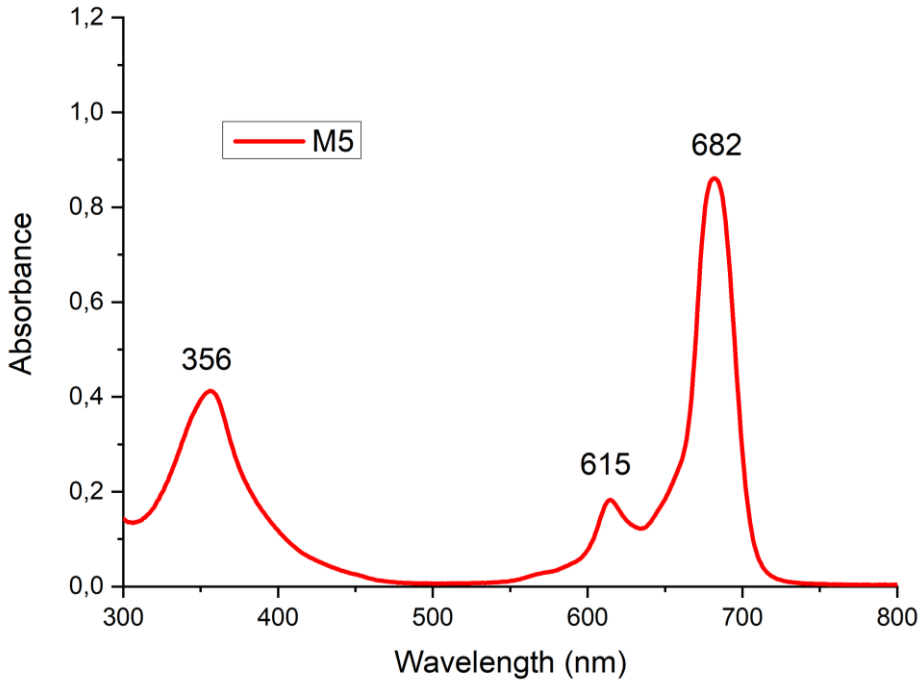

Figure A.32 UV-vis spectrum of monomer M5 in THF

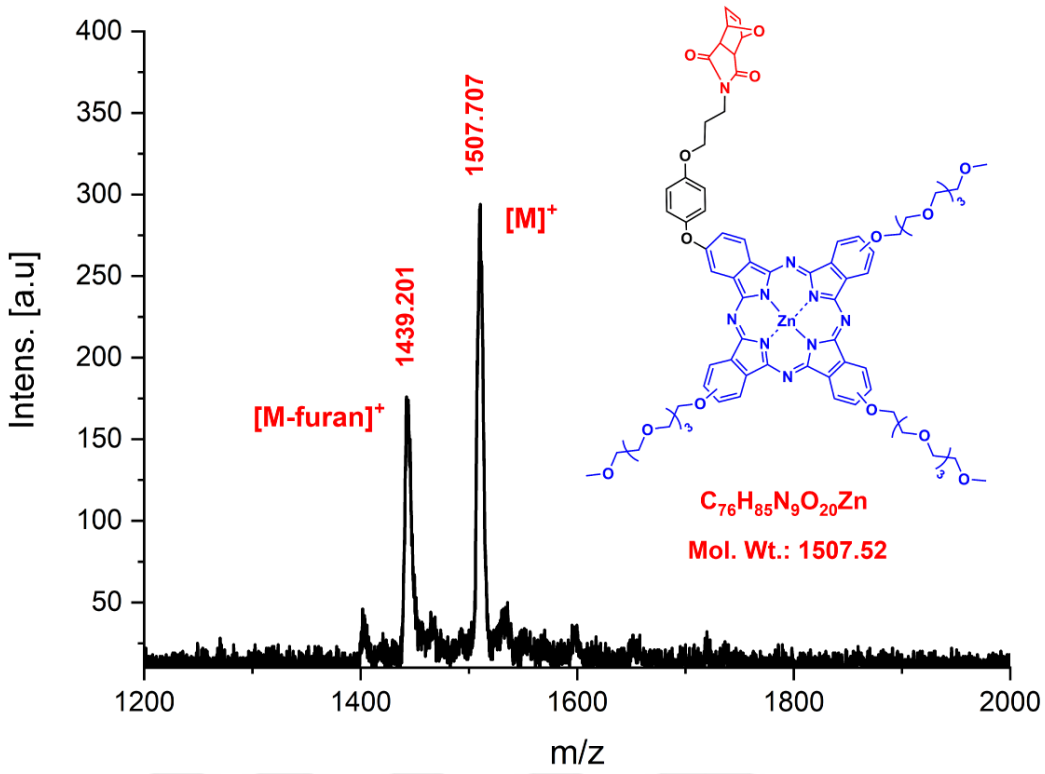

Figure A.33 MALDI-TOF MS spectrum of monomer M5

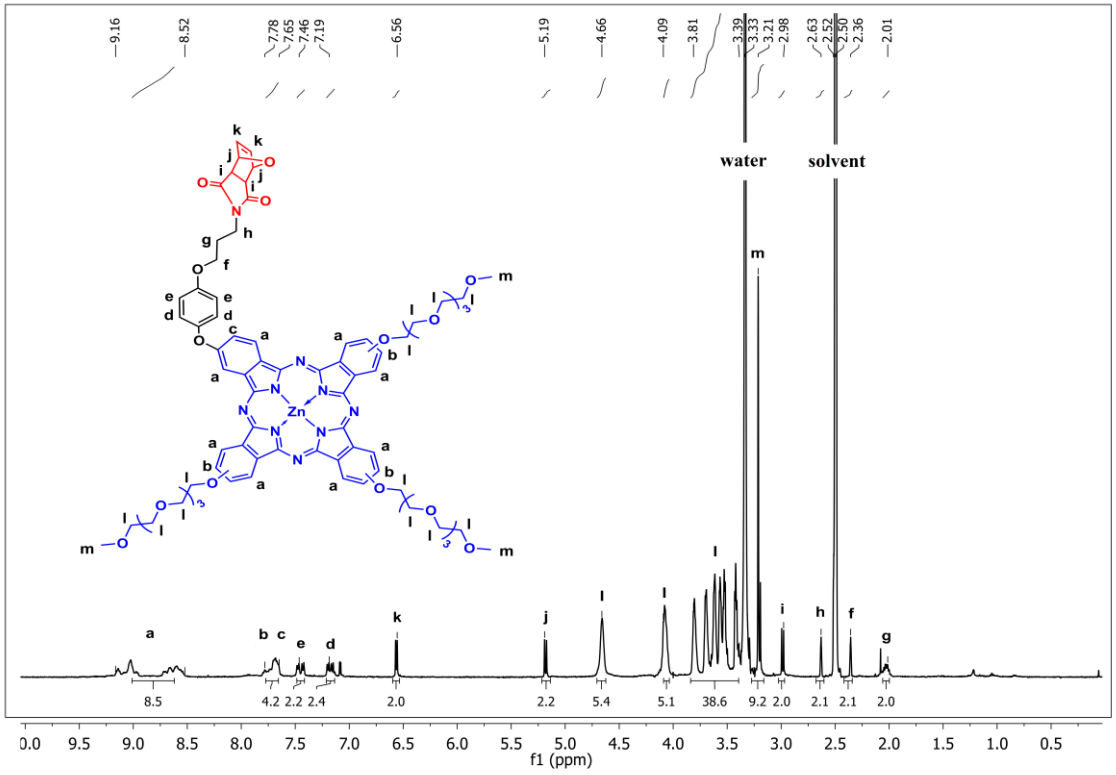

Figure A.34 ^{1}H-NMR spectrum of monomer M5 in DMSO-d_6

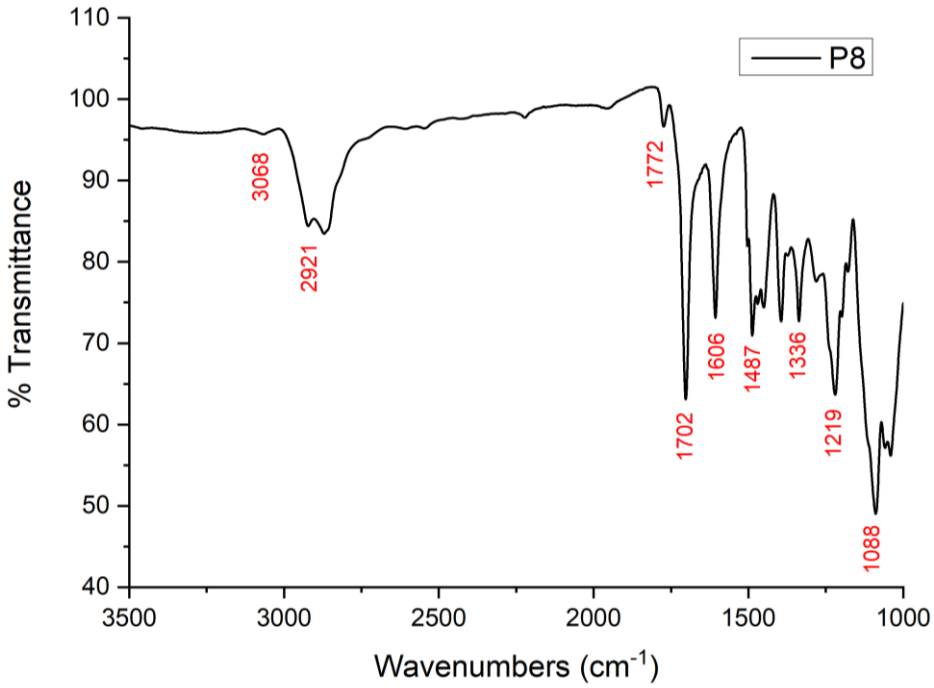

Figure A.35 FT-IR spectrum of P8

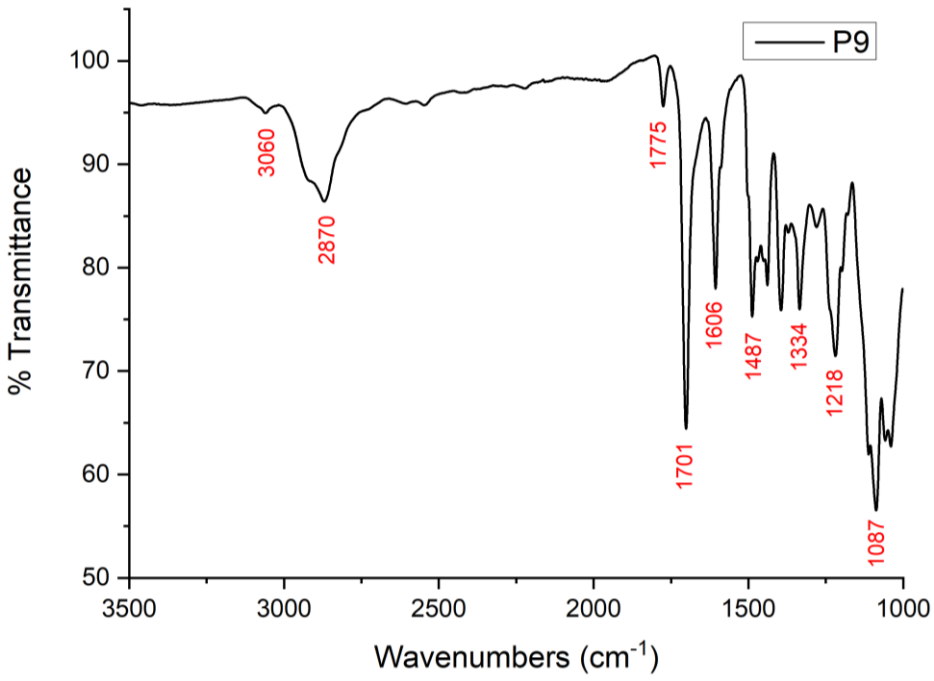

Figure A.36 FT-IR spectrum of P9

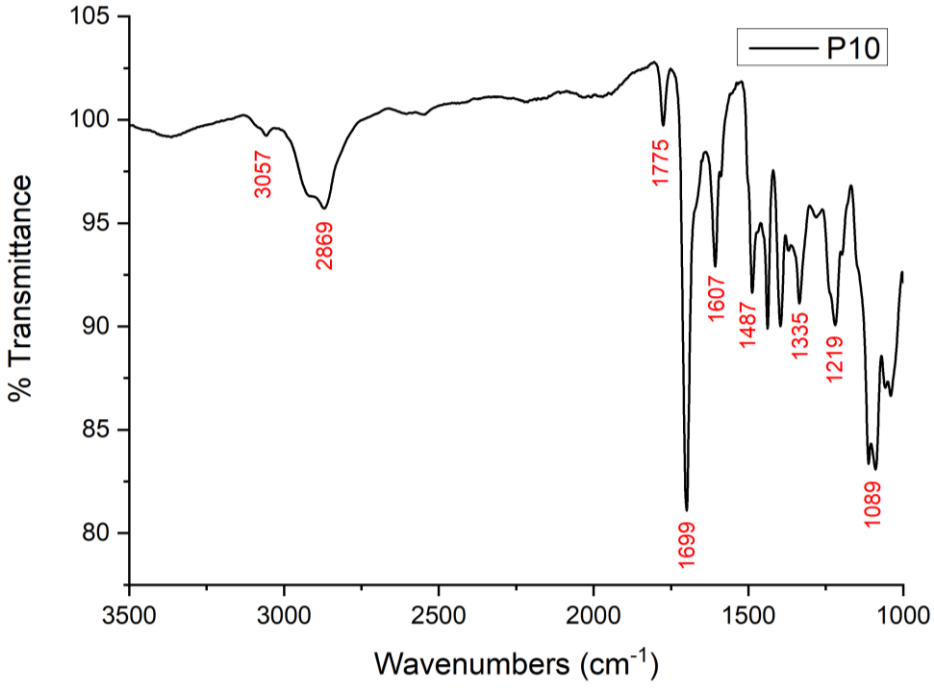

Figure A.37 FT-IR spectrum of P10

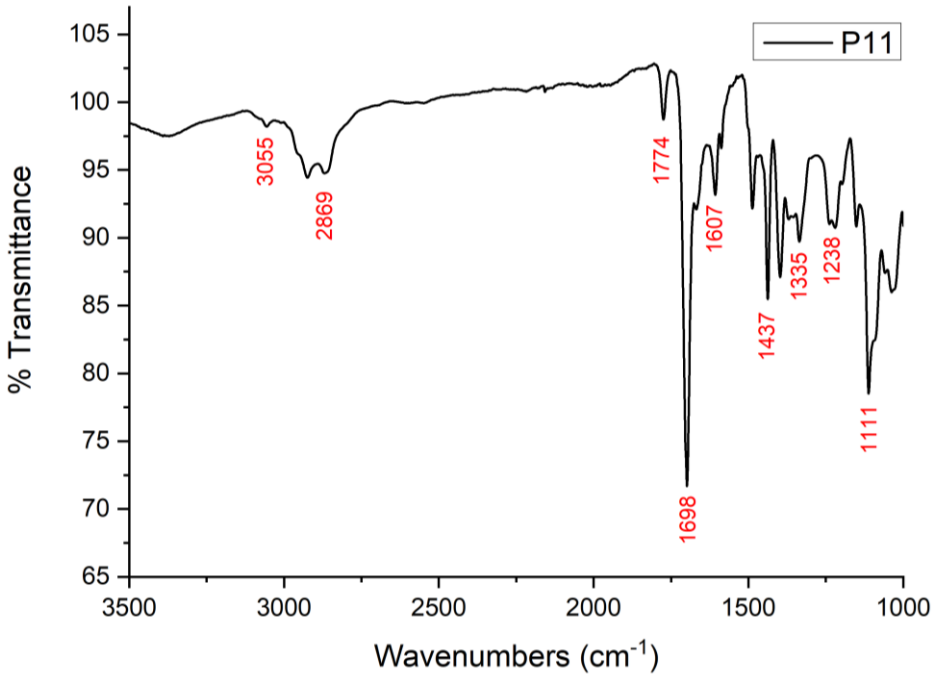

Figure A.38 FT-IR spectrum of P11

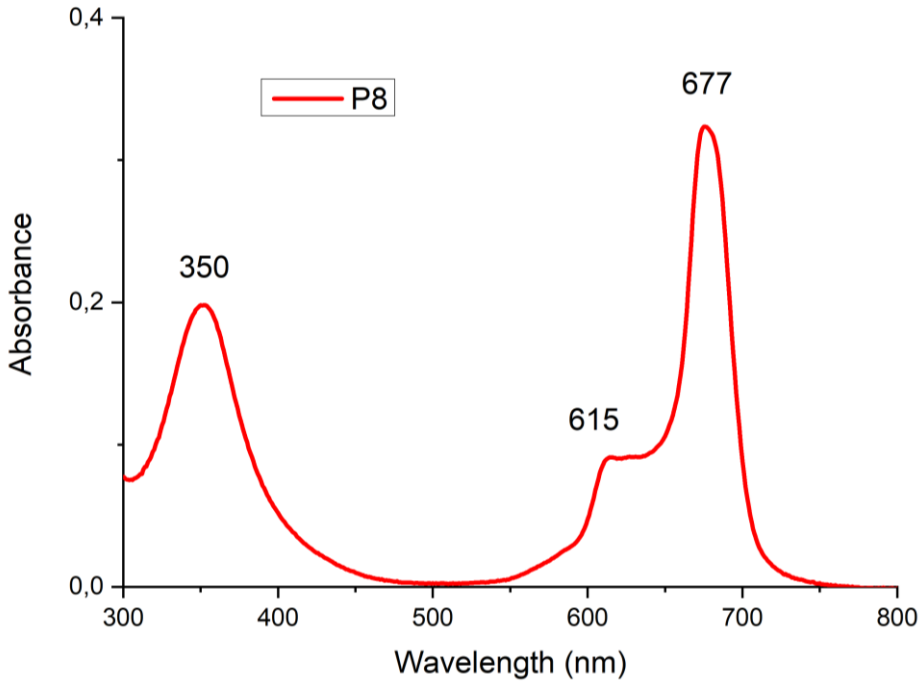

Figure A.39 UV-vis spectra of homopolymer P8 in DMF (concentration: 7 µg/mL)

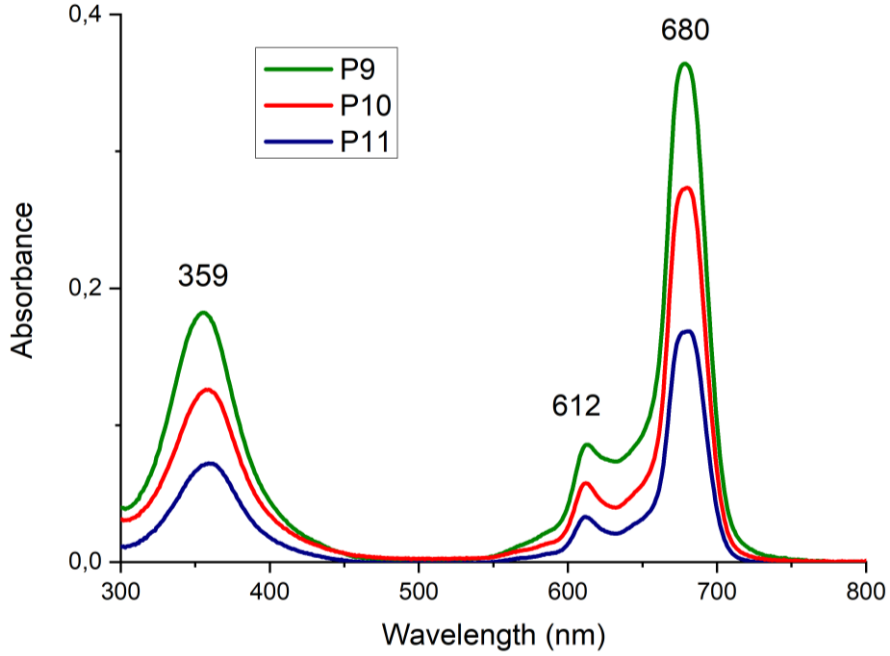

Figure A.40 UV-vis spectra of comopolymer P9-P11 in DMF (concentration: 7 µg/mL)

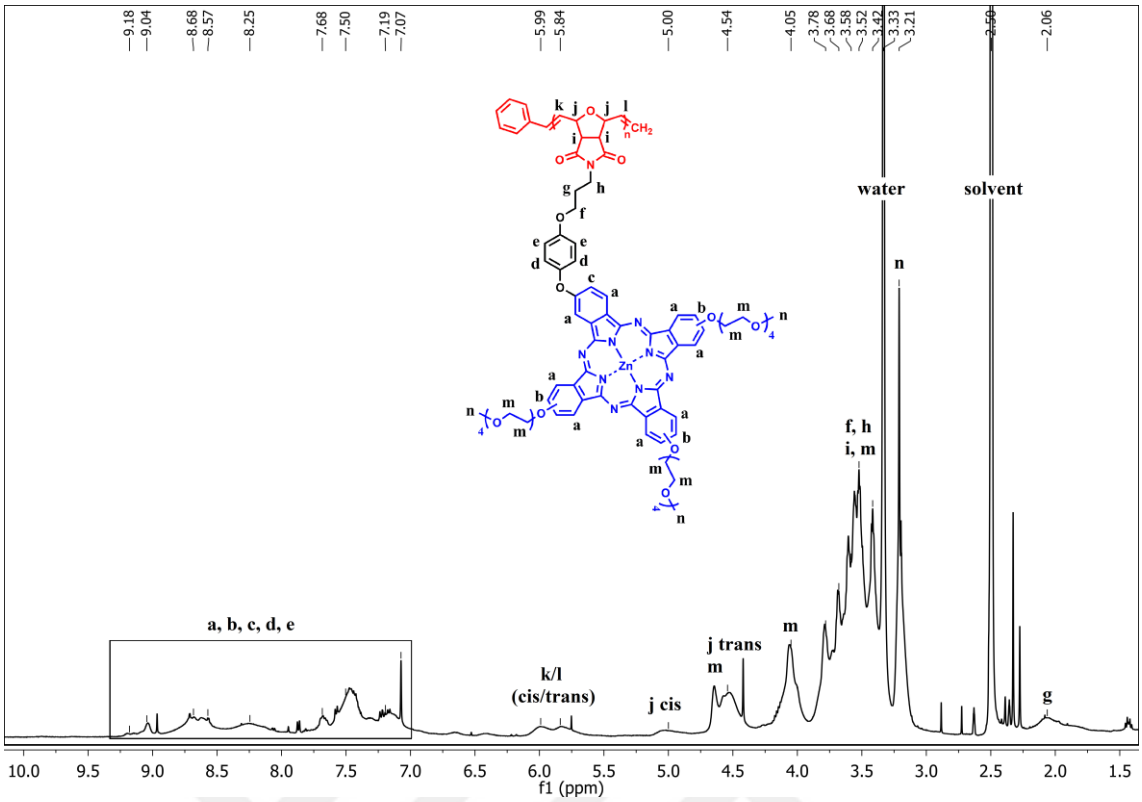

Figure A.41 ^{1}H-NMR spectrum of homopolymer P8 in DMSO-d_6

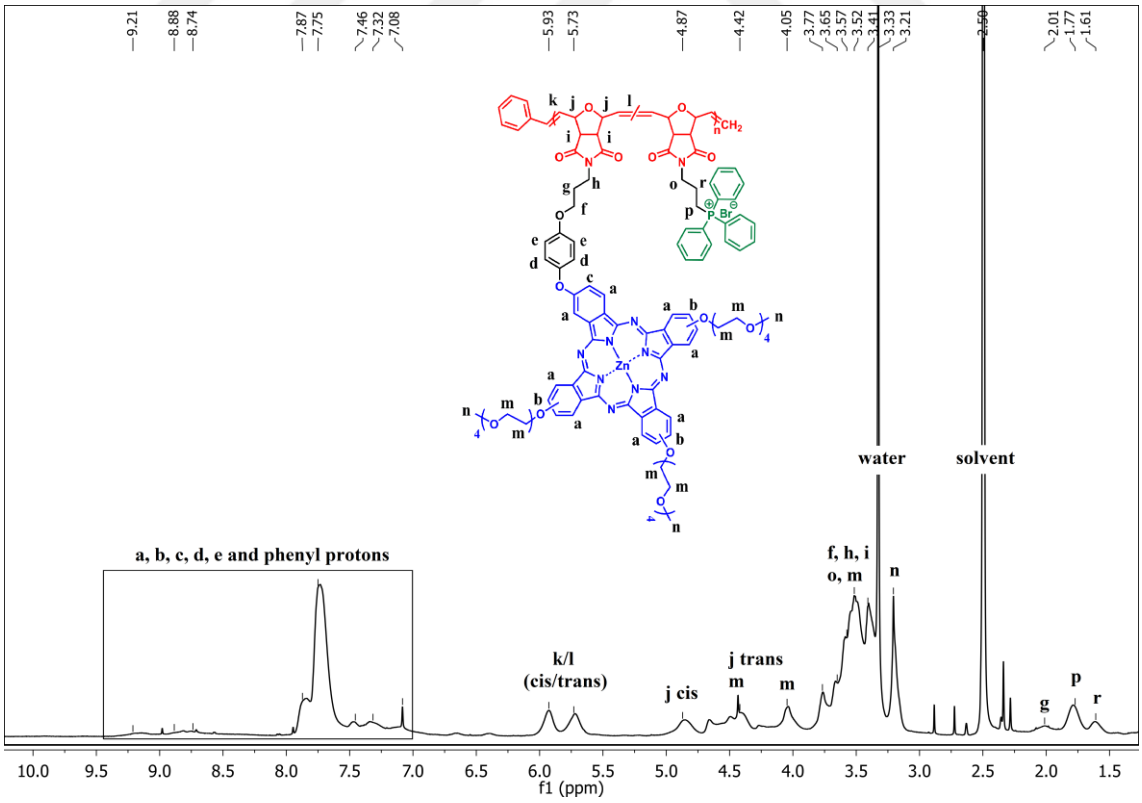

Figure A.42 ^{1}H-NMR spectrum of copolymer P9 in DMSO-d_6

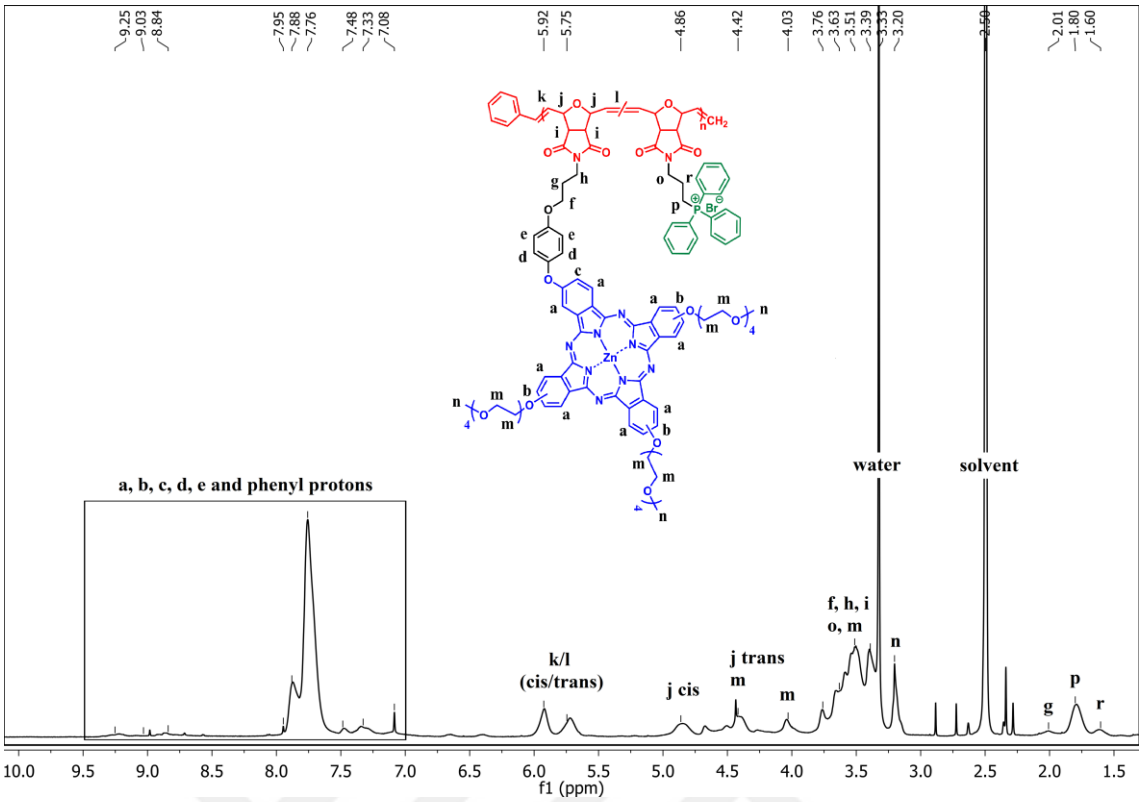

Figure A.43 ^{1}H-NMR spectrum of copolymer P10 in DMSO-d_6

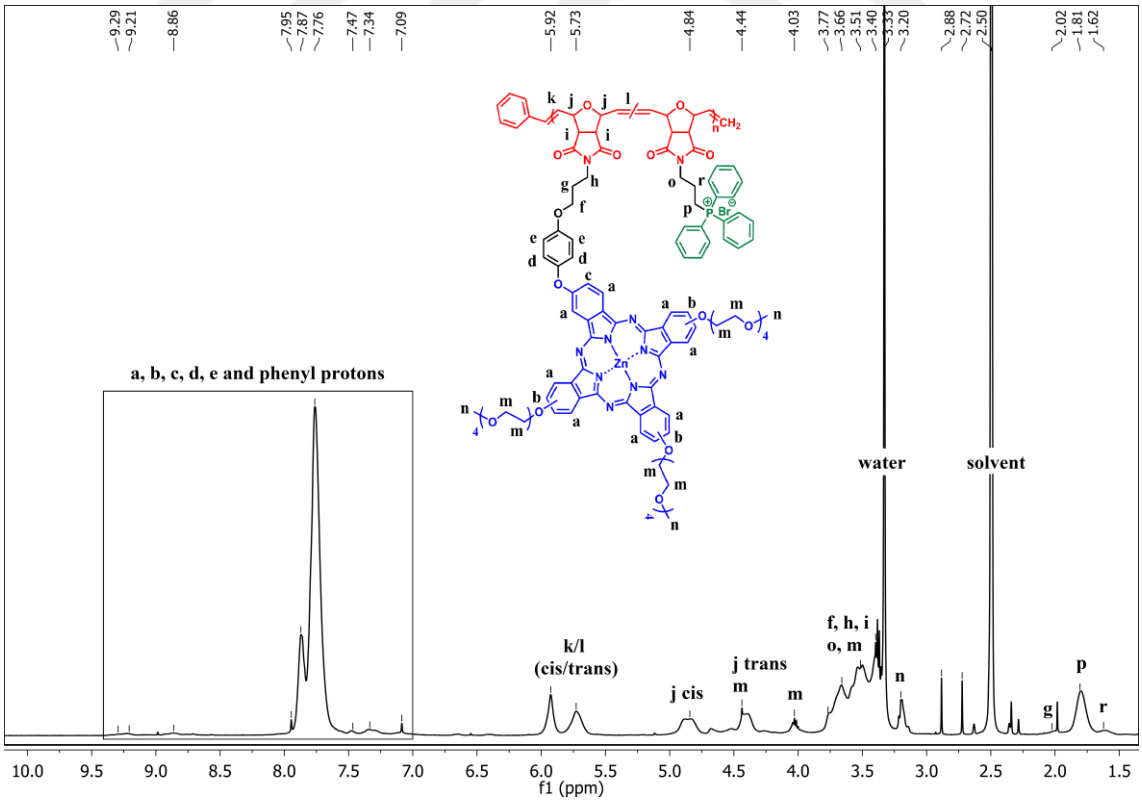

Figure A.44 ^{1}H-NMR spectrum of copolymer P11 in DMSO-d_6

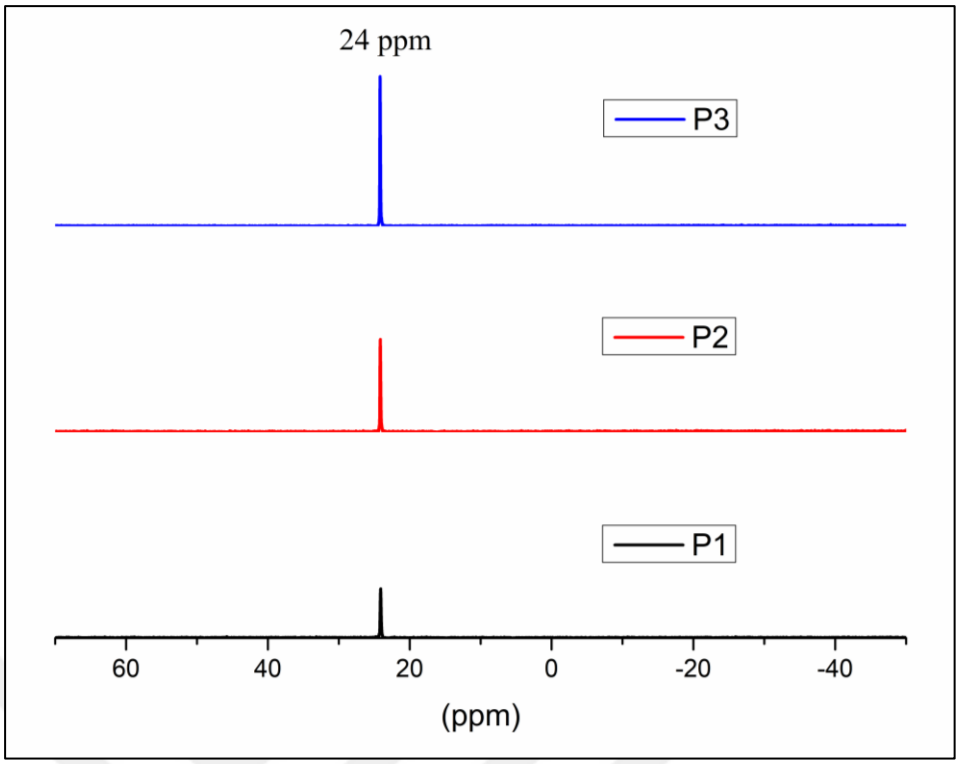

Figure A.45 ^{31}P-NMR spectra of copolymers P9-P11 in DMSO-d_6

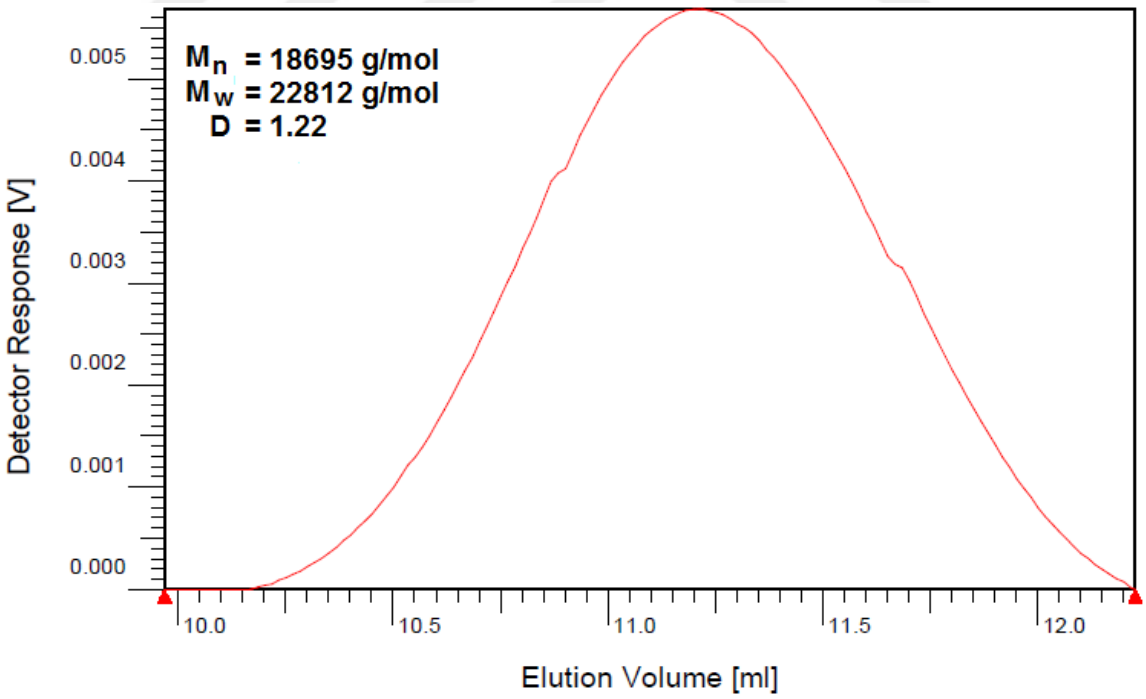

Figure A.46 GPC elugram of the homopolymer P8 in DMAC (RI detector, PMMA standard)

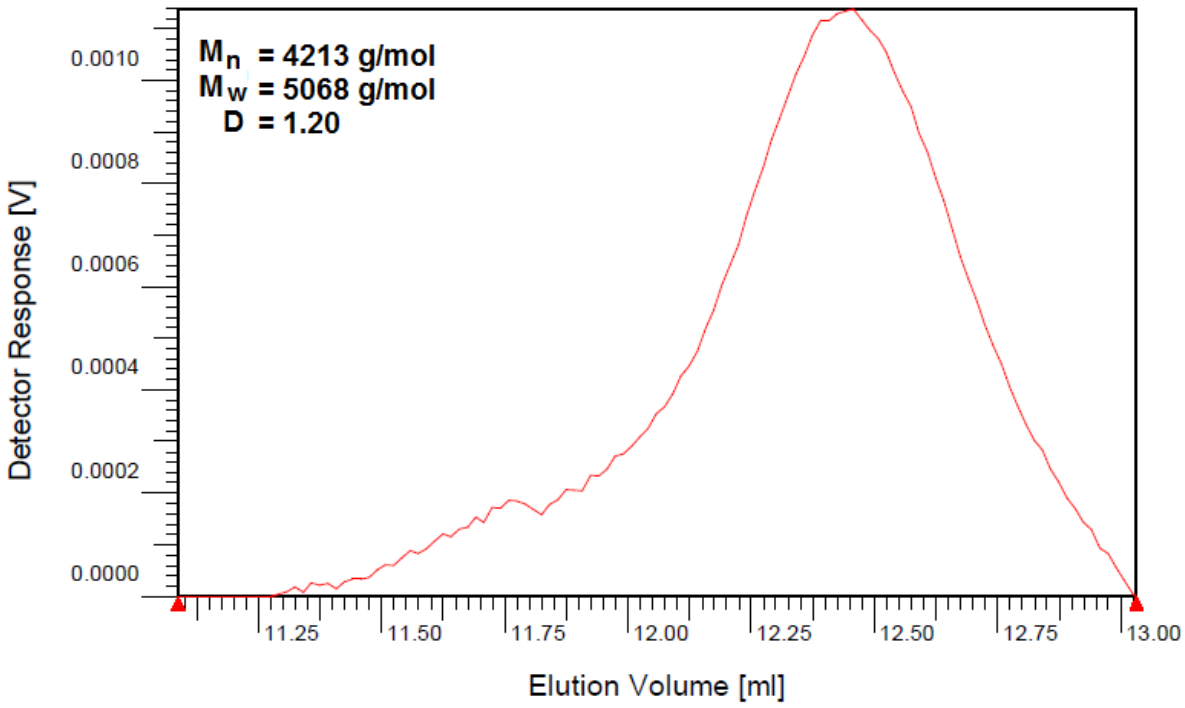

Figure A.47 GPC elugram of the copolymer P9 in DMAC (RI detector, PMMA standard)

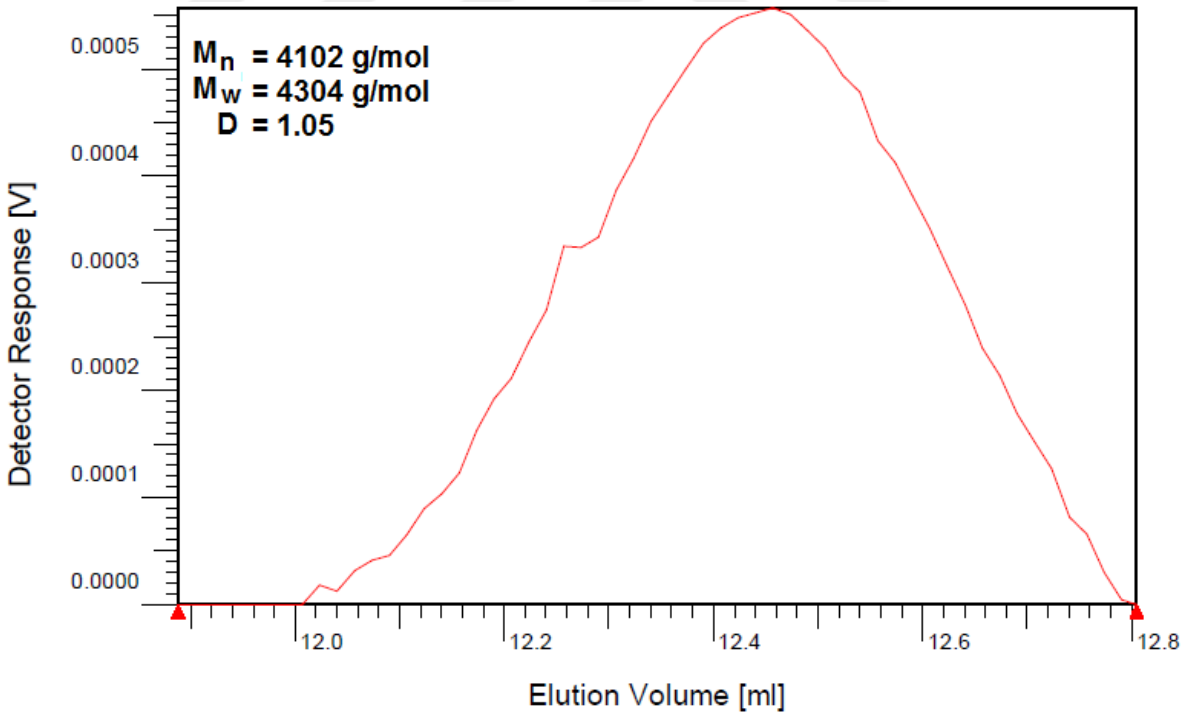

Figure A.48 GPC elugram of the copolymer P10 in DMAC (RI detector, PMMA standard).

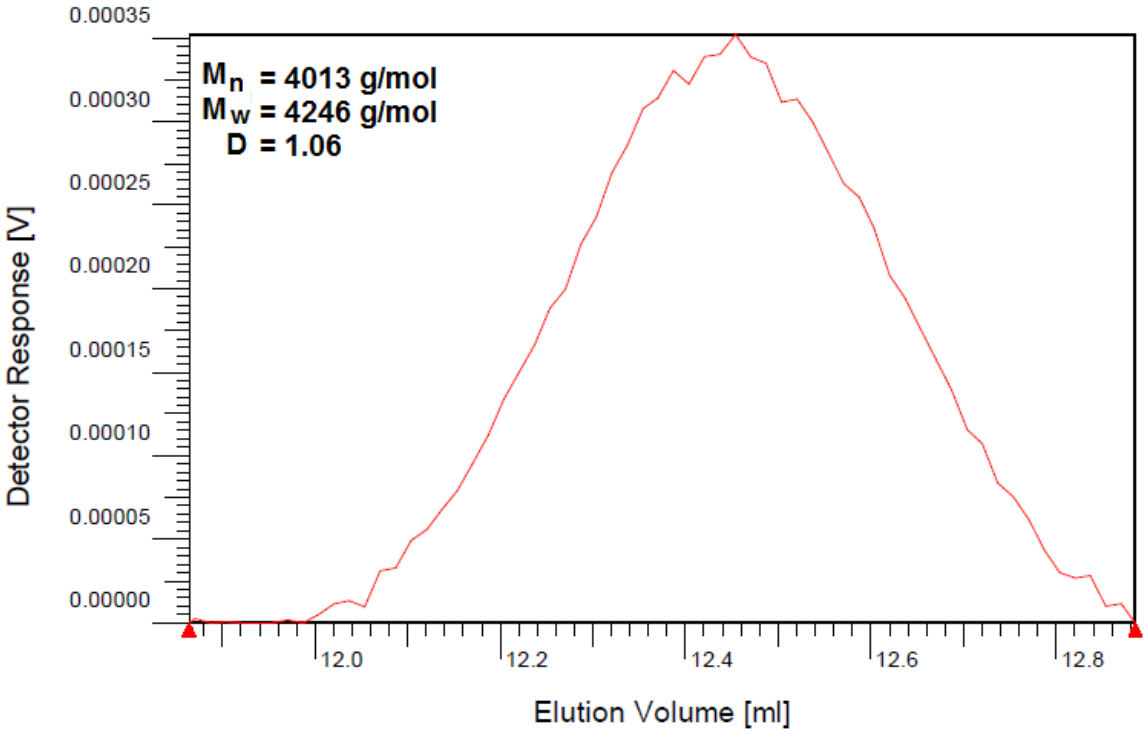

Figure A.49 GPC elugram of the copolymer P11 in DMAC (RI detector, PMMA standard)

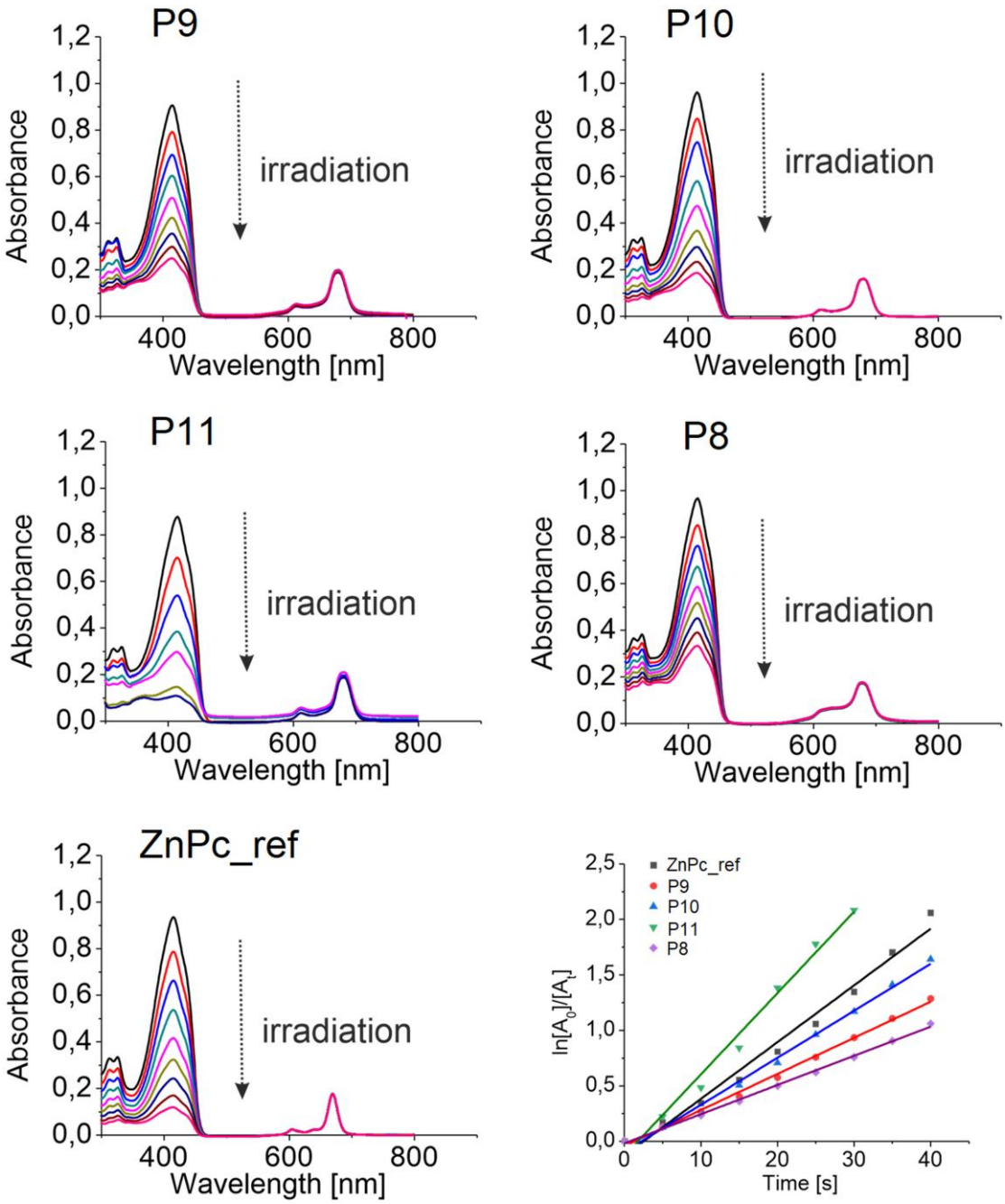

Figure A.50 Time-dependent decomposition of DPBF photosensitized by P8-P11 and unsubstituted ZnPc as a reference in DMF upon irradiation with light of 660 ± 20 nm and corresponding first-order plots

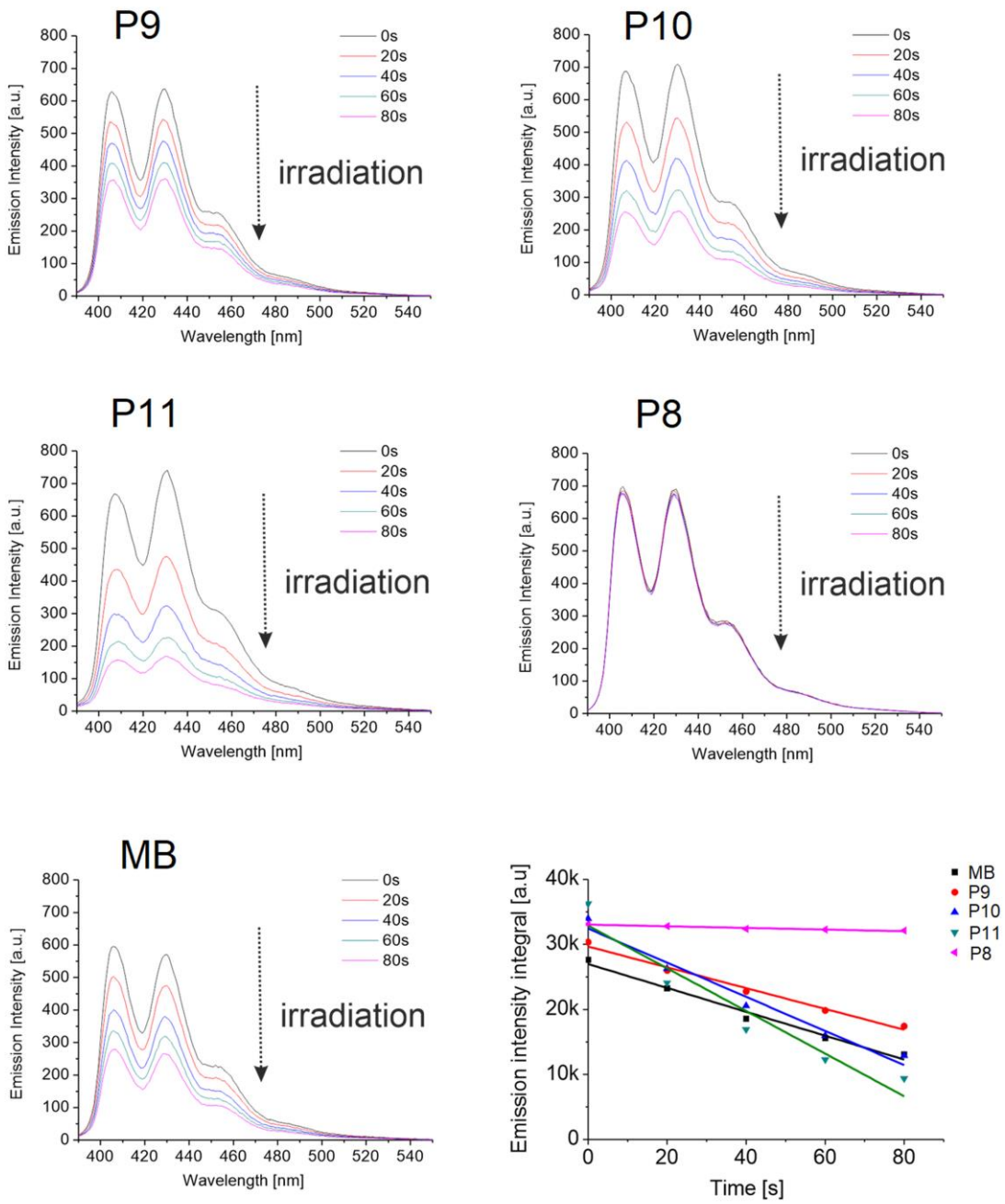

Figure A.51 Time-dependent decomposition of ADMA photosensitized by P8-P11 and MB as a reference in H_2O upon irradiation with light of 660 ± 20 nm and corresponding first-order plots

PUBLICATIONS FROM THE THESIS

Conference Papers

1. Synthesis and photodynamic activity of poly(oxanorbornene)-zinc(II) phthalocyanine conjugates as antimicrobial agents. Ahmetali E., Süer N. C., Galstyan A., Eren T., Şener, M. K. *44th International Conference on Coordination Chemistry*, Rimini, Italy, 28 August **2022**

2. aPDT activity of cationic copolymers with dual function: synergistic effect of poly(oxanorbornene) and phthalocyanine. Ahmetali E., Şen P., Süer N. C., Aksu M. B., Nyokong T., Eren T., Şener M. K. *19th Congress of the European Society for Photobiology*, Salzburg, Austria, 30 August **2021**

Papers

1. Poly(oxanorbornene)s bearing triphenylphosphonium and PEGylated zinc(II) phthalocyanine with boosted photobiological activity and singlet oxygen generation. Ahmetali, E., Galstyan, A., Süer, N. C., Eren, T., M. K. Şener. *Submitted*, **2022**

2. Photodynamic therapy activities of phthalocyanine-based macromolecular photosensitizers on MCF-7 breast cancer cells. Ahmetali E., Sen P., Suer N. C., Nyokong T., Eren T., Şener M. K. *Journal of Macromolecular Science Part A-Pure and Applied Chemistry*, **2021**
https://doi.org/10.1080/10601325.2021.1934012

3. Enhanced light-driven antimicrobial activity of cationic poly(oxanorbornene)s by phthalocyanine incorporation into polymer as pendants. Ahmetali E., Sen P., Suer N. C., Aksu M. B., Nyokong T., Eren T., Şener M. K. *Macromolecular Chemistry and Physics*, **2020**
https://doi.org/10.1002/macp.202000386

Projects

1. Synthesis of phthalocyanine functional poly(oxanorbornene) derivatives via ring opening metathesis polymerization (ROMP) method, investigation of their antimicrobial and photodynamic properties. *TÜBİTAK (The Scientific and Technological Research Council of Turkey)*, 1001 Project, **2019**